THESIS ON INFORMATICS AND SYSTEM ENGINEERING C113

Scalable Open Platform for Reliable Medical Sensorics

MAIRO LEIER

TUT PRESS

Tallinn University of Technology
Faculty of Information Technology
Department of Computer Engineering

Dissertation was accepted for the defense of the degree of Doctor of Philosophy in Computer and Systems Engineering on April 19th, 2016.

Supervisor: Prof. Gert Jervan, PhD
Dep. of Computer Engineering
Tallinn University of Technology
Tallinn, Estonia

Opponents: Prof. Johan Lilius
Dep. of Information Technologies
Åbo Academi University, Finland

Prof. Daniela De Venuto
Dep. of Elettrotecnica ed Elettronica
Politecnico di Bari, Italy

Defense of the thesis: June 13th, 2016

Declaration:
Hereby I declare that this doctoral thesis, my original investigation and achievement, submitted for the doctoral degree at Tallinn University of Technology has not been submitted for any academic degree.

ISSN 1406-4731
ISBN 978-9949-23-953-5 (publication)
ISBN 978-9949-23-954-2 (PDF)

INFORMAATIKA JA SÜSTEEMITEHNIKA C113

Laiendatav avatud platvorm usaldusväärsete meditsiiniliste sensorite jaoks

MAIRO LEIER

TTÜ
KIRJASTUS

List of Publications

This dissertation is based on the following publications:

1. Leier M.; Jervan G. (2013). Sleep Apnea Pre-Screening on Neonates and Children with Shoe Integrated Sensors. *In: Norchip*, Vilnius, Lithuania, 2013, pp. 1-4
2. Leier M.; Jervan G. (2014). Miniaturized Wireless Monitor for Long-term Monitoring of Newborns. *In: Proceedings of the BEC 2014*, Estonia, 2014, pp. 193-196
3. Leier M.; Jervan G.; Stork W. (2014). Respiration Signal Extraction from Photoplethysmogram Using Pulse Wave Amplitude Variation *In: IEEE International Conference on Communications ICC2014*, Sydney, Australia, 2014, pp. 3535-3540
4. Leier M.; Pilt K.; Karai D.; Jervan G. (2015). Smart Photoplethysmographic Sensor for Pulse Wave Registration at Different Vascular Depths *In: EMBC*, Milano, Italy, 2015, pp. 1849-1852
5. Preden S. J.; Tammemäe K.; Jantsch A.; Leier M.; Riid A.; Calis E. (2015). The Benefits of Awareness and Attention in Fog and Mist Computing, *In: IEEE Computer*, 2015, pp. 23-31

Other Related Publications

1. Pilt K.; Leier M.; Silluta S.; Kööts K.; Meigas K.; Viigimaa M. (2015). Pulse wave registration from radial artery using photoplethysmographic method *In: EMBC*, Milano, Italy, 2015, pp. 6425-6428
2. Hollstein T.; Reinsalu U.; Leier M.; (2014). Motivation-driven learning processes at the example of embedded systems *In: 10th European Workshop on Micoelectronics Education EWME*, Tallinn, Estonia, 2014, pp. 3-6

Author's Contribution to the Publications

1. The author proposed sleep apnea detection algorithm and the general system architecture for sleep apnea pre-screening to perform measurements and data analysis. Proposed solution includes the requirements analysis and selection of the hardware that is needed to perform real experiments.
2. The author developed detailed system architecture to meet clinical and technical requirements to perform measurements on infants and children. Also analysis of the embedded algorithms and data communication requirements were done by the author to test whether developed prototype meets defined requirements.
3. The author developed low-complexity algorithm for respiration signal extraction based on the pulse wave amplitude modulation. Proposed algorithm was validated and compared against different methods. As a result we demonstrated that proposed algorithm could effectively be used to derive pulse amplitude variation from the PPG signal.
4. The author was contributing to the several sections of the paper. Design of the optical sensor array, development of the control software and tests were performed in collaboration with the department of Biomedical Engineering at TTU. The result of the paper is device design and the real prototype that was tested using previously developed algorithm. Python based software was written to perform tests.
5. Author was responsible for developing the system architecture of the developed prototype. It included building and testing of the system.

Abbreviations and Definitions

AC	Alternating Current
ADC	Analog-to-Digital Csonverter
ADHD	Attention Deficit with Hyperability
AFE	Analog Front-End
AHI	Apnea Hypopnea Index
AM	Amplitude Modulation
API	Application Programming Interface
BLE	Bluetooth Low Energy
CAGR	Compound Annual Growth Rate
CoHb	Carboxyhemoglobin
CPS	Cyber-Physical Systems
CWT	Continuous Wavelet Transform
DAC	Digital-Analog Converter
DC	Direct Current
DWPT	Discrete Wavelet Packet Transform
DWT	Discrete Wavelet Transform
ECG	Electrocardiography
EEG	Electroencephalography
EMD	Empirical Mode Decomposition
EMG	Electromyography
FDA	Food and Drug Administration
FIR	Finite Impulse Response filter
FFT	Fast Fourier Transform
FM	Frequency Modulation
FRAM	Ferroelectric Random Access Memory
GATT	Generic Attribute
I^2C	Inter-Integrated Circuit Protocol
IMF	Intrinsic Mode Function
IoT	Internet of Things
LDO	Low-dropout Linear Voltage Regulator

LED	Light-Emitting Diode
MCU	Microcontroller Unit
MetHb	Methemoglobin
NIRS	Near Infra-red Spectroscopy
PD	Photo-Detector
OR-MCAR	Order Reduced Modified Covariance Auto Regressive
OSA	Obstructive Sleep Apnea
P_{ETCO_2}	Amount of carbon dioxide present in the exhaled air
PAV	Pulse Amplitude Variability
PCB	Printed-Circuit Board
PD	Photo-Diode
PLMD	Periodic Limb Movement Disorder
PPG	Photoplethysmography
PRF	Pulse Rate Frequency
PRV	Pulse Rate Variability
PSG	Polysomnography
PWV	Pulse Width Variability
RAM	Random Access Memory
RIIV	Respiratory-Induced Intensity Variations
SaO_2	Arterial Oxygen Saturation
SD	Standard Deviation
SoS	Systems of Systems
SPI	Serial Peripheral Interface Bus
SpO_2	Peripheral Capillary Oxygen Saturation
STFT	Short-Time Fourier Transform
TFS	Time-Frequency Spectra
UARS	Upper Airway Resistance Syndrome
UI	User Interface
USB	Universal Serial Bus
UUID	Universally Unique Identifier
UWB	Ultra-Wide Band

Contents

List of Publications **5**

Abbreviations and Definitions **7**

Abstract **11**

Annotatsioon **13**

Acknowledgements **15**

Introduction **17**

1 Modular Architecture for Pre-screening **27**
1.1 Background 27
1.2 Hardware 30
1.3 Software 39
1.4 Experimental results 43
1.5 Chapter summary 46

2 Photoplethysmographic Sensors with Increased Reliability **47**
2.1 Background 47
2.2 Overview 50
2.3 Optical foot sensor 51
2.4 Optical smart photoplethysmographic sensor 56
2.5 Chapter summary 66

3 Low Complexity Algorithms for Sleep Quality Estimation **69**
3.1 Background 69
3.2 Overview 74
3.3 Respiration signal extraction 77
3.4 Experimental results 82
3.5 Chapter summary 86

4 Self-Awareness in Health Monitoring **87**
4.1 Background 87
4.2 Overview 90
4.3 Self-aware health monitor 90
4.4 System architecture 92
4.5 Experimental results 94
4.6 Chapter summary 97

5 Conclusions and Future Work **99**
5.1 Conclusions 99
5.2 Future Work 101

Bibliography **103**

Appendices **113**

Appendix A 115

Appendix B 121

Appendix C 127

Appendix D 135

Appendix E 141

Curriculum Vitae **155**

Elulookirjeldus **157**

Abstract

The objective of this dissertation is to perform research in technologies for health care monitoring. During the last years there have been increased interest in bringing new health care devices into the market. One option to speed up the development of experiments and increase the portability between different devices is to develop devices based on modular architecture. Modularity makes possible to interchange different system components independently. It allows to use more sophisticated signal processing techniques that also requires new types of sensors. This could be achieved by combining different types of sensors to work together or develop further one specific sensor to enhance its sensitivity level or range. Recorded signals that are used to detect the health condition of the patient, need analysis and interpretation. Inclusion of some external sensors, that give an information about the environment, would increase the accuracy of analysis. Having also information about the status of the sensors would help to estimate the reliability of the monitoring system itself. With this knowledge we could estimate how long the system is able to provide reliable information or predict some unexpected issues.

Such application independent solutions must meet the following requirements: (1) it must be portable and have simple functionality, expandable for different research areas, (2) use energy-efficient algorithms designed for portable devices and (3) provide a real-time analysis of measurement data and feedback to the patient. To carry out research and perform real experiments in various medical domains a prototype platform was developed that meets those requirements.

Our focus is on research in sleep quality and arterial pulse wave. To study and perform sleep quality research on children there is a need for optical sensory platform. This is a set of optical and inertial sensors to perform optical pulse wave measurements. An architecture together with prototype was developed. As this set of sensors needs a special analysis hardware it is connected to our developed modular platform. Compared to other similar solutions, our optical sensor allows to enhance optical signal quality by combining signals from different sources of optical sensors and assess their quality in real-time. This method helps to extract the

respiration rate from the pulse wave with increased accuracy.

In order to reduce the required computing power and energy consumption, a new algorithm for respiration rate calculation based on the pulse wave amplitude modulation was developed. Compared to other methodologies calculations are done in time domain, which significantly reduces the required number of mathematical operations, and consequentially requires less energy making it suitable for portable devices.

One of the most widely accepted techniques to quantify the arterial stiffness is measuring the pulse wave velocity. Determining the arterial pulse wave is a time-consuming and precise process. To facilitate this process, a novel optical sensor matrix was developed. It is connected to our platform that enables the sensor to activate only those optical elements that have the best signal-to-noise ratio. The result is enhanced signal quality and decreased measurement time of pulse wave.

To increase the reliability of measurement data for the analysis, one method is to add situation specific information. This method requires measurements from additional sensors that is added as a location and environment-related information. System architecture and prototype with real-time analysis functionality was developed. Our proposed solution enables to add this kind of information and use it for further analysis. This method helps to understand the reason of potential anomaly whether any parameter is changing rapidly or is missing.

This thesis concentrates on research in technologies for health care monitoring. We present a method to speed up real experiments using different types of sensors that may require different hardware. To demonstrate the feasibility of the developed method we have implemented it on our modular platform. We demonstrated how the architecture combined with different sensorics could be used in two different application areas. Finally, we performed several experiments to demonstrate the effectiveness of the developed method.

Annotatsioon

Käesoleva väitekirja põhieesmärgiks on inimese tervise jälgimise tehnoloogiate uurimine erinevates valdkondades. Viimastel aastatel on turule jõudnud üha suurenev arv erinevaid tervise jälgimise seadmeid. Üks võimalus terviseuuringute kiiremaks läbiviimiseks ja erinevate portatiivsete seadmete omavaheliseks ühilduvuse parandamiseks on arendada seadmed, mis põhinevad modulaarsel arhitektuuril. Modulaarsus võimaldab ümber vahetada süsteemi erinevaid komponente üksteisest sõltumatult. Selle tõttu on võimalik kasutada keerukamaid signaalitöötlusalgoritme, mis omakorda nõuavad uut tüüpi sensoreid. See on saavutatav kombineerides omavahel koos töötama erinevaid tüüpi sensoreid või arendada edasi olemasolevaid sensoreid suurendades nende tundlikkust või mõõteulatust. Salvestatud signaalid, mis näitavad uuritava tervislikku seisukorda, vajavad analüüsi ja tõlgendamist. Lisades väliseid sensoreid, mis annavad lisainformatsiooni keskkonnatingimuste kohta, on võimalik suurendada analüüsi täpsust. Omades informatsiooni kasutatud sensorite staatuse kohta on võimalik hinnata monitooringusüsteemi usaldusväärsust. Selle teadmisega on meil võimalik hinnata, kui kaua süsteem on võimeline andma usaldusväärset informatsiooni, või ennetada ootamatuid probleeme.

Sellised aplikatsioonist sõltumatud lahendused peavad vastama järgmistele nõudmistele: (1) see peab olema porditav ja lihtsalt kasutatav ning laiendatav erinevatele uurimisvaldkondadele, (2) kasutama energiasäästlikke algoritme, mis on arendatud portatiivsete seadmete jaoks ja (3) pakkuma reaalajas andmete analüüsimise võimalust ning tagasisidet patsiendile. Uuringute ja reaalsete eksperimentide läbiviimiseks erinevates meditsiinivaldkondades arendati välja prototüüp, mis vastab nendele nõudmistele.

Antud töö fookuseks on unekvaliteedi ja arteriaalse pulsilaine mõõtmise võimaluste uurimine. Viimaks läbi unekvaliteedi uuringuid lastel on vaja kasutada optilisel sensoril põhinevat seadet. See on kooslus optilistest ja inertsiaalsetest sensoritest pulsilaine mõõtmiseks. Arendati välja seadme arhitektuur ja prototüüp. Kuna selline kombinatsioon sensoritest vajab analüüsimiseks spetsiaalset riistvara, on see ühendatud meie poolt arendatud modulaarse platvormiga. Võrreldes teiste sarnaste lahendustega, võimaldab välja arendatav sensor suurendada optiliselt mõõdetud signaali

kvaliteeti, kombineerides signaaliallikaid erinevatelt optilistelt sensoritelt ning reaalajas nende kvaliteeti hinnates. See metoodika aitab suurendada täpsust ka hingamissageduse tuvastamisel pulsilainest.

Vähendamaks vajalikku arvutusvõimsust ning energiatarvet arendasime hingamissageduse tuvastamiseks välja uudse pulsilaine amplituudmodulatsioonil põhineva algoritmi. Võrreldes teiste metoodikatega sooritatakse arvutused ajadomeenis. See vähendab oluliselt vajalike matemaatiliste tehete hulka ja seetõttu nõuab ka vähem energiat, tehes selle sobivaks portatiivsetel seadmetel kasutamiseks.

Üks kõige laialdasemalt kasutatav metoodika arterite vanuse määramiseks on pulsilaine mõõtmine. Arteriaalse pulsilaine mõõtmine on ajamahukas ja täpsust nõudev protsess. Selle lihtsustamiseks arendasime välja uudse optilise sensor-maatriksi. See on ühendatud meie platvormiga, mis võimaldab sensoril aktiveerida ainult neid optilisi elemente, millel on parim signaali-müra suhe. Selle tulemusena paraneb signaali kvaliteet ja väheneb pulsilaine mõõtmiseks kuluv aeg.

Mõõtetulemuste usaldusväärsuse suurendamiseks võib neile lisada situatsioonispetsiifilist informatsiooni. See metoodika nõuab mõõtmiste sooritamist lisaks ka väliste sensorite poolt, mille tulemused lisatakse asukoha ja keskkonnaga seotud informatsioonina. Arendati välja süsteemi arhitektuur ja prototüüp koos reaalajas andmete analüüsimise funktsionaalsusega. Meie pakutud lahendus võimaldab lisada taolist lisainformatsiooni ja kasutada seda hilisemal analüüsimisel. See metoodika aitab mõista potentsiaalsete anomaaliate põhjuseid, kui mõni parameeter muutub järsult või on puudu.

Käesolev väitekiri keskendub inimese tervise jälgimise tehnoloogiate uurimisele. Me tutvustasime metoodikat, mis aitab kiirendada reaalseid eksperimente, kasutades erinevaid tüüpi sensoreid, mis võivad vajada erinevat riistvara. Välja pakutud metoodika teostatavuse demonstreerimiseks arendasime modulaarse platvormi. Me demonstreerisime, kuidas välja pakutud arhitektuuri, ühendatud erinevate sensoritega, on võimalik kasutada erinevates valdkondades. Lõpuks viisime läbi erinevaid eksperimente demonstreerimaks arendatud metoodika efektiivsust.

Acknowledgements

I would like to express my gratitude to everybody who helped me during my PhD studies and without whom this work would not appear.

In particular, I would like to thank my supervisor Prof. Gert Jervan for guiding me through the Master's course to the end of PhD. I have always appreciated his support and wise comments. Interesting and valuable discussions with him helped me to develop the theory and overcome all obstacles that appeared on the way to this thesis.

Special thanks to the head of the Department of Computer Engineering Margus Kruus for creating outstanding environment for productive work and study.

I would like to thank all the people who helped me during my PhD. studies. I would like to express special thanks to my great colleagues Dr. Maksim Gorev, Priit Ruberg, prof. Kalle Tammemäe, Prof. Thomas Hollstein and Dr. Kristjan Pilt for their advises, help and motivation to finish this work.

Furthermore, I would like to acknowledge the organizations that have supported my PhD studies: Tallinn University of Technology, National Graduate School in Information and Communication Technologies (IKTDK), EU's FP7 collaborative research project DIAMOND, European Regional Development Fund through the Centre for Integrated Electronic Systems and Biomedical Engineering (CEBE), Estonian IT Foundation (EITSA) and Technology Foundation for Education (HITSA).

Finally, I would like to thank my parents for their support and motivation. I would also thank for my family for all the care and patience – especially my belowed wife Terje. Thank you!

Mairo Leier
Tallinn, May 2016

Introduction

Would it have been possible to track your daily activities 10 years ago? Probably not, if we don't count our mobile operators nor our national security institutions. During last years, tracking everything has became like a habit. We track how active we are, how do we sleep, how do we perform, what do we eat, etc. We measure everything because it is interesting and we get some feedback about our lifestyle. On one hand we don't have yet the knowledge what we should do with this enormous amount of data. On the other hand this data could be valuable for doctors who could make more accurate diagnosis and start with better treatment.

Even-though we may like to track our everyday life, there are situations where continuous monitoring could be the only preventive way to avoid serious incidents [13]. There are many diseases where such kind of monitoring would increase people safety and decrease costs of health-care. Elderly people living in remote areas may be assisted with tele-monitoring and remote consultancy [47]. People suffering dementia, sleep diseases, cardiovascular problems may need to be monitored for screening and safety purposes. Another advantage is that such remote monitoring allows patients to stay at home and visit the doctor only in case of serious situations or to get the diagnosis of sickness.

The latest technology trend in health-care is personalized medicine that has brought us many portable medical devices. The selection of different monitoring devices covers basically most of the body locations. There are different technologies to perform measurement of the same physiological signal. However, easier methods may be cheaper and easier to use but may perform poorly in real-life situations. Integrating different measurement technologies and combining them is a way forward to avoid people worrying about choosing the best device for health tracking and still support wide range of real-life situations with good results. Great interest have got towards optical sensors as a new non-invasive and energy-efficient way to develop medical devices. There is a wide range of diseases that could be monitored and analysed by combining optical sensors with motion analysis and other types of sensors. For example, sleep quality monitoring that needs unobtrusive and long term screening, especially on babies and chil-

dren [26] [36].

There are different reasons to perform health monitoring but globally number one cause of death are cardiovascular diseases. An estimated 17.5 million people died from cardiovascular diseases in 2012, representing 31% of all global deaths [101]. These are a group of disorders of the heart and blood vessels that are mostly result of unhealthy diet, lack of physical activity, tobacco and harmful use of alcohol. The effects of behavioural risk factors may show up in individuals as raised blood pressure, raised blood glucose or blood lipids, and overweight and obesity. It may take from several months to years before first symptoms may appear. Often, there are no symptoms of the underlying disease of blood vessels. A heart attack or stroke may be the first warning of underlying disease that brings people to the doctor for diagnosis. Usual cardiovascular disease diagnosis may include several tests, for example blood tests, electrocardiogram, stress testing, echocardiography and cardiac magnetic resonance imaging. Some cardiovascular problems are related to a process called atherosclerosis when a substance called plaque builds up in the walls of the arteries. Analysis of the arteries could predict or avoid problems caused by the atherosclerosis which is usually done by analyzing the arterial stiffness. It is a rather quick method where patient have to lie on the bed while his or her pulse wave is being analyzed during few minutes. Shape of the pulse wave reflects the status of the arteries.

When it comes to the data interpretation by a patient or medical personnel, then it highly depends on the qualification of the person. For example, wristbands that are mostly meant for activity tracking show steps counter, pulse rate and burned calories. If those results are collected in controlled environment then they could be compared with results from other patients. While doing your everyday activities it is hard to estimate, is this particular lifestyle healthy or not because there is no information whether those steps were done during the walking in fresh air or doing your homework. Estimating the sleep quality can be grouped into the same category that needs more background information to give relevant diagnosis based on the results. Including different kind of environmental data, like environment temperature, humidity, light conditions, noise level, lifestyle details, could help to interpret the data and to improve the diagnosis. On one hand such kind of enhanced diagnosis needs more complex measurement environment and on the other hand (partly) automated data analysis systems that help to make the first initial estimation about environmental situation. As an example, to perform sleep quality estimation, it needs a set of sensors that are attached to a human. If there are some anomalies during the experiments, the cause of those anomalies could be better explained with the help of additional environmental sensors.

Motivation

Innovation has always been a driving force for increased efficiency and quality in health care. During the last 100 years the quality of health care has improved tremendously allowing us to discover and to treat more diseases. As technology evolves, health care becomes more accurate, cheaper and faster. That leads us to the new paradigm, called personalized medicine to serve people in more efficient way, still ensuring the quality and preventing consequences. It means that the health care is moving away from the hospital to the patient's home bringing us small and wearable remote monitoring devices. Patients could have immediate access to their own records and be able to transmit or carry it from one health care provider to another.

During the last years personalized medicine has became more popular with the help of increased number of portable monitoring devices that are capable of tracking our vital signals in real-time. It makes easier to keep an eye on newborns during the night or to be informed about unexpected health conditions of our elderly parents. Most of such wearable devices need to be attached to the clothes or body to get readings about our current health status. As the electronics get smaller, many of such devices will be embedded into the textile or injected into our body as an implant. That makes personalized health care as one part of our everyday life without even thinking about that.

In spite of rapid technology development it can take years until health care reaches to the technological level when only in rear cases there is a need to visit doctor personally. New types of wearable devices, sensors and automated systems show the direction of the future. More and more new manufacturers appear to bring us new technologies. As a result of research and innovation health care devices get smaller, more powerful and smarter. But as there is a large number of manufacturers, there is an increased need for standardization to decrease the cost for development, increase usability for the end-user and decrease the time for integration with existing systems. Current situation is not promising as we have hundreds of health monitoring devices on the market but most of them can be used only together with application developed for this particular device. In addition, there is no possibility to integrate such devices into some common health care system. Nevertheless, first steps have already been done to increase the compatibility in communication layer. Bluetooth Smart with Health Device Profile [93] is one example that allows to send vital data in predefined format that is understandable for every developer.

The time needed for reliable medical device development is usually several years. For example, there are countless number of wrist bands like smart watches, sleep quality analyzers, fitness trackers. In most of the cases the development of prototype has started from scratch, especially when it

was developed by the start-up company. There is a very large number of prototyping boards available but most of them are large, heavy and need wired connections with the rest of the system. That makes them unusable for portable device prototyping as already the first prototype has to be small with many integrated functions. Having a miniature development kit would give a huge advantage. Instead of designing and building a complete system, one has to focus only to some certain parts that may be missing or need re-design. As the market for different kind of measurement devices increases rapidly, providing a fully flexible and open-source hardware and software would make developing portable medical and health-care devices cheaper, faster and increase compatibility on the lower level.

Problem formulation

There are about 100 million units of wearable devices shipped in each year with market value more than 10 billion US dollars [96]. As the health care in last years is moving more towards personalized medicine, it is expected that many of those wearable devices could be used for remote monitoring and screening purposes. In medical industry standardization is one of the most important aspect that every manufacturer has to follow. It covers everything from design up to delivery and the outcome, among others, is increased usability. By that we mean easier integration with other systems, better functional extension possibilities and more understandable user interface for end-user. As the number of wearable device manufacturers is growing, many of those devices are monitoring particular disease and there are countless number of places on the body they could be attached to, the standardization is hardly achievable goal. For each particular disease there are tens of competitive devices that are able to perform exactly the same measurement operation. For the end-user large number of devices makes hard to choose the best suitable option for his or her particular needs. Such kind of highly competitive market decreases confidence for the end user. There is no assurance if that particular chosen device is on the market next year or production has stopped because of high competition and decreased demand. Another situation would be if customer needs have slightly been changed then replacing the device with another one that has some additional features is costly, time consuming and may also need to redesign some part of the supportive infrastructure to perform measurements. This situation would be improved by developing open standards to support developing devices with increased modularity that are able to extend each-other features. Modular devices also help to decrease time to perform experiments.

Modular architecture

During the last years there have been increased interest in bringing new health care devices into the market. Modular architecture would give a possibility to speed up the development of experiment and increase the portability between devices. Modularity itself means that the system consists of many parts that are interchangeable. In this case we focus on the system modules that are used to build a complete system. As an example, the core of the system is on processing module. Interface between analog sensors and the rest of the system is on analog front-end. Some external sensors are located on sensor module. By connecting those boards with each other we can get working system that has modularity on hardware level. This means, for example, in case we need to replace the signal processing module with the more powerful one, we don't have to make any changes in the rest of the system. Or another example. If we are going to develop a new type of sensors then we would like to use these with existing systems. Signal processing module can remain the same and we only switch an analog front-end and sensor module with the new one, achieving a device with completely new functionality. There are lack of such modular systems on the market, but the need is there, specially forn the research and prototyping purposes. By having such modular system would enable us to perform research experiments with starter kit and increase its functionality over the time without changing the core system. That would help to save experimenting and development costs and focus more to the research problem.

Another aspect is that any kind of disease needs some kind of diagnosis from the doctor. For good quality diagnosis, it is required to perform experiments that may include several different measurement devices. Depending on the type of the disease, there are several physiological signals that are measured during the experiments. The main purpose of experiments is to collect good quality data that is used to give a diagnosis. Usually it requires to have many different devices but by using devices with modular architecture would reduce the number of those devices dramatically. That makes diagnosis faster, more reliable and reduce the cost for health-care.

Non-invasive sensorics

The current trend in health care sensorics is to make as little harm and discomfort to the patient as possible. Non-invasive electro-chemical, electrical and optical sensors have won popularity in most of the health care sectors. One of the leaders in non-invasive optical measurement is pulse oximetry. It is harmless, relatively low power and does not need sophisticated signal processing to get reliable results.

The advantage of modular architecture for medical sensorics over the conventional wearable devices is the possibility to add a new functionality to the system with lower costs. Modular architecture makes possible to use more sophisticated signal processing that also requires new type of sensors. This could be achieved by combining different types of sensors to work together or develop new specific sensor to enhance its sensitivity level or range. As new sensors get smaller in dimensions integrating more sensors does not cost much extra space. Physiological signal measurement is complicated process that brings in addition to useful signal also different kind of noises and measurement results could be affected by many related in-body processes. Suppressing the noise level and enhancing measurement range would increase the accuracy of processed signal and different features extracted from that signal.

One application area that takes the advantage from increased sensitivity and new types of sensors is a pulse wave registration from arteries. This technique requires to exclude the influence of the peripheral blood vessels (arteroiles, capillares) that have many challenges [28]. The development of new types of sensors would give physicians new methodologies and faster ways to analyse the health condition of the patient. If the communication interface of new sensors were compatible with the existing ones, it would need minimal effort to increase the device sensitivity and functionality. This kind of approach would decrease the overall infrastructure and training costs of the health-care sector that already takes a huge amount of the budget.

Data processing and system awareness

As the number of available portable devices is increasing and there are new types of sensors, there is a continuous development how to make recorded signals more robust, reliable and accurate. Although new types of processors, specially designed for portable devices, become more powerful, there is always a trade-off between the battery life, amount of data processing and communication. The number of sensors connected to one monitoring device is increasing. Having many similar sensors near-by could make it possible to add some level of cooperation to balance the load for data processing. For example, if there are similar devices nearby that are capable of measuring the same signals but using different type of sensor. Depending on the capabilities and needs it can be decided which sensor is used for data recordings. There are many parameters like amount of power required for recordings, battery status, required device lifetime or the speed of wireless link. Depending on the need it would be even possible to decide which signal processing algorithm to use. Either the one that provides real-time analysis with decreased accuracy or get the best possible signal quality for

medical diagnosis.

All recorded signals that are used to detect the health condition of the patient, need analyzis and interpretation. Most wearable devices have only limited number of sensors integrated. Including also some external sensors that give an information about the environment, would increase the accuracy of analysis. Having also information about the status of used sensors would help to estimate the reliability of the monitoring system itself. Without this knowledge we could not be able to estimate how long the system is able to provide reliable information or predict some unexpected issues. This kind of awareness gives the system some level of autonomy to make decisions up to some level of confidence. There is a lack of such available systems because of the complexity.

Contributions

The main contributions of this thesis are the following:

- A new approach for system level design that extends the possibilities to use the same hardware for the development of different health monitoring and screening devices. Proposed architecture enables to extend the functionality of the system and replace some of its functionality without complete redesign of the system. Together with the hardware a system firmware is built to support the same modularity.
- A method to increase the quality of the optical signal. To validate the method, a dual optical sensor for infant sleep quality monitoring was developed. The purpose is to increase the signal quality by continuously analyzing signal to noise ratio of the acquired signal from different optical elements. If there is an efficiency decrease below predefined level, a signal from another optical element is used for further analysis.
- A smart optical photoplethysmographic sensor for automatic pulse wave registration. In order to record a pulse wave from the artery, the position of the artery has to be estimated. Developed sensor detects the position of the artery and enables only those optical elements that produce the best signal to noise ratio.
- A new efficient low-power algorithm to extract the respiration rate from the PPG signal. Developed algorithm is a power efficient alternative for using in wearable systems that has limited processing power and where sophisticated signal processing algorithms are not possible. It is based on detecting the amplitude changes in the PPG signal to estimate the respiration rate.
- The model of adaptive and situation aware self-aware health moni-

toring system to collect the data from different medical and environmental sensor and to make decisions. As the proposed system enables different functionalities and type of sensors that all could measure different parameters, there is a need for the system that receives all measured and pre-analysed signals and make decisions based on the situation. Decision mechanisms could help to decide in which situations and when to send critical information about the patient to the caregiver or parent. As a next step, architecture for the real-time system was designed and developed although not yet published. Still, initial results with real-time systems are promising.

Thesis organization

This thesis consists of 5 chapters and 5 appendices.

Chapter 1 gives an overview about the modular architecture of the portable health monitoring system. Background information gives on one hand an overview how this architectural solution could increase the system level compatibility. System prerequisites are defined and based on the prerequisites proposed solution of the modular system is described. System functionality and its extension possibilities in hardware and software level are discussed.

Chapter 2 starts with an overview of photoplethysmography and in which areas of health care it is used. Also the challenges of optical measurements are discussed. As one example an architecture of optical foot sensor for sleep research and sleep quality analysis is proposed. The focus is on newborns and children as the foot sensor could be one of the most comfortable ways to perform long term monitoring. In the second part of the chapter an architecture of smart photoplethysmographic sensor for pulse wave registration from arteries is proposed. As this solution is designed for adults it is one example using the same modular platform for different age groups and diseases.

Chapter 3 focuses on low complexity algorithm development for sleep quality estimation. Also background information to give an overview about sleep and sleep diseases is provided. As one of the most important components in sleep monitoring is respiration signal, a low power algorithm for respiration signal extraction from pulse wave is proposed. Also experiments together with similar methods are discussed.

Chapter 4 starts with the definition of fog and mist computing, and situation awareness for health monitoring. The architecture of self-aware health monitoring system is proposed. The initial architectural description starts with the off-line system and continues with the real-time system. Initial experiments were also discussed to show the feasibility of such systems.

Chapter 5 concludes the thesis and discusses possible directions for future research.

The appendices 1 to 5 present research papers that form the basis of this thesis.

Chapter 1

MODULAR ARCHITECTURE FOR PRE-SCREENING

The current trend in health care technologies is connected and personalized medicine. The future of medical device industry is to assist people in achieving healthier lifestyle, allow quick and remote diagnosis of possible disease without leaving the everyday environment. Most of health monitoring devices are developed for special purpose and do not provide any modularity to extend its functionality.

In this chapter we propose a design for a reliable modular system that supports research in various medical domains. The proposed modular system is the basis to provide measurement abilities for different diseases and for different patient groups. Those systems are mostly portable with limited processing power and energy capabilities. Combining recordings with other types of sensors, for example environment information, and exchanging information between those sensors leads us to a self aware health system that has capability to perform some level of autonomous decisions. Main results of this chapter have been reported in [55] and [56].

1.1 Background

Health care together with automotive, nuclear and aerospace belong to highly regulated industries. The health care sector can be divided into two main groups - health care equipment and services, and pharmaceuticals and biotechnology. Medical devices with their software belong to the health care equipment and services group. The 20th century was the time when the pace of medical advances quickened on all fronts [43]. New understanding of diseases brought new treatments and cures for many of these conditions. Together with other areas there were also breakthroughs in technology that brought us first medical devices. For example, the first pacemaker implant was installed in 1958. The first pacemaker failure occurred in 1972 that

highlighted urgent need for regulations applicable to medical devices. In 1976, the legislature passed medical device amendments to ensure safety and effectiveness of medical devices [46]. Medical devices are grouped into different categories based on their design complexity, use characteristics and potential of harm if misused.

Moving further from traditional to personal medicine, the biggest value would come from saving doctor's time by serving more patients and giving correct diagnosis with minimum amount of time. One option is to apply personalized medicine together with remote doctor visits and monitoring. As the technology evolves, there are many medical devices that could be brought out from the clinical environment to use for pre-screening purposes with remote connectivity. For long-term monitoring a wireless blood pressure monitor [41] together with wireless pulse oximeter [42] and wireless scale [100] could improve the general overview about patient's health condition. In some cases an Electrocardiography (ECG) monitoring with wireless ECG system from LifeSync could be used in hospital and outpatient settings [60]. The number of such wireless devices is increasing rapidly. Combining different similar devices could provide an early detection of possible diseases without the need to visit a doctor after a first sign of abnormal health condition.

During the forecast period of 2015-2020, the diagnostic and and therapeutic market is projected to grow remarkably at 21.3% to generate revenue of 41.3 bn US dollars by 2020 [81]. The diagnostic devices market is propelled by Polysomnography (PSG) devices, particularly clinical PSG devices. The usage of Ambulatory PSG devices is expected to increase in the next few years due to patient preference to be tested at home for convenience reasons, patient's inclination to skip the unfamiliar environment of sleep labs, and cost-effectiveness of these devices. The global demand for screening devices such as respiratory polygraphs, two channel screening devices, single channel screening devices, and actigraphy systems is also on the rise due to their low costs. These devices serve as cost-effective and convenient options, as compared to PSG devices, especially for the low-economic class patient pool.

Even more development is happening on the screening device market. Stardust II Sleep Recorder device is capable of measuring respiratory airflow, pulse, Capillary Oxygen Saturation (SpO2), chest effort and body position without wireless transmission [77]. Its main purpose is to diagnose Obstructive Sleep Apnea (OSA). Luna bed cover helps to track the sleep quality by tracking sleep phases, heart rate and breathing rate [64]. There are also sleep mats available which are measuring breathing and waking movements and mats which are put 8-11 cm below foam or sprung mattresses.

As babies and children are one of the main target groups, there are

several real-time systems on the market for infant monitoring. Most of them have the functionality to measure heart rate, body temperature and motions [87] [86]. Some of them have additional body sensor which is attached to the baby's lower abdomen with micro-pore tape. Some of these are built for infants which use UWB technology [106] or have a possibility to have respiration and humidity level information [62]. Placing a sensor on the feet is considered one of the most comfortable places for infants. It allows a quick replacement of the sensor and has a reliable signal quality [86].

As the most care is needed for babies and elderly people, they are the biggest target groups who may need continuous care and help. One aspect of this care is to perform different kind of health care analyses for better diagnosis. One possible solution for this is depicted on Figure 1.1 that describes the architecture of health monitoring solution. As it varies highly which kind of disease is being diagnosed, it may require some environmental sensors or monitoring device with minor changes in the functionality. By collecting measurements during longer period of time it is possible to detect also an abnormal behavior from everyday patterns. It helps to detect and predict severe health condition changes before they appear as a result of wrong life-style.

Technology development in recent years have made possible to perform such monitoring sessions in addition to hospitals also at home or even while continuing with your daily routines. As some type of monitoring activities may last several days continuously the system should have some level of autonomy to send results in automated way to the caregiver or family members as shown on Figure 1.1. The patient may not even be aware of continuous monitoring and data transmission process. In this way it is possible to increase the health care system efficiency.

That leads us to the main topics of this thesis. All mentioned measurement types are connected to each other to fulfill one of the main objectives of this thesis - design a reliable modular system to perform better diagnosis for different age groups. By that we mean that the proposed modular system is the basis to provide measurement abilities for different diseases and for different patient groups. Those systems are mostly portable with limited processing power and energy capabilities. Combining recordings with other types of sensors, for example environment information, and exchanging information between those sensors leads us to a self aware health system that has capability to perform some level of autonomous decisions.

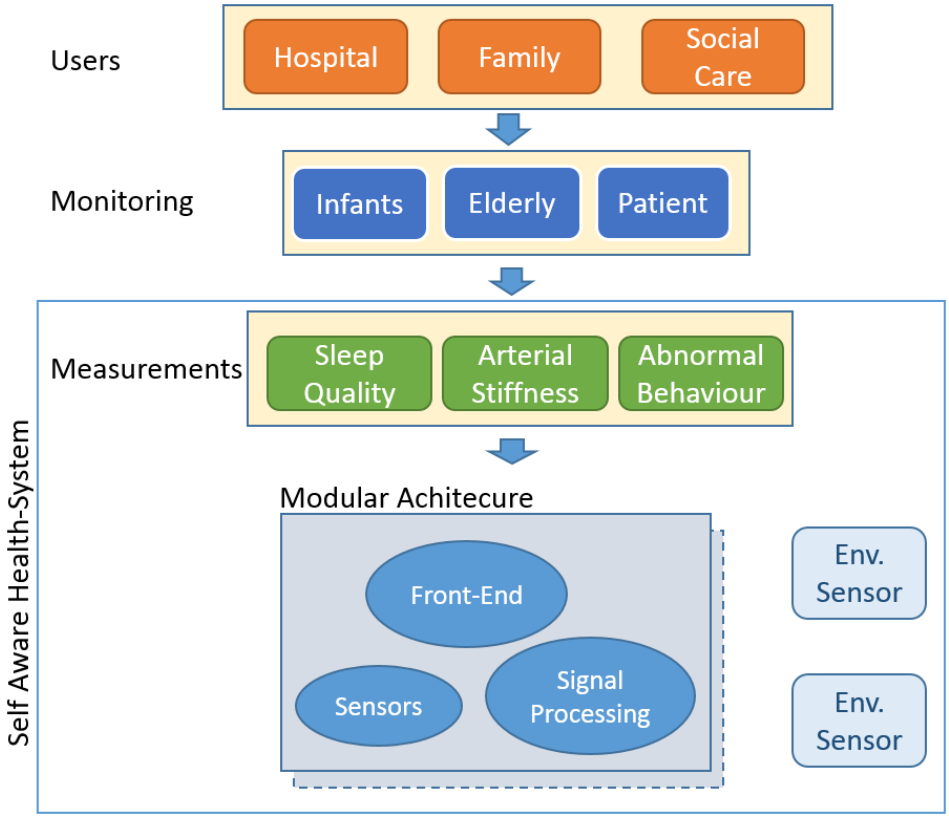

Figure 1.1: Health care solution description

1.2 Hardware

The goal of this chapter is to provide an overview about the developed modular architecture for health monitoring for different age groups and diseases. Developed prototype is used thorough the thesis to perform different type of measurements. Depending on the age and diseases, they all require different functionalities of the monitoring device. For example, infant monitoring devices need to be lightweight and have small dimensions. Elderly people monitoring may need another type of sensors and in some cases also an alarm button or automatic alarm system. There are also many diseases that may need only short time monitoring. For short term monitoring it is not important to have a long battery life or real-time connection. The most critical part is to have a good quality sensor to perform measurements fast and easily. All those situations introduce new requirements to the monitoring device.

1.2.1 System Prerequisites

According to the Food and Drug Administration (FDA) a device is a medical device when it is intended to use in the diagnosis of disease or other conditions, or in the cure, mitigation, treatment, or prevention of disease, in man or other animals, or intended to affect the structure or any function of the body of man or other animals, and which does not achieve its primary intended purposes through chemical action within or on the body of man or other animals and which is not dependent upon being metabolized for the achievement of any of its primary intended purposes ([23]). By that it means that all health-care devices have to meet specific regulatory requirements. For clinical trials the monitoring device should meet the several clinical and technical requirements. Technical requirements are chosen based on the normal monitoring process so that it does not need much additional effort to perform the measurement. They are divided into several sections, starting from the most important ones.

Modularity

To cope with the requirements started earlier, system architecture must be modular. For extended modularity the system should be divided into modular groups where each group represents one particular task. There should be one group to perform power management and processing. Another group should perform an analog to digital conversion to support different kind of sensors. The third group is a sensor that is connected directly to the analog module. All these modular groups should be interchangeable and compatible with each other whichever module is currently connected. It needs to have a pre-defined physical communication standard and communication protocol between those boards. As it should be possible to connect either optical sensor, electrodes or sensor that has its own processor included, the interface between the analog front-end and sensor should include digital, analog and supply connectors.

Small Dimensions

The system should be usable for monitoring all age groups - from infants up to elderly people. Even when the system is being used for adults the suitable dimensions for babies should be taken into account. Based on the studies, one of the most comfortable place for long-term monitoring on infants is the foot [86]. This method is widely used also in hospitals where all infants have their pulse oximeters attached to the foot. Based on our measurements and research, the length of the infant foot is ca 8 cm and the width starts from 3.5 cm. In case the monitoring device is placed on top or under the foot, dimensions may not exceed those given values. The

height of the system is not so critical and depends highly on the height of the components, battery and thickness of the cover.

Processing Power

Processing unit should be reasonably chosen taking into account the signal type, sampling rate and what kind of data processing algorithms will be executed on that unit. Based on our needs, we are working mostly with optical signals, motion and temperature data. As the analog front-end takes care of receiving an analog signal from sensor and converting it into discrete signal, it loads off some required processing power from the Microcontroller Unit (MCU). As the chosen analog front-end supports sampling rate up to 5 kHz with 24-bit signal in parallel from two channels, MCU should be able to handle this amount of real-time processing.

To filter out noise or unneeded parts of the signal, chosen MCU unit should be capable of signal pre-processing. For example, to create an Finite Impulse Response filter (FIR) filter, an hardware multiplication should be used that is available for example in Texas Instruments MSP430 micro-controllers. To support up to 5 kHz sampling rate with 24-bit signals in parallel from two channels, there is a need for at least 512 byte of Random Access Memory (RAM) for each channel to store the signal into circular buffer. One should also take into account that one channel gives out four signals in parallel.

In some cases there is be a need to apply Fast Fourier Transform (FFT) calculations to determine a dominant frequency. No floating point precision is needed and sampling rate is up to 250 Hz. An average MSP430 at 25 MHz could handle it. For example 256 point FFT would take 4.7 ms according to performance tests [20]. If more computational power is needed, DSP or ARM based micro-controllers should be used. In our modular system it requires to replace signal processing module with more powerful one.

Power Consumption

Power consumption of the whole system depends highly on the used MCU, analog front-end, number of attached optical sensors, amount of signal processing and frequency of wireless communication. For long term monitoring, the system should have an autonomous power at least one full day. For example, the average time infants sleeps per day is ca 18 hours. With some reserved capacity, we could say that at least 24 hours of autonomous power without charging would be required.

1.2.2 System Architecture

To perform monitoring of different diseases on wide range of ages, we have defined system prerequisites that has to be fulfilled with our proposed system architecture. Figure 1.2 describes the proposed hardware design. The hardware architecture is divided into three parts - digital board, analog front-end and sensors. Analog front-end takes care of driving of the optical sensors. In the analog front-end Digital-Analog Converter (DAC) controls the intensity and timing of each LED as they need to be switched on and off with the sampling rate of 1kHz. LED driver amplifies the current that is needed to illuminate the LED. Photo-detector receives the light that is not absorbed and current changes are converted into the voltage changes with the trans-impedance amplifier. Acquired signal is filtered with several filters to eliminate high frequency noise and 50/60 Hz line interference and converted into digital form. Taking into account that prototype should consist as less similar hardware on different hardware modules because of the limited size and weight, most of these filters have to be applied in the software. 22-bit Sigma-delta analogue-digital converter (ADC) converts analogue value into digital form. The benefit of using sigma-delta ADC is higher stability and higher resolution at low cost.

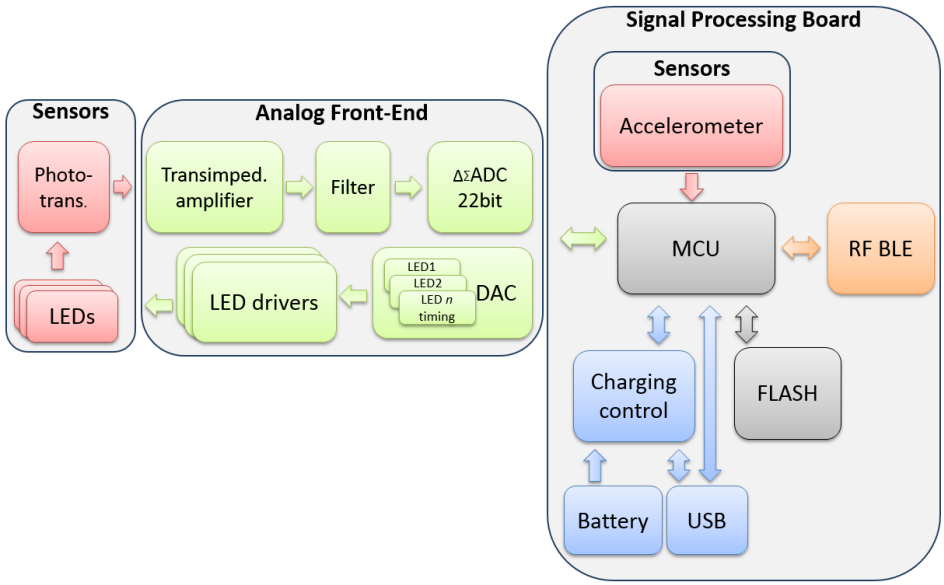

Figure 1.2: Functional block diagram of the proposed modular system [55]

The current version of the proposed system has dimensions 33.4 x 27.4 mm. These dimensions are dictated by the used 400 mAh Li-ion battery to power the system. It is required that all other boards should have smaller dimensions. Developed dual analogue front-end has dimensions 29 x 19.5

mm. With these dimensions the system is suitable for using from newborns up to adults.

Power management is managed by the charging system. Estimated battery lifetime is around 48 hours of continuous monitoring which covers 2-3 full sleep cycles of newborn. Device is recharged over the USB connection. Li-ion battery charging takes around 2 hours until fully charged. It is approximately the same time a newborn stays awake between the sleep cycles.

Signal processing board takes care of the data processing and temporary data storage. In addition to that it has power management components to power up a whole system and provide communication with external systems. There is also a wireless module for wireless communication. This set of components makes possible to change the processing unit of the system with another one in case there is a need for more processing power, more efficient processing unit, larger on-board memory or another type of wireless communication. Wireless communication is hidden into higher software abstraction layer to make it independent from the rest of the system components. As there are certain Application Programming Interface (API) commands used for inter-system communication, it does not affect other parts of the system if processing unit is replaced with another type of unit.

Signal processing board, that is the system core, consists of processing unit and storage. MCU is chosen based on the required computational power in order to perform filtering and features extraction with compression. Processed data is stored on FLASH/uSD card in case wireless connection is not available.

Radio module connects over Bluetooth Low Energy (BLE) protocol. Compared to the Bluetooth, it provides less throughput but smaller latency and better power handling that makes it perfect solution for the wireless portable devices.

The type of supported sensors is highly dependent on the type of analogue front-end used. It is not limited which kind of sensors can be driven. We have implemented two types of sensors. One type is a dual optical sensor for infants that includes opto-pairs, temperature and humidity sensor. Another is an optical sensor array that includes on-board processing unit and drivers to drive optical sensors. Detailed description of these sensors can be found in Chapter 2.2.

Current configuration of proposed modular system, depicted in Figure 1.3, is composed of:

1. Flexible board with optical and temperature sensors.
2. Analog board which provides an analog to digital conversion of optical signals.
3. Processing board which provides processing features for the monitor-

ing system and wireless transmission.

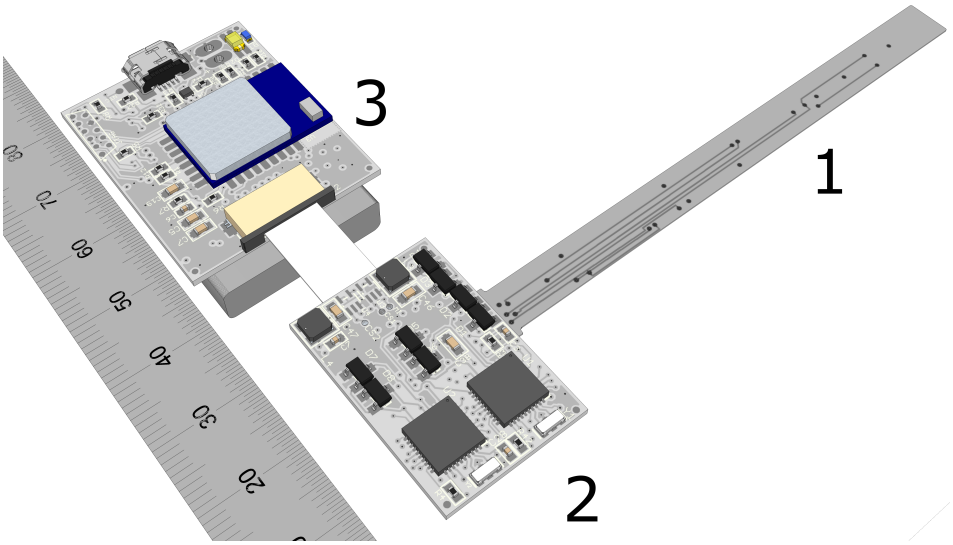

Figure 1.3: Proposed modular monitoring system [56]

Flexible board with optical sensors is attached as an example how similar sensors could be attached. There is also flexible connector between the digital processing and analogue board.

1.2.3 Signal Processing Board

The purpose of the signal processing board is to handle communication between all system components and to provide high level interface for the end user for system management. The choice of hardware was done based on the previously specified requirements. Figure 1.4 depicts the architecture of processing board and communication interfaces in between each component.

Red color marks power related components. Micro-USB connector is used for battery charging and data transfer. Battery charger BQ24072 from Texas Instruments (TI) chosen to support Li-Ion and Li-Polymer batteries and configured to support up to 500 mA charging current from the USB port. All components on the processing board get their power through Low-Dropout Linear Voltage Regulator (LDO) TPS73633 from TI. It can power up to 400mA system load with the system operating voltage of 3.3V with low noise level 30 μVrms.

For analog board, a separate LDO TPS7A4901 from TI in order to achieve very low noise level 16 μV_{RMS}. Separate power unit for analog board helps to decrease the overall noise level that the digital board may

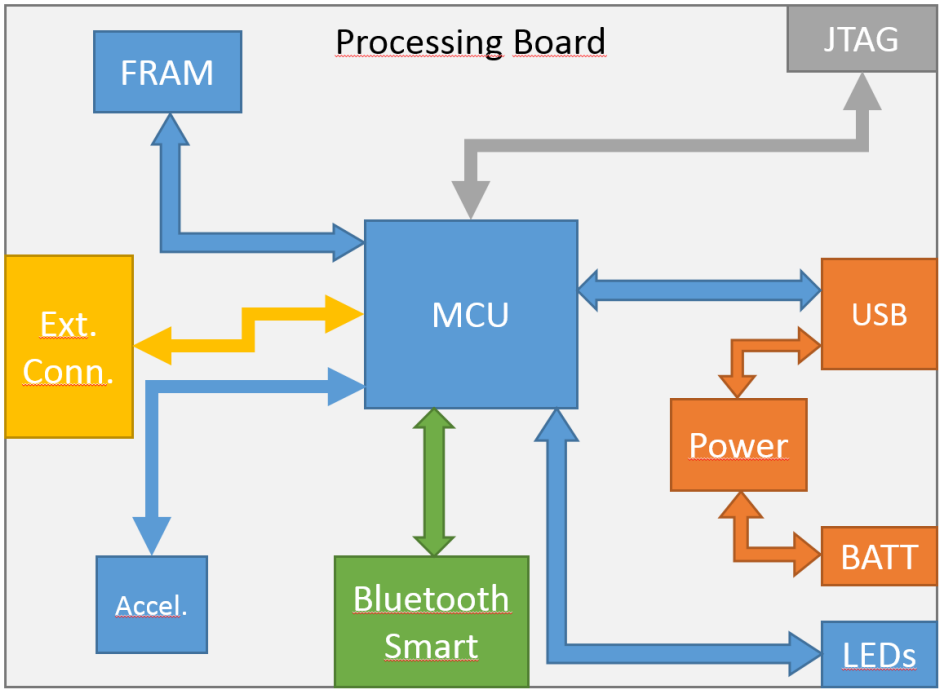

Figure 1.4: Block-level description of digital processing board

generate. All power related component have built in reverse current, short-circuit and thermal protection functionality that shuts down the system in case of accidents and malfunction.

Accelerometer

As the purpose of the system is to be a miniature and portable monitoring device, there is a need for activity and movement detection to notify the user about events or give to the system additional autonomy. It was decided to add on-board accelerometer that has low power requirements and has digital output to decrease the overall power consumption. At the time of the system design, the smallest size accelerometer with very low power requirements was provided by Bosch Sensortec. BMA280 has 2x2 mm package size, and large number of interrupts that can be used for automatic system sleep and wake-up.

Micro-Controller Unit

A MCU is the main processing unit for the whole system. As it is used in portable device that is designed to perform also long-term monitoring

sessions, MCU has to meet to the following requirements:

- 16-bit or 32-bit architecture
- Enough RAM to perform analysis of four 32-bit signals simultaneously
- Low power consumption in low power mode
- small footprint to minimize system physical dimensions

There are large number of MCUs available from different manufacturers. Some of them are designed for low-power applications, others for signal processing. At the time of designing, the author was the most familiar with devices from Texas Instruments and especially in low-power microcontrollers. Therefore the MCU with the highest speed and largest flash and RAM, that still has low-power capabilities, was chosen. MSP430F5528 has 128 KB of flash and 8KB of RAM. The example of flash and RAM allocation is described in [56]. Depending on the type of analogue front-end and sensors, there may be a need for more RAM or faster processor. For the first prototyping and proof of concept design, chosen micro-controller has fulfilled all the needs.

If there is a shortage of RAM for pre-processed signal, there are also two on-board Ferroelectric Random Access Memory (FRAM) memory modules FM24V10 [14]. Altogether they can store up to 256 kB of temporary data. Compared to FLASH-based memory, FRAM type memory provides ultra-fast, up to 100 times faster data throughput, and consumes 3 times less power.

1.2.4 Analog Front-End

The type of analogue front-end (AFE) depends on the application. Current application is designed for optical pulse wave detection. Texas Instruments has developed a special purpose AFE for optical photoplethysmographic sensors that includes built-in ADC, operational amplifier, trans-impedance amplifier and digital configuration possibilities. Chosen AFE4490 component has 22-bit resolution and sample rate up to 5 kilo-samples per second. High integration density into single chip decreases the noise to very low level. All sampling timings are fully configurable digitally through the set of registers. There is also a built-in sleep mode that decreases the power consumption of the chip to the marginal level. For better usability there is also an integrated optical test procedure to detect all short-circuits and open connections on the optical sensor.

Analogue front-end connects directly to the processing board. As there could be any kind of modifications on the analog board, there are SPI and I^2C communication possibilities in parallel to support the most common

connection interfaces. In addition, analogue front-end has ability to use several GPIO pins from the processing unit as depicted in Figure 1.5.

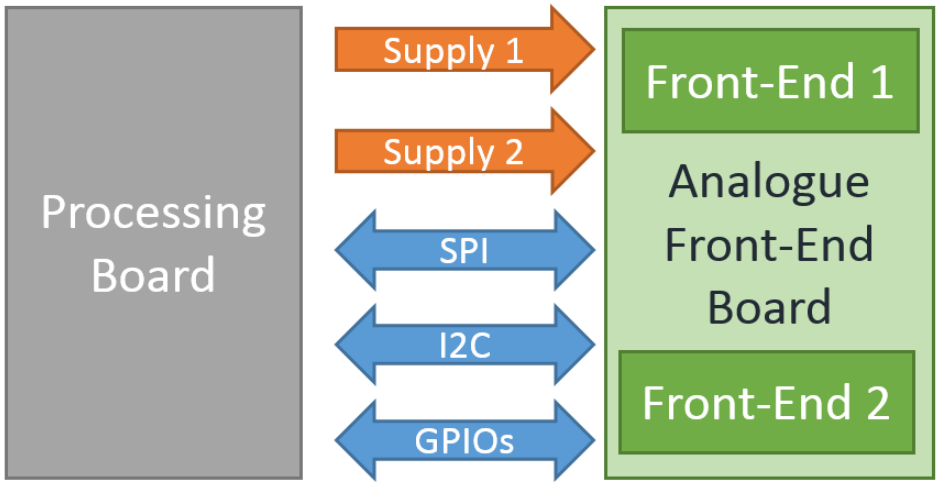

Figure 1.5: Electrical connections between processing unit and analogue front-end

The maximum speed of SPI and I^2C lines depend on the used processing unit. The current version of the analog front-end board includes two identical analogue front-end units in one board to increase the reliability of optical signal.

Figure 1.6 depicts one possible communication solution between the AFE and sensor. In this case, the sensor is an optical sensor that may have additional on-board MCU and additional sensors for temperature and humidity measurements.

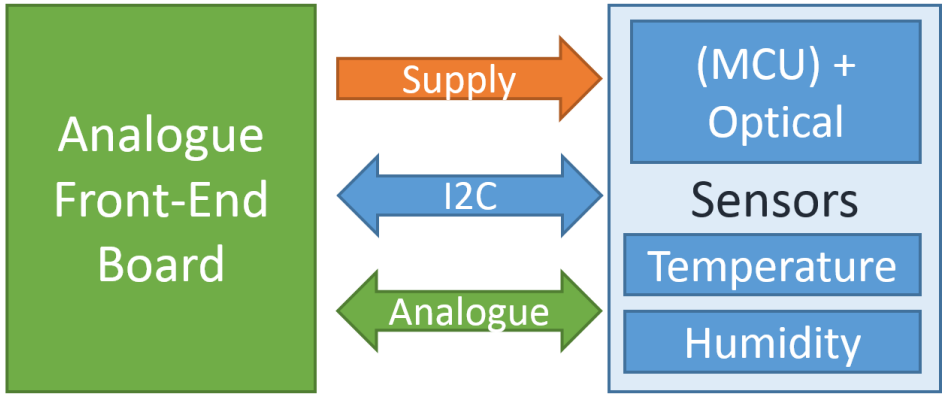

Figure 1.6: Electrical connections between analogue front-end and sensor

For data communication between the AFE and sensor, I^2C up to 400 kHz can be used. The advantage over SPI is less amount of wires and possibility

to connect multiple sensor to the same signal line. On the other hand, the drawback is slower communication speed that may not be suitable for very high speed data transfer or strict timing requirements.

1.3 Software

In this section software architecture is described. The system management commands and communication interfaces are presented. It is also described how system wide functionality tests were performed.

1.3.1 Software Architecture

System software is written in embedded C. To meet the low power requirements, the system stays always in low power mode unless there is something to process. In case of internal or external interrupt from USB, sensors or internal clock, the system wakes up and continues from the place where it stopped and goes back to sleep.

Data processing is solved by using flags. To start or stop continuous task processing, it is needed to send a command to the system that enables or disable that particular flag. If the flag is enabled, system is working autonomously until next command is received that disables the flag. It is possible to enable different types of tasks simultaneously. For example, sending continuous temperature, acceleration data and perform pulse wave analysis do not disturb each other and each one of them can be independently enabled or disabled.

1.3.2 Command Processing Flow

There is a certain packet structure how the system is communicating with external systems and user interface. Through the USB interface it is possible to control the whole system functionality. Developed packet structure is flexible and supports new devices and data types without modifying the existing structure. Table 1.1 describes the packet structure.

Table 1.1: Packet structure

Abbrev.	**Description**	**Length**
HDR	Packet header	1 byte
DEV	Device type	1 byte
CMD	Command	1 byte
FUNC	Function	1 byte
DATA	Data value	0..59 bytes
FOOT	Packet footer	1 byte

To recognize the command, each packet has to start with a header and to end with a footer. All packet structure elements, except DATA have length of 1 byte. The second byte defines device type that can be on-board sensor, module or external sensor or board that is connected to the digital processing board or AFE. Defining a device makes it easy to talk only to a specific device. Command field defines what kind of communication is expected from that specific device. It could be configuration, measurement, diagnostic or some other type. Function defines what kind of data that device should give us or is previously configured to perform. Data is a real value that is sent to the device or from the device. In some specific cases we may skip sending data value if there is no need to send any value. Data value can be up to 59 bytes as the whole packet can be up to 64 bytes which is also the limit of USB buffer of the used micro-controller.

Device type definition makes it easier to configure or get data from a specific device. However it is possible to get measurements simultaneously from more than one device. Table 1.2 lists device types that are currently supported.

Table 1.2: Device types

Device ID	**Definition**	**Description**
0x01	DEV_MCU	MCU on the main board
0x02	DEV_ACCEL	On-board accelerometer
0x04	DEV_AFE1	Optical analogue front-end 1
0x05	DEV_AFE2	Optical analogue front-end 2
0x06	DEV_TEP	Ext. temperature sensor
0x07	DEV_MCU2	MCU on the smart optical sensor
0x08	DEV_BLE	On-board bluetooth smart

There is also a list of supported commands in Table 1.3 that are used for system management. The first one *CMD_NO_COMMAND* means that if there is some data sent to of from the device, it should not be processed as a command.

The rest of the commands are actual commands to configure the system. The last one *CMD_FW_UPGRADE* makes possible to perform automatic system firmware upgrade without a need for specific programmer. System image file has to be pre-compiled and loaded into the device that is done automatically after initiating firmware upgrade.

1.3.3 Wireless Communication

If health monitoring is performed over long period of time and there is a need for real-time feedback about possible threats, it is required to have a wireless communication between the monitoring device and control device.

Table 1.3: Command list

Command ID	Definition	Description
0x00	CMD_NO_COMMAND	No command
0x01	CMD_START	Start reading data
0x02	CMD_STOP	Stop reading data
0x03	CMD_DIAGNOSTIC	Perform system diagnostic
0x04	CMD_R_CONF	Read register
0x05	CMD_W_CONF	Write register
0x06	CMD_READ_DEV_ID	Send device ID
0x07	CMD_CONF_LED	Configure LEDs
0x08	CMD_CONF_PD	Configure photodiode
0x09	CMD_POWER	Configure power settings
0x0A	CMD_FW_UPGRADE	Firmware upgrade

Wireless interface gives patient more freedom him or herself and reduces the complexity of handling wires. As smart-phones have became very reliable and comfortable devices, also for health and lifestyle tracking, they are usually the best option for control devices. Almost all smart-phones have built in Bluetooth, Bluetooth Low Energy (BLE) and WIFI connectivity. Among those Bluetooth Low Energy, also called as Bluetooth Smart, has the lowest power consumption and is well suitable for personal area networks like health and activity monitoring.

Bluetooth Smart is an interface to communicate with the device over radio node using BLE communication protocol. Its throughput is limited to around 60 kbps in case of unacknowledged packets. In a typical environment the fastest reliable throughput with acknowledged packets, according to Bluegiga Technologies tests, is 8-10 kbps [7].

Transmitting raw Photoplethysmography (PPG) signal with sampling rate of 250 Hz and 22-bit of data, we need throughput of 5,9 kbps. 14-bit digital accelerator with the sampling rate of 100 Hz needs 1,6 kbps. In total there is a need for throughput of up to 7,5 kbps.

Current version of Bluetooth Smart is based on Bluetooth version 4.1. As it has limited data throughput and in case of higher sampling rate it may become a limiting factor, we use Bluetooth Smart module only for sending processed data and receiving commands to manage the device. Bluetooth Smart 4.2 has almost triple times higher throughput that increases further possibilities for sending raw data. First chips that support the new version, will be available during year 2016.

Bluetooth Smart communication is based on Generic Attribute (GATT) profiles. Services that are advertised under each according profile by our proposed monitoring system are listed in the Table 1.4.

First column describes name of the service. Second column defines

Table 1.4: Bluetooth Smart profiles [56]

Service name	Service type	Update interval	Value descriptor
Device Information	global	N/A	uint16
Health Thermometer	global	1 Hz	uint16
Heart Rate	global	1 Hz	uint8/uint16
Respiration Rate	local	1 Hz	uint8
Blood Oxygen Level	local	1 Hz	uint8
Body Position	local	1 Hz	uint8
Activity	local	1 Hz	uint8
Alert Status	local	1 Hz	uint8

whether the service is globally defined by the Bluetooth Smart specification or defined by us. The biggest difference between the global and local service is that global services are defined by specifications and with known Universally Unique Identifiers (UUID) but local services can be defined according to specific need and with own-generated 128-bit UUID. Supporting globally defined services adds better integration with Bluetooth Health Device Profile [8]. Third column defines the frequency of each service update interval. If particular service does not support notification based automatic update it is marked with N/A. Last column defines number format of the service descriptor value. Type "uint" means unsigned integer and number after uint is the number of bits that represents the length of data. Heart Rate service supports two type of lengths depending the value that is currently transmitted. Because of the limited throughput and depending on the sampling rate, there is currently no support for raw data transfer. However, for development purposes, this data is still accessible over the Universal Serial Bus (USB) interface.

1.3.4 System functionality tests

System functionality can be verified with functionality tests. In this chapter we describe which hardware was developed for testing and which functions are covered with tests.

Hardware

To perform hardware and software debugging a special testbed was developed. To program the system a processing board is fastened between the middle and bottom board as depicted in Figure 1.7. Top board has connectors for MCU and BLE module programmer.

Power and all programming signals are connected through the pogo-pins to the test-board. It is possible to connect an AFE module and USB cable

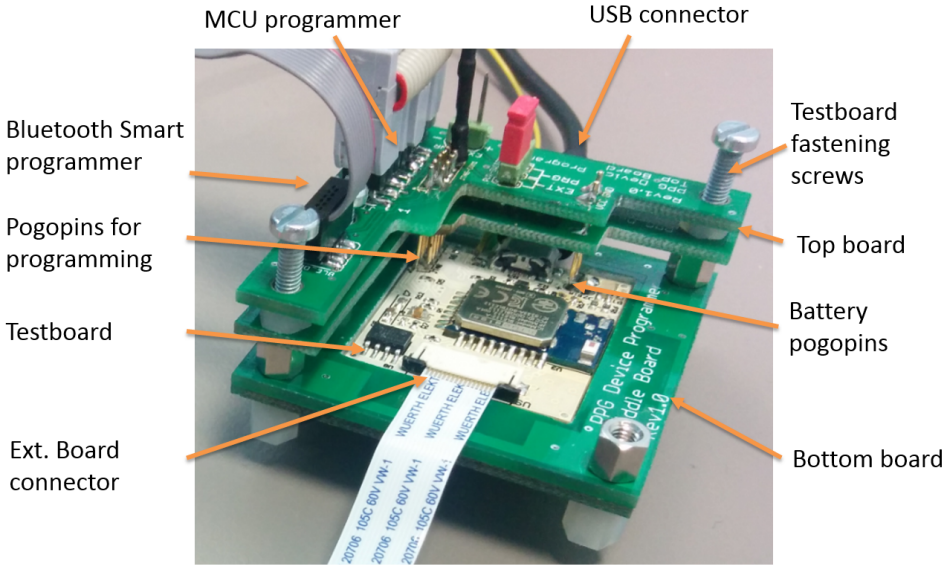

Figure 1.7: Testbed for debugging

while test-board is fastened to the test-bed.

Software

As the whole system consists of many components, there is a need for system wide tests to ensure the reliability. It is possible to ask for system revision information, get battery level, charging information and perform full system diagnostic. The system diagnostic command gives an output of all components. Figure 1.8 describes the system test functionalities. Upper part of the figure up to the Bluetooth Smart shows the check for system core functionalities. Middle part shows whether the AFE is functional. Below part of the figure shows the results how the currently connected sensor is working and are there any short-circuits or disconnections.

System test starts with visual Light-Emitting Diode (LED) blinking where all three LEDs blink once. Battery level information is given in hex format as a value in millivolts and the percentage. All tests output either a PASS for successful test or FAIL for failed test. All system tests will take few hundred milliseconds to complete.

1.4 Experimental results

Results can be categorized into two different groups. First group describes, how good is the user experience in terms of usability and reliability for all age groups. Second groups describes, how the hardware dimensioning

```
LED1 (blue):  ON ->            OFF
LED2 (red):   ON ->            OFF
LED3 (green): ON ->            OFF
USB:                           <FAIL/PASS>
Battery level:                 0xABCD mV (0xAB %)
Battery level:                 <FAIL/PASS>
Accelerometer:                 <FAIL/PASS>
Bluetooth Smart:               <FAIL/PASS>

AFE1:                          <FAIL/PASS>
AFE2:                          <FAIL/PASS>

Temperature:                   <FAIL/PASS>
AFE1: Photo-diode alarm:       <FAIL/PASS>
AFE1: LED alarm:               <FAIL/PASS>
AFE1: LED1 open:               <FAIL/PASS>
AFE1: LED2 open:               <FAIL/PASS>
AFE1: LED short:               <FAIL/PASS>
AFE1: OUTP shorted to ground:  <FAIL/PASS>
AFE1: OUTN shorted to ground:  <FAIL/PASS>
AFE1: Photo-diode open:        <FAIL/PASS>
AFE1: Photo-diode short:       <FAIL/PASS>
AFE1: INN pin to ground:       <FAIL/PASS>
AFE1: INP pin to ground:       <FAIL/PASS>
AFE1: INN pin to LED:          <FAIL/PASS>
AFE1: INP pin to LED:          <FAIL/PASS>

AFE2: (identical to the AFE1 output)
```

Figure 1.8: System functionality diagnostic

meets the real world needs. All experiments were performed with connected optical sensor that is introduced in the next chapter.

Initial results with optical foot sensor cover tests with infants from 3 months up to children 6 years old, and adults. Results were promising as the dimension and weight of the device was appropriate and did not disturb normal movements of the foot. There were no problems during the sleep, however it was not an easy task to align the sensors correctly to the foot. Wrong placement of the sensors is causing increased amount of corrupted signal that needs to be excluded from the further analysis.

Another approach was to test the reliability of the device as there are

several physical connections in-between different hardware modules. The weakest part was an optical foot sensor itself that stopped working after several sensor bending movements on the foot. Disconnection was caused by the micro-crack in the copper that caused signal loss between the LED driver and LED. This is considered as a design issue that can be fixed with slight modifications in the design, but it is very time consuming because of the long manufacturing process. As the system includes built in functionality for self test then each hardware failure is alarmed immediately. All data is transferred via wireless connection that makes it easy to perform data collection remotely and get always the latest status of the system.

Another type of tests was performed using smart photoplethysmographic sensor. During the test PPG signal was measured. Signal quality was good without system generated artifacts or noise. As measurements were performed on the wrist, there were no issues with the hardware. Acquired data was transferred via micro-USB cable to the PC that did not introduce any comfortability issues while the device was on the wrist.

1.4.1 Memory footprint

Including all functionality the measurement system requires 1,5 kB of RAM and 22,8 kB of program memory. The biggest size of the program memory is occupied by USB, accelerometer and functionality that analyses the digitized optical signal. Algorithms that are handling accelerometer and optical signals consume also most of the used RAM.

1.4.2 Power consumption profile

In the "operating" mode, the total system power budget is 71 mW. The measured average MCU active duty-cycle is 40% yielding to an average power consumption of 28,4 mW that meets well the requirement #12 that is introduced in [56]. It represents about 50 hours of autonomy for a 400-mAh battery. For data storage we use an external FRAM memory modules that support over 100 times faster data throughput and consume 3 times less power compared to FLASH based modules. Figure 1.9 illustrates power consumption breakdown of the measuring device.

The biggest amount of power is consumed by the MCU that has several tasks. Embedded algorithms that are activated by external interrupts consume most of the MCU active mode. PPG signal sampling with the rate of 250 Hz adds a new sample in every 4 ms. If there are at least 5 continuous unprocessed samples a pulse-wave detection algorithm is executed. Acceleration information is sent only if there is a movement over the preset threshold. The remaining, 60 % of the time, MCU is idling that leaves room for additional processing algorithms.

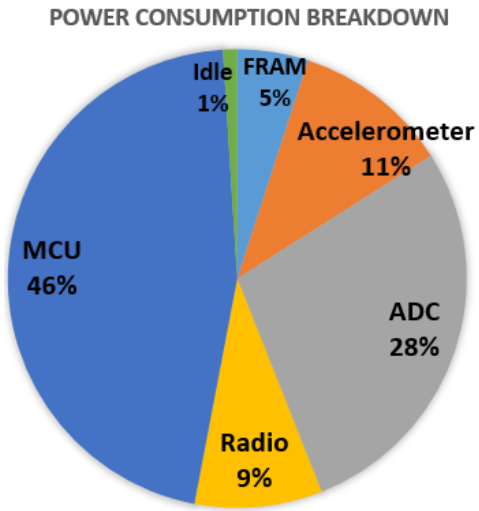

Figure 1.9: Power consumption of the measuring device [55]

1.5 Chapter summary

As the technology evolves, traditional medicine is replaced more and more with personalized medicine. There are many medical devices that could be brought out from clinical environment to use for pre-screening purposes with remote connectivity. There are wide range if diseases that could be monitored remotely. Our proposed modular architecture together with self-aware system, that is discussed in the next chapters, would suit those needs to monitor different age groups and diseases.

Currently there are no good solutions on the market that would allow to perform health monitoring on wide range of ages and for different diseases. As it requires another level of modularity, there are additional requirements introduced for the health monitoring devices. Those requirements and the proposed architecture were discussed and presented in this chapter.

If the system hardware has been designed to be modular, then software must support it on the same way. For this purpose the software architecture was presented as well. As the system hardware includes wide range of sensors and modules, we have also developed system functionality tests to perform quick hardware debugging.

As any system has to be tested in real life situations, we presented experimental results. It gives an summarized overview how the designed system is able to perform its tasks with different sensors.

Chapter 2

Photoplethysmographic Sensors with Increased Reliability

The modular system that was developed in Chapter 1 can be used on different age groups for short and long-term monitoring. In this chapter we propose two new types of optical sensor designs. First design is focusing on sleep quality analysis with increased optical signal quality in longer period of time. The purpose of the second sensor design is to perform short time measurements and get the pulse wave with the best signal-noise ratio in different penetration depths. Compared to the conventional pulse oximeters we have increased the number of optical elements to increase the reliability of the acquired signal. Main results of this chapter have been reported in [54].

2.1 Background

The history of medical sensors goes back to the 19th century when first bio-monitoring electrodes were developed. In 1838 Carlo Matteucci, professor of physics the University of Pisa, showed that an electric current accompanies each heartbeat. In 1887 the first human electrocardiogram was published [17]. At that time also the first studies of electricity in muscles started. As the technology has evolved sensors have became smaller and more reliable. It is expected to have 3 billion wearable sensors by 2025 [40]. The biggest size belongs to chemical sensors, inertial measurement unit sensors and optical sensors. On the other hand, the greatest growth rate belongs to stretch and pressure sensors (Compound Annual Growth Rate (CAGR) 40%), chemical sensors (CAGR 32%) and optical sensors (CAGR 13%).

The first study with PPG was done in 1936 when two research groups (Molitor and Kniazuk of the Merck Institute of Therapeutic Research, New Jersey, and Hanzlik *et al* of Stanford University School of Medicine) de-

scribed similar instruments used to monitor the blood volume changes in the rabbit ear following venous occlusion and with administration of vasoactive drugs [2]. Molitor and Kniazuk also described recordings made with a reflection mode PPG system from human fingers. Hertzman and Dillon split the alternating current (AC) and direct current (DC) components with separate electronic amplifiers and monitored vasomotor activity [34]. Potential sources of error with the technique have been identified in [33], where it was emphasized that good contact with skin was needed, but without excessive pressure that would result in blanching. It was advised that movement of the measurement probe against the skin should be avoided. During recent decades there have been considerable improvements in the size, sensitivity, reliability and reproducibility of PPG probe design.

2.1.1 Principle of photoplethysmography

PPG is a simple and low-cost optical technique that can be used to detect blood volume changes in the micro-vascular bed of tissue. It is often used non-invasively to make measurements at the skin surface. The PPG waveform comprises a pulsatile AC physiological waveform attributed to cardiac synchronous changes in the blood volume with each heart beat, and is superimposed on a slowly varying DC baseline with various lower frequency components attributed to respiration, sympathetic nervous system activity and thermo-regulation [2]. Although the origins of the components of the PPG signal are not fully understood, it is generally accepted that they can provide valuable information about the cardiovascular system.

Light from a light source, e.g. LED, laser, halogen lamp, is emitted to the examined tissue, where it is scattered and absorbed. The transmitted or back-scattered light intensity changes from the tissue can be detected by using a photo-diode. This technique has been clinically widely used for example in pulse oximetry systems, where the blood oxygenation rate is calculated based on the simultaneous amplitude measurement of PPG signal on two or more wavelength bands [72]. However, the research and application areas of the PPG technique have been expanding during the recent years. The PPG signal registration and analysis has been used for heart and breathing rate measurement, heart rate variability analysis, pulse transit time, arterial stiffness and vasomotion estimation [2]. PPG sensors are designed mainly for the pulse wave registration from peripheral vascular beds, such as finger, ear lobe, forehead etc. Nevertheless, the pulse wave registration from the artery is needed in order to exclude the influence of the peripheral blood vessels (arterioles, capillaries) and to estimate the stiffness changes of the central arteries or certain segment of artery [28]. The PPG technology has been used in a wide range of commercially available medical devices for measuring oxygen saturation, blood pressure and

cardiac output, assessing autonomic function and also detecting peripheral vascular disease. The principle of PPG is in more detailed level described in [97].

Photoplethysmography measurement modes

PPG can be measured in two modes - transmission and reflectance mode. Figure 2.1 depicts two modes of PPG. In tramission mode, the light transmitted through the tissue is detected by a Photo-Diode (PD) opposite the LED source, while in reflectance mode, the PD detects light that is backscattered or reflected from tissue, bone or blood vessels.

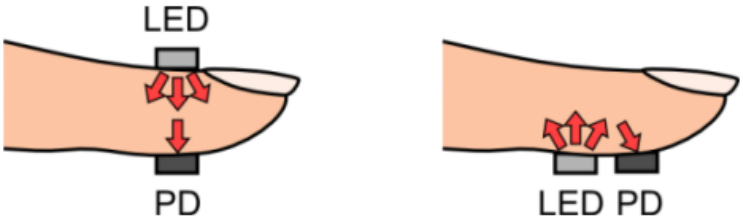

Figure 2.1: LED and PD placement for transmission- and reflectance-mode photoplethysmography (PPG) [97]

Transmission mode is usually capable of obtaining better signal quality compared to reflectance mode. The limitation is the measurement site. The fingertip and earlobe are the preferred monitoring positions but they have limited blood perfusion. In addition, the fingertip and earlobe are susceptible to environmental extremes, such as low ambient temperatures. On the other hand, reflection mode PPG is more affected by motion artifacts and pressure disturbances. Pressure disturbances can deform the arterial geometry by compression influencing the AC amplitude of the PPG signal.

2.1.2 Challenges in PPG measurement

There are several factors that affect the quality of PPG recordings. As described previously the location of the LED and PD, and measurement type affects the signal quality and robustness against motion artifacts [49]. Although PPG sensors are commonly worn on the fingers due to the high signal amplitude, most daily activities involve the use of the fingers. In recent years, different measurement sites for PPG sensors have been explored, including the ring finger, wrist, brachia, earlobe, external ear cartilage, and the superior auricular region. The perfusion of 52 anatomical sites in healthy subjects showed that the fingers, palm, face and ears offer much highest perfusion values compared with other measurement sites [99]. Earlobe provides the largest perfusion value.

The PPG sensor monitors changes in the light intensity via reflection from or transmission through the tissue. In reflectance-type PPG, the PPG signal waveform may be affected by the contact force between the sensor and the measurement side. The waveform of the obtained PPG signal differs depending on the PPG probe contact pressure. Several studies have shown that moderate pressure on the sensor can improve the PPG signal. Insufficient pressure results in inadequate contact and consequently low AC signal amplitude. However, PPG signal recording under excessive pressure conditions can also lead to low AC signal amplitude, as well as distorted waveforms caused by the occluded artery beyond the PPG probe.

PPG signal is sensitive to motion artifacts that is mainly random low-frequency interference. Several signal processing techniques can be applied, including those that use referencing from an acceleration signal or those that minimize the motion artifact with synthetic noise generation. However, attempts to minimize motion artifacts reported to date do not appear to correlate well with real-world noise sources. The moving average method is commonly used to reduce motion artifacts and works well for a limited artifact range. A Fourier analysis, model-based algorithms, adaptive filters like least mean square adaptive algorithm, Kalman filter [53], timer frequency methods, wavelet transformation [52], principle component analysis and several other signal processing techniques have been applied to reduce artifacts. Although it is possible to recover distorted signal and remove most of the noise, there is a need for better accuracy and reproducibility of real environments to eliminate motion artifacts.

2.2 Overview

The AC component in the PPG signal is synchronous with heart cycle and it is related to the heart generated pulse wave [2]. The pulse waveform carries important clinical information about the arterial system, including the micro-circulation of the skin. Characterization and analysis of pulse wave is well described in [2]. The detection of the PPG signal from different tissue layers may give a better understanding of the changes in the arterial system [94]. Techniques and applications to obtain the information from deeper tissue layers, such as blood flow monitoring in the tibial anterior muscle [105] [90], foetal oxygen saturation monitoring [107], estimation of pulse wave velocity in larger arteries [63] have been developed.

The light penetration volume-depth in skin depends on the selection of the wavelength [3]. Absorption of the light in the visible and near infrared wavelengths depends mainly on chromophores such as water, hemoglobin, and melanin. There is an "optical window", where the light is less absorbed by tissue. Therefore, red and near infrared light can penetrate deeper layers

of tissue than shorter (green, blue) or longer (infrared) wavelengths and the absorption of blood is more prevalent. In addition to the absorption, tissue is a highly scattering medium, where the light behaves diffusely. Photons are scattered from cell membranes and organelles. Generally, in shorter wavelengths the light is more scattered than in longer wavelengths. Due to the scattering and absorption properties of the tissue there is possibility to obtain the PPG signal from different tissue layers, which is based on the combination of wavelength and distance between the LED and PD [61]. In addition, earlier studies, using extremely short light pulses and time-of-flight analysis, have reported that the distance photons travel in tissue is approximately 4-6 times the distance between the light source and PD [11]. Generally, in case of short distance between the LED and photo-diode, and short wavelength (green, blue), the penetration volume-depth is small. On the other hand in case of long distance between the LED and photo-diode, and longer wavelength (near infrared), the penetration volume-depth is larger.

As babies and children are the most affected by the sleep problems and SpO2 level is one of the most frequently used measurement, different studies have been done measuring the SpO2 level. For that purpose reflectance pulse oximeter based on Near Infra-red Spectroscopy (NIRS) technique was used which is more comfortable in long term monitoring [80]. Prototypes with reflectance sensors embedded in soft foam and fabric materials give an opportunity to integrate them into snuggle and mattresses where baby lays for most of the time. Drawback of this solution is that it is very sensitive to the movements and requires certain body positions that may give many false alarms. Pulse oximetry and accelerometer has also been integrated into the infant shoe [86]. Accelerometer is used as an actimetry, position measurement of infant and to reduce the oximetry motion artifact. On the other side, this data was not used to perform sleep quality analysis and extract the respiration rate from the PPG signal.

Comparing the accuracy of oximeters by different manufactures some claim confidence limits $\pm 2\%$ or $\pm 4\%$ for readings above 70% [88]. Therefore greater likelihood of false alarms is caused by a false low reading or no reading at all. The studies of neonates and children found that 44-63% of all critical care alarms were caused by pulse oximeters, 94% of oximeter alarms were considered clinically unimportant, and 71% were false alarms [88].

2.3 Optical foot sensor

If adults are able to detect their sleep problems by themselves then such kind of issues on children may become undiscovered for a long time. Sleep

quality monitoring on babies and children has a long-term affect by increasing their life quality. Those measurements could only be done in remote monitoring conditions. For this purpose we need a small size and modular device suitable for long term monitoring that was proposed in chapter 1. One of the best places for sensors is foot [86]. For this purpose there is also a need to have an appropriate size optical sensor for PPG measurements.

New hardware and more advanced software algorithms are being developed to reduce false alarms and provide more reliable readings under conditions of low perfusion. Signal processing algorithms are one way to compensate motion artifacts but it does not increase the quality of raw signal. There are three main factors that affect pulse oximetry readings. A straight incident light to tissue scattered wavelength-dependently until about 2 mm depth because the inner structure of tissue is not uniform. The effect of the tissue has to be considered that affects total optical density. If using three-wavelengths, two simultaneous equations give the Peripheral SpO2 without the effect of tissue coefficient dependency. At last, the effect of venous blood could be removed with five wavelengths.

Oxygen saturation is defined as the measurement of the amount of oxygen dissolved in blood, based on the detection of Hemoglobin and Deoxyhemoglobin. Two different light wavelengths are used to measure the actual difference in the absorption spectra of HbO2 and Hb. The bloodstream is affected by the concentration of HbO2 and Hb, and their absorption coefficients are measured using two wavelengths 660 nm (red light spectra) and 940 nm (infrared light spectra). Deoxygenated and oxygenated hemoglobin absorb different wavelengths. Deoxygenated hemoglobin (Hb) has a higher absorption at 660 nm and oxygenated hemoglobin (HbO2) has a higher absorption at 940 nm [24].

Conventional oximeters use two wavelengths (λ_n) to perform measurements. Later technologies use wider area of wavelengths in order to increase the system reliability. Different research groups are using 3 to 12 wavelengths in oximeter. In addition to $\lambda_1 = 660$ nm and $\lambda_2 = 940$ nm, used in conventional oximeters, the most used wavelengths are $\lambda_3 = 700$ nm, $\lambda_4 = 730$ nm, and $\lambda_5 = 805$ nm [21] [68] [4].

For detection of Carboxyhemoglobin (CoHb) and Methemoglobin (MetHb), four wavelengths are in principle sufficient [21]. The use of additional wavelengths allow further correction of disturbances and improves the accuracy. Using three-wavelength method improves the accuracy of SpO2 when the tissue constants are appropriately selected. It does not matter how many wavelengths are used, motion artifacts elimination is still considered difficult [4]. Signal artifacts are mostly caused by the body movements. With two optical sensors it is possible to reduce artifacts caused by the local movements. Sensors have to be placed on the body away from each other by at least few centimeters. To calculate pulse wave velocity (PWV) us-

ing two synchronized, wireless pulse oximeters, placed on the wrist and fingertip of the same hand has been used in [59].

The purpose of our optical sensor is to increase the reliability of the signal by adding more optical sensors and compare the quality of the signal to choose the optical element that gives better signal to noise ratio at that particular time.

2.3.1 Sensor architecture

The architecture of the sensor is depicted on Figure 2.2. It consists in total four PDs and two LED-pairs. There is one pair of LEDs and two PDs for each AFE. For both AFE, one LED has the wavelength $\lambda_1 = 660$ nm and another one $\lambda_2 = 940$ nm. The sensor is connected to the monitoring device, which was described in Chapter 1.2. The Figure 1.3 in Chapter 1 describes how this optical sensor is physically connected to the device to perform measurements.

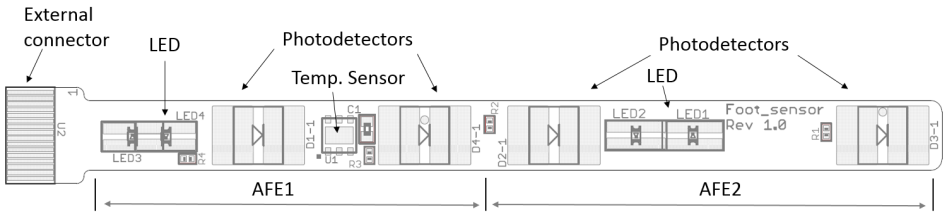

Figure 2.2: The architecture of dual channel optical sensor

With the help of this optical sensor we can detect the pulse wave using optical elements, calculate SpO2, heart rate and respiration rate. The sensor includes also digital temperature sensor for skin temperature. To get the oxygen saturation, we are using LED pair with red and infrared wavelength.

Dimensions of the sensor are chosen to fit for baby foot for long-term monitoring. There is one pair of LEDs for each AFE as sown on the picture 2.2. There are also two photo-detectors (PD) for both AFEs. It is not possible to switch automatically between those PDs as they have to be pre-soldered manually to enable one of those. The purpose of two PDs is to find the best placement of the sensor while it is being carried on the foot. Figure 2.3 depicts the location of arteries on the foot.

The placement of the LEDs is selected to be as close as possible to the lateral tarsal artery or medial plantar artery to increase the amplitude of pulse wave and acquire better signal. Figure 2.4 depicts the sensor attached to the foot.

All locations of the PDs and LEDs are marked. On the top of the foot, there is a monitoring system with Li-ion battery. It can also be seen that

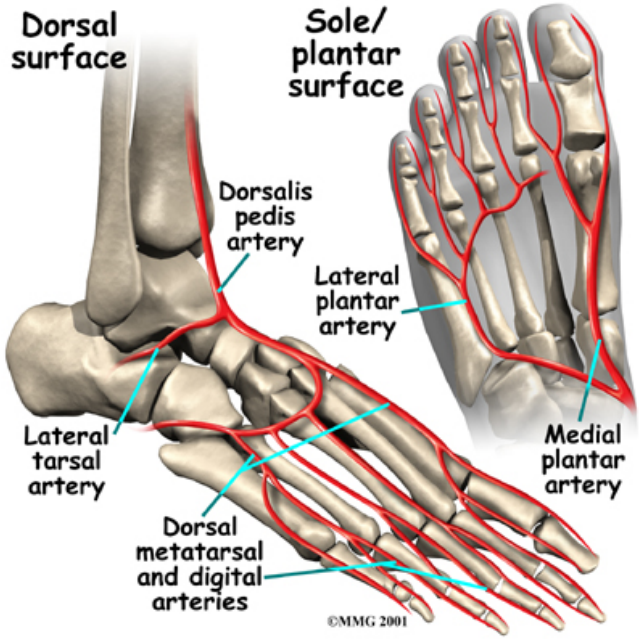

Figure 2.3: Foot anatomy [19]

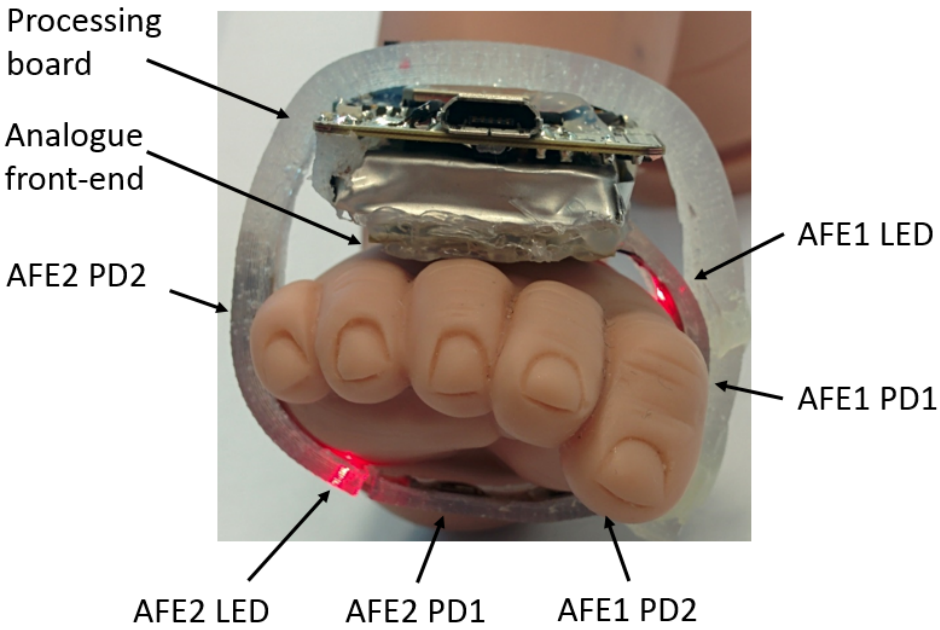

Figure 2.4: Optical sensor attached to the foot

AFE1 LED and AFE2 PD has some air gap between the sensor and skin. As the foot is being moved frequently, it affects drastically the quality of

the signal. Therefore it is needed to perform continuous measurement of the signal quality between different optical elements and use only those that give the best signal to noise ratio.

2.3.2 Experimental results

The aim of the experiments is to develop a methodology to choose between optical elements that give the best results. As the signal quality varies depending on the movement of the foot, there is a need for a method to receive always a signal with the best quality.

For experimental results we have developed an additional part for the user interface that is used for smart optical sensor, described in Section 2.4.3. The interface is depicted on Figure 2.5. It gives a real-time information about the current efficiency of the signal. Efficiency averaging functionality over 5 seconds has been implemented. If the average efficiency drops below predefined threshold, an automatic switch to the another AFE is executed to measure the efficiency on different sensor. If the efficiency on the second sensor is better, then further measurements will be performed with the second AFE. In real measurements efficiency above 10% percents is considered as a result of artifact and therefore skipped. If the signal efficiency stays continuously between 1% to 5% no switch to another source signal is done.

As the efficiency could change dramatically there is also a need to change the sensitivity of the PD and LED current. Current implementation is tested only with mentioned user interface. It gives us better overview about the applied thresholds and further development of algorithm to give adaptability depending on the user and how well the sensor was positioned. As mentioned in the beginning of this chapter, signal quality depends highly on the placement of the sensor on the foot.

The same efficiency calculation method is used in smart PPG sensor to automate the task in which opto-pairs give the best signal-noise ratio and should be used to perform measurements. This kind of parameter change is called calibration that needs to be done in case of change of sensor location. The only difference is that in case of foot sensor, this kind of calibration is done frequently after each foot movement and in case of smart PPG sensor only initially and only after the misplacement of the sensor.

The only drawback that appeared during the measurements was the reliability of the optical sensor. Caused by the design issue one physical connection between the AFE and LED got frequently broken that caused the loss of the signal. The root cause was a copper disconnection on the flex board next to the LED pad that appeared after several bending movements. The result of this incident caused automatic switch to another AFE as the signal quality dropped dramatically.

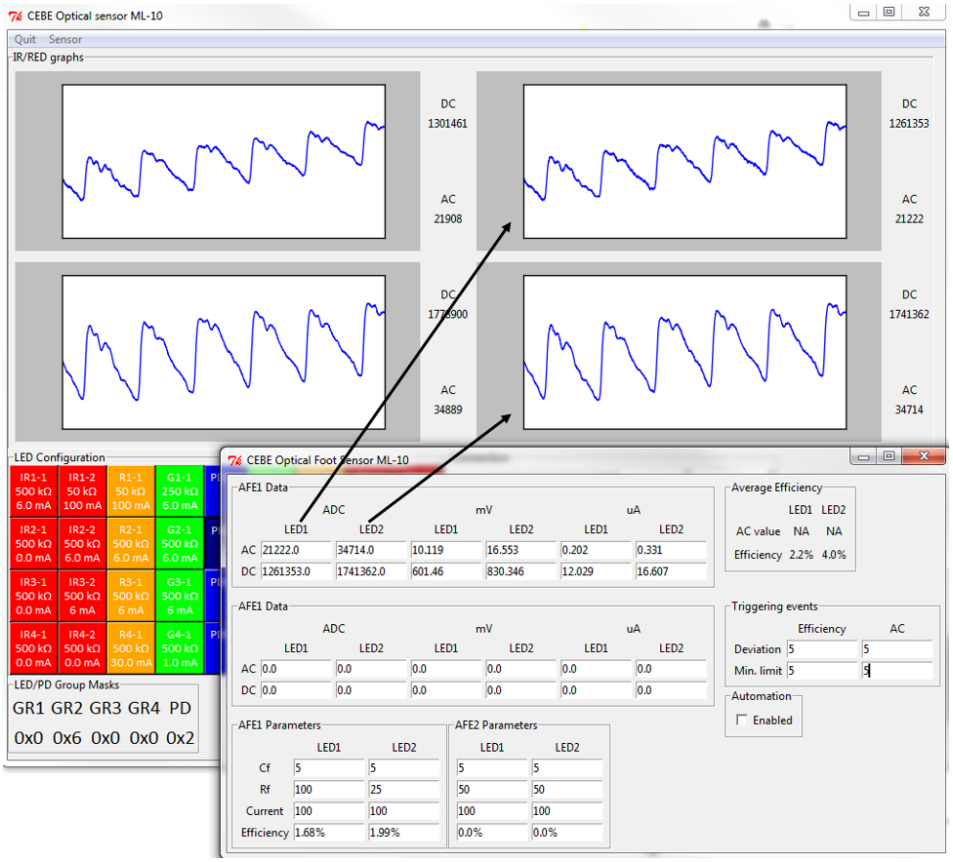

Figure 2.5: Signal efficiency measurements on foot sensor

2.4 Optical smart photoplethysmographic sensor

Combining LEDs with different wavelengths in the same way as described in previous chapter would increase the measurement results also in other application areas. As an example, pulse wave registration from the artery is needed in order to exclude the influence of the peripheral blood vessels (arterioles, capillaries) and to estimate the stiffness changes of the central arteries or certain segment of artery [28]. For this purpose we propose a new optical smart sensor design that is used for pulse wave registration for adults. This is a new type of sensor, that automates and speeds up obtaining the pulse wave signal from the radial artery with the highest possible signal to noise ratio.

PPG sensor development for the signal registration from the different penetration volume-depths, has been described earlier [105] [90] [89]. The advantage of our proposed sensor is to combine PDs and LEDs with dif-

ferent wavelengths into groups so that they can be driven independently. The selection of the distance between the LEDs and PDs and choice of the wavelength in the proposed smart PPG sensor has been made based on the previously mentioned studies.

Our proposed sensor consists of 32 LEDs in four different wavelengths and four photo-diodes. Distances between the photo-diodes and LEDs varies to analyze different tissue layers. LEDs can be grouped in order to analyze automatically larger tissue areas without moving the sensor on the skin. The sensor is controlled by the miniaturized monitoring device [56]. The designed PPG sensor is tested for the pulse wave registration from radial artery.

2.4.1 Sensor architecture

The proposed sensor architecture is part of the developed system. The architecture and the functionality of the system has been discussed in [56] and [55]. Smart PPG sensor consists of LED and photo-diode array with control logic and optical measurement functionality.

The proposed system consists of three main parts. Figure 2.6 illustrates the system architecture how the smart PPG sensor is connected to the AFE module and rest of the system.

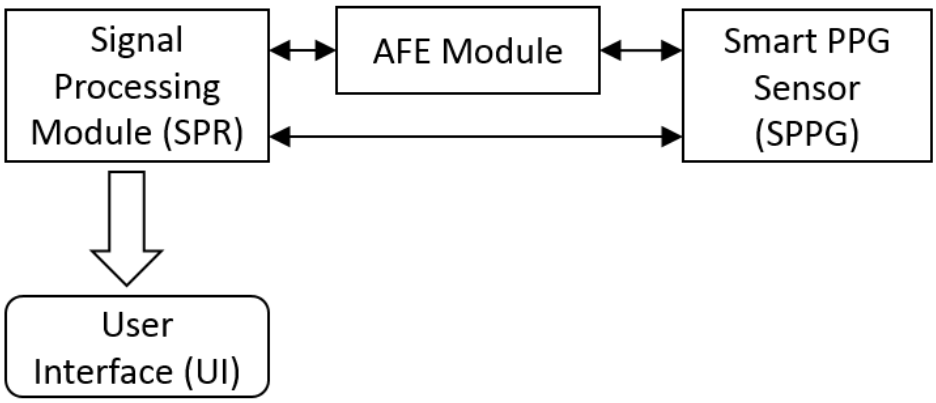

Figure 2.6: System Architecture

Signal processing module (SPR) manages the whole system, performs signal pre-processing and data transfer between the user interface and rest of the system. The architecture and the functionality of processing and AFE module has been discussed in [55] and [56]. Smart PPG sensor (SPPG) consists of LED and photo-diode array with control logic and optical measurement functionality. Acquired optical signal is at first received by the AFE module and then sent to the SPR module for pre-processing. Digital logic on the SPPG module is also controlled by the SPR module. The SPR

module supports wide range of system management commands via User Interface (UI). It is possible to control every individual on-board sensor and module through the UI.

Figure 2.7 depicts the architecture of the optical sensor module. There are four independent LED and PD groups, and two independent channels. A channel means that all signals that are measured in this particular group are connected with one particular AFE module. In total there are two identical AFE components integrated into one AFE module that are working in parallel. Each group, separated with red borders, has one PD, green (G), red (R) and two infra-red (IR) LED emitters.

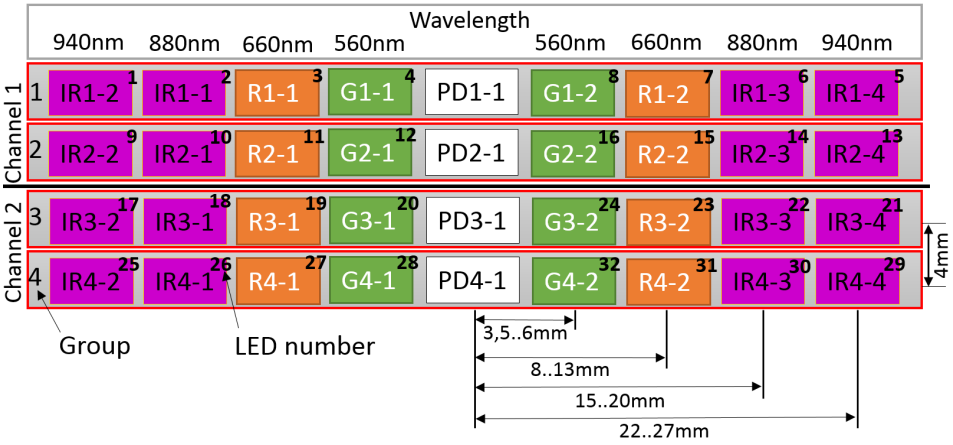

Figure 2.7: Structure of optical sensor array [54]

Four different wavelengths in each group are used. Green LED 560 nm, red LED 660 nm, inner infrared LED (IRn-1 and IRn-3) 880 nm, and outer infrared LED (IRn-2 and IRn-4) 940 nm. All vertical and horizontal distances between LEDs and PDs are based on the previous studies.

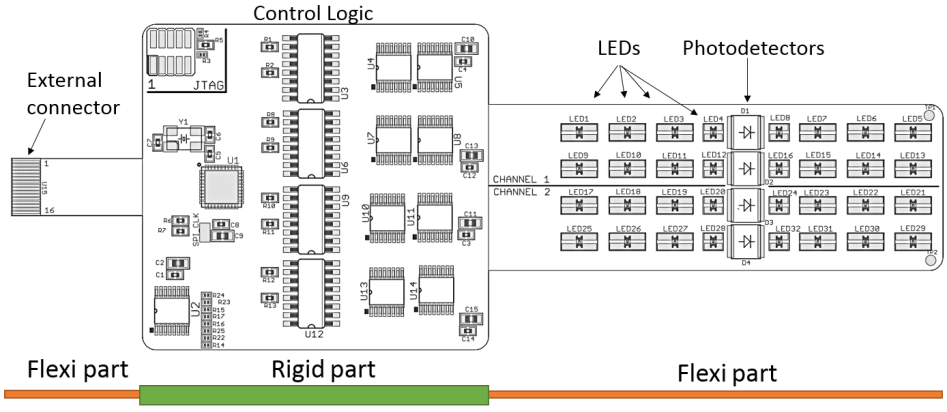

Figure 2.8: A structure of smart optical sensor

Sensor driving is done through the API to enable or disable individual optical elements or its groups. Figure 2.8 depicts the architecture of the optical sensor module. There are four independent LED and PD groups, and two independent channels. A channel means that all signals that are measured in this particular group are connected with one particular AFE module. In total there are two identical AFE chips integrated into one AFE module that are working in parallel. Each group, separated with red borderline, has one PD, green (G), red (R) and two infra-red (IR) LED emitters.

Communication

Device is controlled by the user interface via USB connection. For better sensor management we have developed a Python based graphical user interface (GUI) that allows to set individually the current of each LED, feedback resistors and capacitors, to view the received signals and save the raw data into the file. From Analogue front-end we receive 6 signals: LED1, LED2, LED1 ambient, LED2 ambient, LED1-LED1 ambient and LED2-LED2 ambient. All signals are 22-bit long. Automatic ambient measurement and cancellation is done by the AFE.

2.4.2 Driving logic

Sensor configuration must follow certain hardware and software limitations. This chapter describes how the sensor elements can be configured by following pre-defined limitations. It is also described how the sensor configuration could be extended by grouping different optical elements.

Driving phases

The LED array driving process has two main phases. At first, the array has to be calibrated which is mandatory to start the measurement process. Calibration process analyses the acquired signal and determines LED groups that have the best signal quality.

For the calibration we group two LEDs into one group. In Figure 2.7 LEDs IRn-1 and IRn-2 form one group, Rn-1 and Gn-1 second, Rn-2 and Gn-2 third, and IRn-3 and IRn-4 fourth group. The same grouping methodology is defined in each group and on both channels. Altogether we get 16 LED groups. Each group is switched on and off for a short period of time with different pre-defined configurations.

Calibration with each group is started by setting the LED current to 100mA and amplification with the feedback resistor to the maximum level. If the signal strength goes into saturation, amplification is decreased until the AC component has the maximum value and DC component is not in

the saturation. Based on the the AC and DC component, we calculate the efficiency. At first, a received photo-current is calculated:

$$I_p = \frac{V_{out}}{2 * R_f}, \tag{1}$$

where I_p is photo-current, V_{out} is photo-voltage analog-digital conversion (ADC) value divided by 22-bits, R_f is feedback resistor of the amplifier. With that equation we can calculate photo-current for AC and DC component. Efficiency is calculated with the following formula:

$$\gamma_{eff} = \frac{I_{AC}}{I_{DC}}, \tag{2}$$

where γ_{eff} is the efficiency, I_{AC} is photo-current of AC component and I_{DC} is photo-current of DC component.

After all groups are toggled once with their own best settings, signal quality analysis follows to detect the presence of pulse wave. The group with the highest amplitude of AC component will be chosen automatically to start the continuous measurement process. If there are signals with identical quality from more than one group we can redefine groups and repeat the same process to find only those LEDs that give the best signal for our needs and group these into one group that will be used during the analysis.

Configuration of light source driver

The AFE module is capable of generating up to 5 kHz Pulse Repetition Frequency (PRF). In each period there are two times ambient and LED sampling. The sample rate is four times PRF, up to 20 kHz. For pulse wave detection the common sampling rate is 250 Hz and up but using higher sampling rate it is possible to use built in hardware averaging functionality that increases signal quality. In our current configuration we are using sampling rate of 500Hz and no averaging.

As we are using two AFEs concurrently, we can sync them by using interrupt that is generated every time when pulse repetition period starts. Combining timings between both AFE modules, it is even possible to emit the light with one channel and perform the measurements with another one. In this way we could increase possible combinations of finding the best signal for blood vessels detection.

Figure 2.9 illustrates the usage of multiple emitter groups. Each PRF starts with "ADC Ready" interrupt. Duty cycle of each sample can be in-between 5% to 25%. There is also a hardware averaging built into the ADC but it decreases the sampling rate accordingly. If we would like to

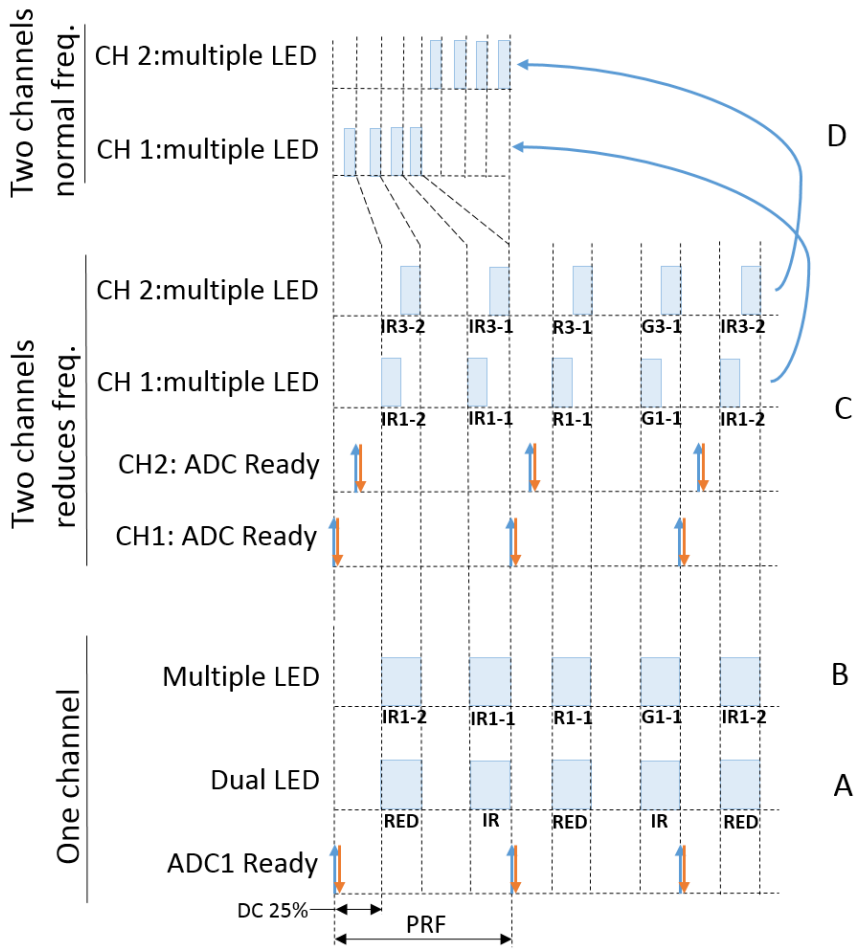

Figure 2.9: Multiple LED switching. A) Sampling with one channel and dual LED configuration. B) Sampling with one channel and four LED configuration. C) Sampling with dual channels and reduced frequency. D) Sampling with two channels and normal frequency

sample at the rate of 5 kHz with 4 averages then the PRF becomes 1250 Hz.

Multiple Group and Channel Measurements

The most common optical pulse wave measurement device is a fingerprint sensor. It has red and infrared LEDs and one PD. Both leds are switched continuously with the duty cycle of 50%. In some cases there is also an ambient sampling added to reduce the noise level. Same mechanism is described in the part A in Figure 2.9. With one channel the sampling rate

can be up to 5 kHz because the ADC sample rate of 20 kHz will be divided between four cycles - two times ambient and LED sampling.

In case of multiple LEDs or LED groups, as in our proposed solution, we could define which emitter will be switched on in every cycle. In multiple LED configuration, part B in Figure 2.9, we start by switching IR1-2, then continue with IR1-1 and up to G1-1 until the same cycle starts again. With this configuration we could increase the number of emitters but the sampling rate gets smaller the same amount of times. For one channel we have up to 16 independent LEDs. with this configuration, using the equation below, we could achieve the sampling rate up to 625 Hz without averaging.

$Fs_{desired}$ - desired sample rate
SPS - ADC sample rate (up to 20 kHz)
N_{LED} - number of independent emitter groups
N_{CH} - number of ADC channels

$$Fs_{desired} = \frac{(SPS) * N_{CH}}{2 * N_{LED}}, \tag{3}$$

For the two channel configuration we have a possibility to decrease the duty cycle to alternate the sampling using two channels. In Figure 2.9 part C describes a two channel configuration and increased number of LEDs. The cycle of channel starts with the ADC ready interrupt. The duty cycle of emitter is reduced to the 12.5%. This gives the possibility to use the rest of 12.5% for the second channel because the maximum duty cycle could be up to 25%. For that we shift the second channel ADC ready interrupt half of the duty cycle forward that makes possible to use the second channel while there are all LEDs turned off on the first channel. With this 2-channel configuration we could go through all 32 LEDs and still achieve sample rate of 625 Hz without averaging.

By using two channels we could also decrease the ambient and LED sampling duty cycle. This gives a possibility to finish all sampling for one channel only during part of the full pulse repetition period and use the rest of time for other channels. In Figure 2.9 part D illustrates a situation when the first channel has finished sampling, and the second one starts with sampling within one period of pulse repetition. With this configuration we could go through all 32 LEDs with sample rate of 1250 Hz. The maximum duty cycle is 6.25% which is above the allowed minimum of 5%. The number of possible configurations are not limited to the discussed ones. It shows the flexibility of our proposed solution for using it on different emitter and detector configurations.

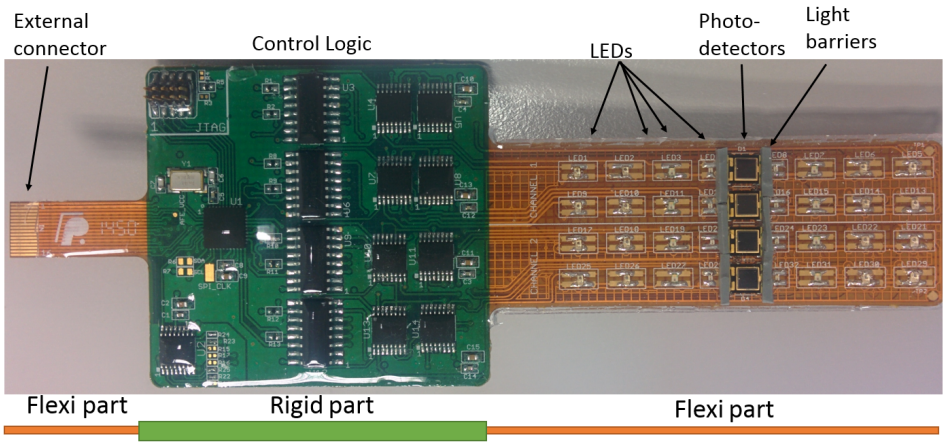

Figure 2.10: Sensor module overview [54]

Figure 2.10 depicts the build-up of the sensor module. Module has a connector to external system connection, that is built on the flex Printed Circuit Board (PCB). All control logic is placed on the rigid PCB as it helps to increase the mechanical reliability because the rigid does not bend. All optics are on the flex PCB as it touches directly the skin and needs to be bent accordingly. All electronics, including LEDs and photo-diodes, is poured into the medical silicone to minimize the effect on the skin.

Rigid and flex PCBs have 4-layer design to suppress the noise and increase the stiffness to the appropriate level. Extra care has been taken with the signal line routing of the detectors. As the length of the whole sensor part is 138 mm, there is a risk for increased noise. For that reason all detector lines are routed on the middle layer and also surrounded with shielding traces.

2.4.3 Experimental results

Signals were collected with the user interface developed in Python. Figure 2.11 depicts the user interface (UI) for managing smart PPG sensor. Upper part of the UI shows received signal with numeric values of AC and DC components from active sensors. It is possible to change the current and feedback resistor value for each LED.

All values are saved automatically into the configuration file that can be reloaded later if needed. Starting or stopping saving the received signal can be set in real time. During the real experiments we have got results that verify our expectations about obtaining the best pulse wave signal from the radial artery only from the LED and photo-diode pair with the highest efficiency, that is calculated using formula 2.4.2.

Measurements were performed by placing the sensor on the wrist, as

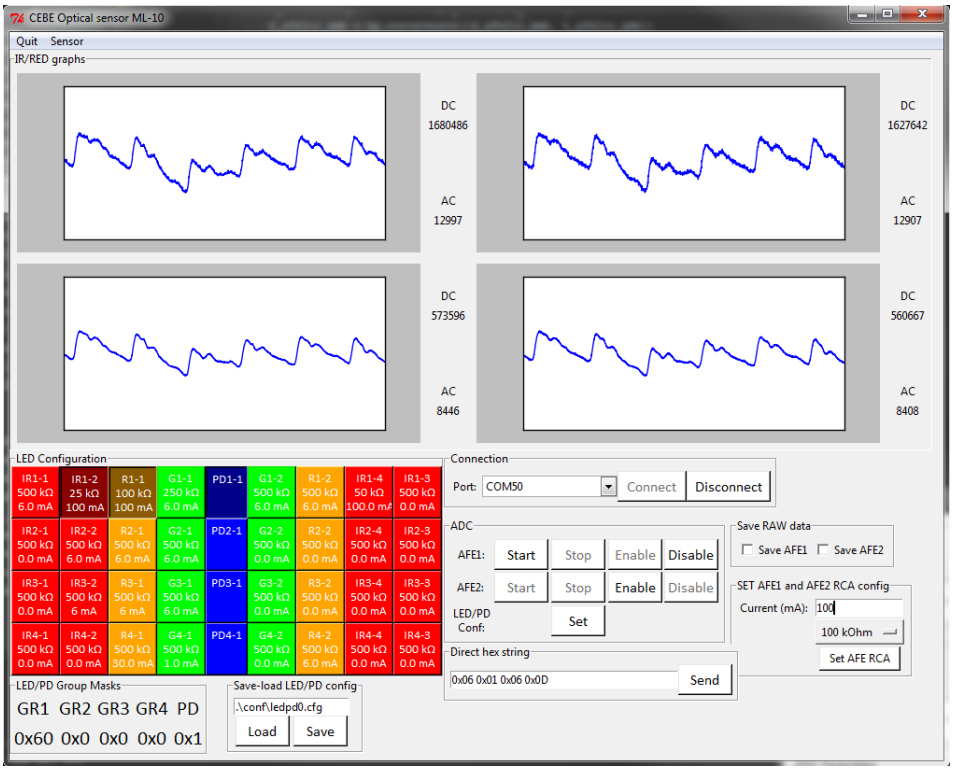

Figure 2.11: User interface for smart photoplethysmographic sensor driving

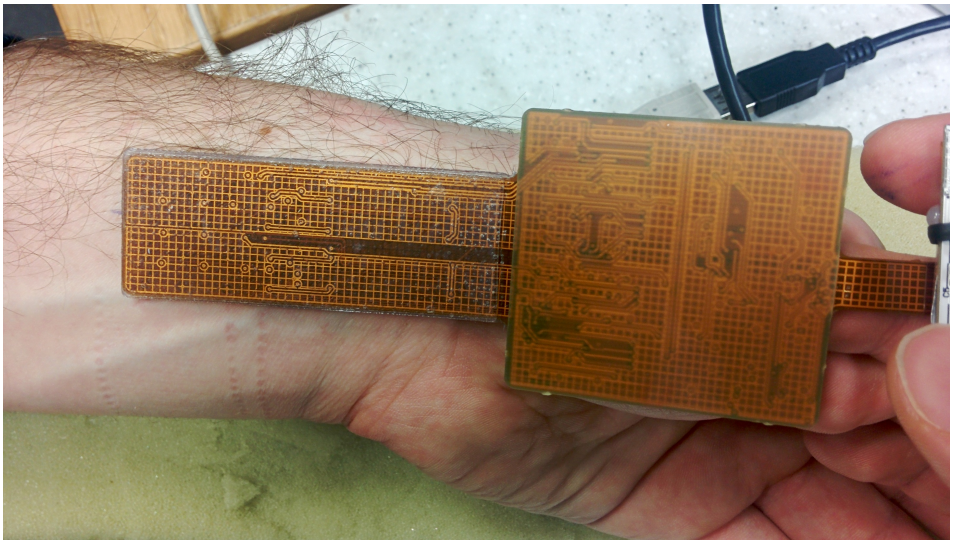

Figure 2.12: Sensor placement on the wrist [54]

depicted on figure 2.12, and fastening it using bending strap. Experiments were performed on different days during few hours on both days, but on the same test person. The signals were recorded from the left hand radial artery. Efficiency was calculated as described in the previous section. Table 2.1 depicts the relative signal efficiency for each LED and photo-diode pair.

Table 2.1: Test results [54]

Day 1

IRn-4	IRn-3	Rn-2	Gn-2		Gn-1	Rn-1	IRn-1	IRn-2
0,68%	0,58%	0,33%	0,59%	PD	1,09%	0,36%	0,52%	0,67%
1,11%	1,10%	0,68%	0,00%	PD	0,83%	0,68%	1,61%	1,37%
0,89%	0,84%	0,51%	0,47%	PD	0,63%	0,62%	1,07%	1,02%
0,63%	0,58%	0,43%	0,37%	PD	0,48%	0,55%	0,60%	0,79%

Day 2

0,31%	0,26%	0,41%	0,32%	PD	0,36%	0,29%	0,42%	0,65%
0,69%	0,48%	0,51%	0,00%	PD	0,37%	0,49%	0,79%	1,46%
0,50%	0,50%	0,46%	0,23%	PD	0,26%	0,35%	0,61%	1,05%
0,29%	0,29%	0,32%	0,16%	PD	0,21%	0,38%	0,53%	0,71%

The optopair with highest efficiency on each vertical group is colored. Red color marks infrared, orange red and light green marks green LED. Efficiency more than 1% is considered usually as a good signal. The bigger the efficiency number the better signal to noise ratio we get. The signal with the highest efficiency is received with the LEDs that have the longest wavelength, marked with red. Comparing the left and right side, the signal with highest efficiency is on the right side because radial artery is more close to the surface of the skin on the wrist side. As it can be seen from Table 2.1, there are also some differences between measurements on different days. However, it is visible, that the results are repeatable and the radial artery can be detected under certain optopair.

For the reference we have also measured noise level of photo-diode by shutting down LED driving part of the AFE module and putting the sensor to the dark. The average noise is 0.256 mV and it is not dependent on the feedback resistor in Eq. (1).

Figure 2.13 depicts the results of one LED pair. Upper part describes the signal measured with IR2-3 and lower IR2-4. Both signals have already ambient subtracted and LED current is calculated based on Eq. (1) and

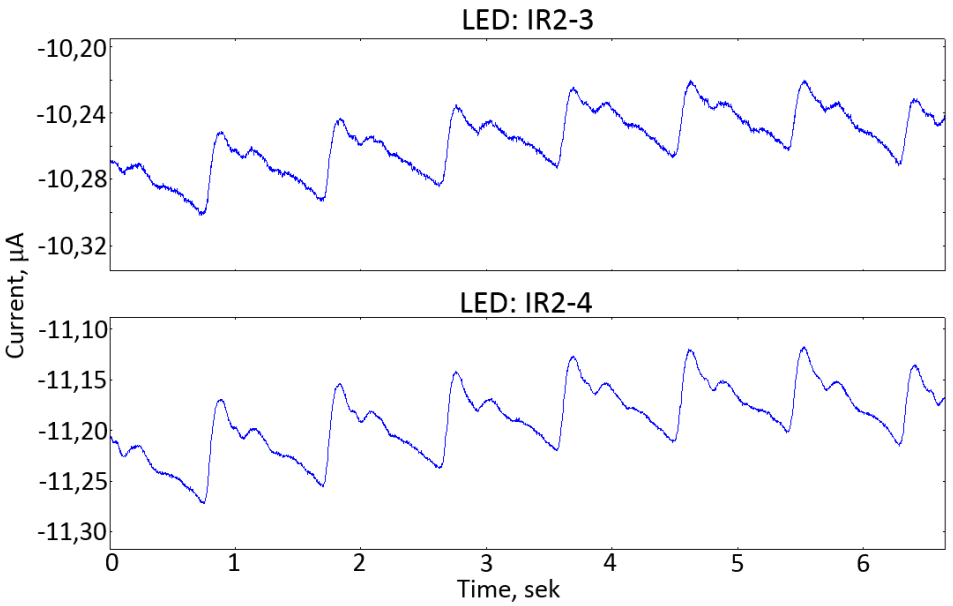

Figure 2.13: Measured PPG signals; Top: IR2-3, bottom: IR2-4

(2). As this figure belongs to the measurements made on the second day, it correlates well with the lower part of Table 2.1. Efficiency values in that table show also that IR2-4 has slightly better efficiency compared to IR2-3, 0.69% and 0.48% respectively.

2.5 Chapter summary

The goal of this chapter was to provide an overview about proposed optical sensors for pulse wave registration. The purpose of the developed sensors is to increase the reliability of the optical signal and automate the measurement process by getting the best possible signal that any combination of sensors could give at each particular time. A lack of comparison with other similar solutions is caused by the method of experiments. Results can be compared only if the measurement conditions, place, sensors settings and human anthropometric data is known and identical. Based on our experiments with different persons under controlled experiment environment results were correlating and could be repeated with similar results. Therefore we are not focusing on comparison but to the quality of the measurements. Although there were some differences between measurements on different days the radial artery can be detected under certain optopair and results are based on real experiments.

The first part of this chapter gave an overview about PPG and its challenges. Two types of PPG methods are described together with several

factors that may affect the quality of PPG measurement.

The second part of this chapter gave an overview and state of the art about similar solutions developed by others. It is discussed about the advantages and drawbacks of different solutions.

The third part of this chapter introduced an optical foot sensor that is suitable for infants and babies up to few years old. This sensor is used to develop a methodology to receive a signal from that optical element that has the best signal to noise ratio.

The fourth part of this chapter introduced an optical smart photoplethysmographic sensor for pulse wave registration at different vascular depths. A complete new architecture and driving logic decreases the time needed for pulse wave registration and artery detection. Also initial experiments were demonstrated.

Chapter 3

Low Complexity Algorithms for Sleep Quality Estimation

Long term patient monitoring needs small size and reliable devices that consume a little power. This restriction also limits the amount of signal processing, the device is able to perform. Proposed modular platform, described in Chapter 1, is designed taking into account the same limitation. To increase the battery lifetime, it has limited processing capabilities that require to use low complexity algorithms for signal processing. As one of the use cases is monitoring sleep quality, there is a need for an low complexity algorithm to perform PPG signal analysis in real time.

The main contributions of this chapter are summarized in [57] and [55]. The aim of this chapter is to demonstrate possibilities to apply the previously proposed architecture and sensors for disease diagnosis and propose a low complexity algorithms for sleep quality estimation. In this chapter we propose an efficient low-power algorithm to extract respiration rate from PPG signal. We analyze amplitude variations in the PPG signal that are caused by the respiration and demonstrate experimentally efficiency of our proposed algorithm. Compared to other methods it performs well also in limited processing power conditions. As a result the extracted respiration rate can be used for sleep quality estimation and pre-screening. Main results of this chapter have been reported in [57].

3.1 Background

Sleep research requires to have background understanding what the sleep is, what are the methods to measure sleep. An overview about most common sleep diseases is given and how ti classify it.

3.1.1 What does sleep mean

Human bodies regulate sleep in the same way that they regulate eating, drinking, and breathing. Going without food produces uncomfortable sensation of hunger, while going without sleep makes us feel overwhelmingly sleepy. And just as eating relieves hunger and ensures that we obtain the nutrients we need, sleeping relieves sleepiness and ensures that we obtain the sleep we need. But the question still remains, why do we sleep?

There are few theories, why do we sleep. One of the earliest theories, called inactive theory, suggest that inactivity at night is an adaption that served a survival function by keeping organisms out of harm's way at times when they would be particularly vulnerable. Although there are few more theories like energy conservation and restorative, the most recent one is brain plasticity theory [32]. It says that sleep is correlated to changes in the structure and organization of the brain. Even these theories remain unproven, it is one of the driving forces of sleep research to understand better why do we sleep.

3.1.2 Background of sleep research

The history of sleep research starts in 1913 when French scientist Henri Pieron authored a book entitled "Le probleme physiologique du sommeil" [95]. In 1953 Dr. Nathaniel Kleitman, known as the "father of American sleep research", and his students made the landmark discovery of rapid eye movement (REM) during sleep. Sleep research comprises many different areas like narcolepsy research, sleep and cardio-respiratory research, circardian rhythms, shift work and it's effects on sleep, sleep deprivation, sleep and aging, infant sleep etc. There are approximately 84 different known sleep disorders. The most common disorders are sleep apnea, narcolepsy, parasomnias during sleep, infant sleep problems and insomnia. Many of them have also several sub-categories.

3.1.3 Instrumentation for sleep research

Polysomnography (PSG) is the most frequent test to diagnose sleep disorders. Full PSG is an overnight monitoring in the sleep laboratory. Each subject is monitored with Electroencephalography (EEG), right and left electrooculogram, submental EEG, Electromyography (EMG), ECG, chest and abdominal wall motion by respiratory inductance plethysmography, oronasal airflow, SaO2, P_{ETCO2} by infrared capnometry at the nose. Subjects are also monitored with infrared video camera [48].

For screening purposes simplified tests using portable equipment may be used at home. These tests usually involve measuring heart rate, SpO2 level, airflow and breathing patterns. In case of sleep apnea, the test results show

drops in the SpO2 level during apneas and subsequent rises with awakening. As there are less types of measurements taken, portable monitoring devices don't detect all cases of sleep apnea. In some cases you still may go through the full PSG even if your initial results are normal. However, screening is considered also as a reliable and comfortable way to diagnose the OSA in babies and children.

3.1.4 Sleep apnea

Sleep apnea, that is one of the most common sleep disorders, has many variations. Depending on the type of sleep apnea it needs different methods to detect it. In this section an overview of the sleep apnea classification and detection is given.

Sleep apnea classification

One of the most common types of sleep disorders is sleep apnea. The term apnea means absence of spontaneous breathing. It is a common disorder that is estimated to occur in about 7% of the population of which more than 85% remain undiagnosed. There are four major types of sleep-related breathing disorders - central apnea, obstructive apnea, hypoventilation associated with sleep and non-specific sleep disorders. Central apnea is rare disorder on unknown cause. It is more prevalent in the middle-aged and elderly people. OSA is currently estimated to affect 4% and 2% middle-aged men and women repsectively and between 1% and 3% of 2- to 8-year old children. It is most commonly found in children between 3 to 6 years of age.

The 2007 AASM scoring manual respiratory rules for children require that obstructive apneas last at least 2 breaths, be associated with at least a 90% decrement in air flow from baseline, and be associated with continued or increased respiratory effort for the duration of the event [75]. Arousals or desaturation of SpO2 levels are not required for scoring of obstructive apneas [37].

Above mentioned scoring rules require that hypopneas last at least 2 breaths, be associated with at least a 50% decrement in nasal pressure or alternative flow signal from baseline, and be associated with arousal, awakening, or at least a 3% desaturation of SpO2. Use of esophageal pressure monitoring often demonstrates crescendo increases in respiratory effort when hypopneas are obstructive in nature.

Central apnea may be scored on pediatric PSGs whenever respiratory effort is absent for at least 20 seconds or whenever respiratory pauses lasting at least 2 breaths are associated with arousal, awakening, or at least a 3% desaturation of SpO2. Polysomnographers should take care to distinguish

when frequent central apneas meet criteria for the diagnosis of periodic breathing or Cheye Stoken respiration.

Increased resistance of the upper airway is the characteristic PSG feature of Upper Airway Resistance Syndrome (UARS), a condition where chronic partial airway obstruction and increased work of breathing disturbs sleep in the absence of scorable respiratory events and gas exchange abnormalities. Altough flow limitation is occasionally apparent using PSG methods in patients with UARS, esophageal pressure monitor represents a more sensitive measure of partial airway obstruction in these patients.

PSG features of periodic limb movement disorder in children are comparable to those of adults. Other sleep related movement disorders occasionally observed in children include being sleep myoclonus of infancy and alternating leg muscle activation.

Corkum and colleagues studied the sleep of 25 medication-free preadolescent children and reported sleep problems such as bedtime resistance, restless sleep and longer sleep duration were significantly more frequent in the Attention Deficit with Hyperability (ADHD) group. The study found significantly increased night-to-night variability of sleep onset and duration for the ADHD group during the five consecutive nights [29]. A series of 50 children with polysomnography proven OSA demonstrated hyperactivity in 42% of subjects and decreased school performance in 16% [30]. A subsequent examination of the natural history of snoring between 4 to 7 years of age found that hyperactivity, restless sleep and excessive sleepiness were significantly more common among habitually snoring children compared with youngsters who had never snored, lending further support to the notion that a causative relationship may exist [1].

There is also an emerging evidence that periodic limb movement disorder (PLMD) may be associated with prominent attentional/behavioural symptoms in children. Diagnostic criteria for PLMD is typically met when PSG exhibits greater than five PLMs per hour of sleep and symptomatic sleep disruption is reported, although universally accepted pediatric criteria have not yet been established [98].

Existing research suggests that daytime inattention, hyperactivity and behavioral problems are likely to be caused or worsened by OSA or PLMD for a substantial minority of patients. This will remain an active area of investigation, with substantial efforts toward development of reliable and cost-effective screening tools which will permit screening for these primary sleep disorders without the time and expense of a full PSG. Development of outcome-based treatment guidelines for these conditions will improve assessment of the impact of treatment on day and night time symptoms [35].

Sleep apnea detection

Normal waking and asleep SpO2 levels in healthy child or adult are 96-99% and 94-98%, respectively. Sleep apnea has specific pattern in which order all symptoms appear. Cumulative time when saturation level is below 90% is also often an early sign of trouble and pointed out in the summary of clinical PSG tests [79]. The typical cycle of sleep apnea is:

1. saturation level decrease 3-4% from the baseline
2. decrease of the amount of air through the lungs at least 50% with the duration over 10 seconds
3. heart rate falls below normal
4. brief awakening with few large breaths
5. heart rate speeds up above normal heart rate
6. oxygen level returns to near normal

One such cycle is calles apneic episode that may repeat tens of times per hour. Apnea Hypopnea Index (AHI), the number of apneic episodes per hour, is used to detect the severity of sleep apnea.

- AHI of 5-15/hr - mild sleep apnea
- AHI of 16-30/hr - moderate sleep apnea
- AHI of +30/hr - severe sleep apnea

The standard definition of AHI determined during attended laboratory PSG is calculated using following formula[12]

A_{wofl} - apneas where 10 sec without flow
R_{flow} - hypopneas with reduced flow with 5% of desaturation
St_{tot} - total sleep time in hours

$$AHI^s = \frac{(A_{wofl} + R_{flow})}{St_{tot}}, \tag{6}$$

Even as the AHI index is widely used as a metric for OSA diagnosis, clinicians generally do not rely solely on AHI for OSA diagnosis and for determining treatment plans. In addition to that, symptoms, sleep architecture, arousal indices, degree of saturation and examination of raw PSG data is taken into account to diagnose OSA.

3.2 Overview

The term sleep quality lacks an established definition. Sometimes it is used to refer to a collection of sleep measures including total sleep time, sleep onset latency, total wake time, sleep efficiency and sleep disruptive event like apnea. As discussed previously there are many different physiological signals measured during the sull sleep study that makes it expensive and uncomfortable. By replacing it with pre-screening, there are less signals measured that makes it more comfortable and possible to perform the monitoring remotely at home.

As the need for remote health monitoring systems increases, the complexity of such systems also grows significantly. Signals measured by few attached sensors consist usually complex signals that are used to extract different features. Those systems are usually wearable and have limited processing power that limits using sophisticated signal processing algorithms.

Pulse oximetry is frequently used in clinical situations for non-invasive measurement of heart rate and arterial oxygen saturation. PPG is obtained by optically illuminating the skin and measuring changes in light absorption with the pulse oximetry. In many clinical situations breathing rate is extracted from the PPG, which is known to cause a minimum inconvenience to the patient. A number of methods for deriving the breathing rate from the PPG have been suggested in the literature. Respiration rate extraction is used in several application areas. The diagnosis of an OSA is one of them. It is a respiratory disorder characterized by recurrent airflow obstruction caused by total or partial collapse of the upper airway.

Physiological monitoring of breathing interval is important in many clinical settings, including critical and neonatal care, sleep study assessment and anaesthetics. Respiration causes variation in the peripheral circulation, making it possible to monitor breathing using a PPG sensor attached to the skin. The low frequency respiratory-induced intensity variations (RIIV) in the PPG signal are considered that RIIV includes contribution from the venous return to heart caused by alterations in intra-thoracic pressure and also changes in the sympathetic tone control of cutaneous blood vessels. The physiological mechanisms relating to the RIIV are, however, not fully understood. Different research groups [74, 48] have found that increased respiratory effort occurs throughout the night in OSA patients, with the subsequent hypoxia and arousal, may become one of the useful parameters for the OSA screening of snoring children.

3.2.1 Respiration signal extraction from pulse wave

There are several methods extracting respiratory information from the PPG signal. Pulse rate variability (PRV), pulse amplitude variability (PAV)

and pulse width variability (PWV), which all are related to respiration [51], are used to estimate the respiration using a spectrum-based algorithm [6]. Respiratory estimation errors are quite comparable and stay around $-0.26 \pm 7.30\%$.

Empirical Mode Decomposition (EMD) method, that is robust, simple and makes use of derived Intrinsic Mode Functions (IMF), have shown good results in [66] with the accuracy of estimating respiratory rate between 98.73% and 99.87%. Some research has been done to efficiently extract respiration from the PPG using Order Reduced Modified Covariance Auto Regressive (OR-MCAR) technique [67]. It gives an improvement in the frequency resolution compared to the traditional Fast Fourier Transform (FFT) method.

Discrete Wavelet Transform (DWT) is widely used when extracting respiration signal from ECG [91]. An absolute average error of 6.8% was obtained, considered highly acceptable for ambulatory patient monitoring. One variant of the DWT is Discrete Wavelet Packet Transform (DWPT) which tiles the frequency space in a discrete number of intervals. According to the literature [84] the accuracy of the DWPT technique is 85%. Wavelets have advantages over traditional Fourier methods in analysing physical situations where the signal contains discontinuities and sharp spikes. Daubechies wavelet based method was used and proved to be efficient in reducing motion artifacts restoring all the morphological features of the PPG signal [85].

By filtering the data, it is possible to extract respiratory rate harmonic from the filtered signal. In [71] suggested the use of a 3rd order Butterworth band-bass filter with a pass-band from 0.1 to 0.3Hz to filter the PPG signal. Autoregressive based method [22] is aiming to provide more accurate results than existing techniques but it needs to be tuned to an individual, or at best, to specific age groups and/or for specific time periods. Some more complex techniques are using Time-Frequency Spectra (TFS) for analyzing non-stationary signals. In this category, several studies have utilized Short-Time Fourier Transform (STFT) and Continuous Wavelet Transform (CWT) [58] to extract the respiration rate from the PPG signal. While the studies show relatively good results, the CWT is impractical because the extraction of the RR is done in some cases with the use or Frequency Modulation (FM) while in other cases with the Amplitude Modulation (AM) of the heart rate. This requires additional adaptive decision-making schemes, to determine when to use either FM or AM of the heart rate signal, making this kind of approach not suitable for a low power resource constrained application.

Choosing suitable method depends on the requirements for the signal quality and available processing power. Taking into consideration that wireless portable devices have usually limited processing power there is a

need to have a lightweight algorithm to extract the respiration signal from the PPG signal in near real-time. To the best of our knowledge, most of the respiration extraction algorithms require signal spectral analysis that requires more computational power than our proposed algorithm. Therefore we propose a method that is suitable for using in energy constrained systems.

3.2.2 Photoplethysmographic signal

SpO2 is usually measured by using a finger probe or ear lobe saturation with transmittal sensor that has usually better signal quality. This is considered as a reliable and practical when patient is steadily in the bed. There are also experiments where SpO2 readings were taken on wrist and chest belt [65] with good quality readings. Studies [73] also show that pulse oximetry measurements on foot are reliable and have also good correlation with foot perfusion index. It is also stated that oximeter performance is mostly affected by low peripheral perfusion states and patient motion. The features of PPG signal are more discussed in detail in 2.

Detecting correctly the pulse wave is important for the further analysis. The biggest difference between adults and neonates is the heart rate and breathing rate.

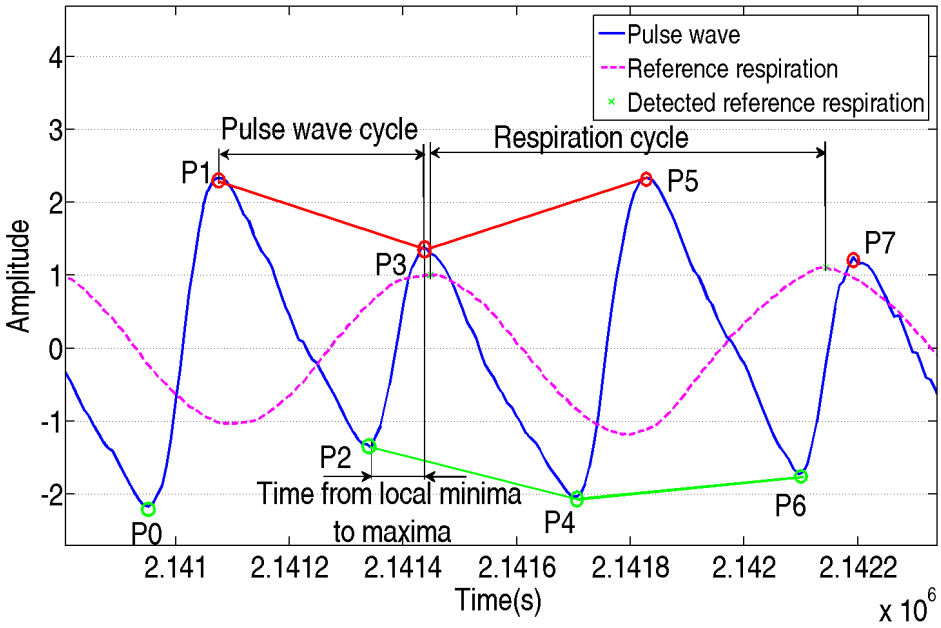

Figure 3.1: Analysis of pulse and respiration wave [57]

Strong sympathetic stimulation can increase the heart rate in young adults from the normal rate of 70 beats per minute up to 180 to 200 and,

rarely, even 250 beats per minute. Resting heart rate for the newborns is similar, 70 to 190 beats per minute. In case of 250 beats per minute time between every beat is 240 ms and biologically it can not be less than 200 ms which defines minimum required timeslot for the pulse wave analysis.

Respiration affects the pulse wave modulating it during the exhalation and inhalation. This modulation can be analysed to calculate the respiration rate. Figure 3.1 describes morphological changes of the pulse wave. Time from local minima ($P2$) to maxima ($P3$) is about 80 ms. To compare the shape of the currently analysed signal with the next one, it has to be buffered. It causes a slight delay for the analysis but helps to detect whether the next local minima or maxima belongs to the current respiration pattern or is the beginning of the next one. Respiration pattern is one full respiration cycle, starts with the inspiration and ends with the expiration. In order to take into account abnormal conditions like some possible missing beats, buffering 5 seconds at the time is enough to include the next pulse wave and not to cause big delays in case some critical changes have happened.

3.3 Respiration signal extraction

The proposed algorithm is focusing on infants from the newborn up to the first year and children between the years 2 to 8 who need to be monitored in case sleep apnea is suspected. Newborn babies have very sensitive skin and because of the small dimension of their body it is much more complicated to place the sensors and perform long-term measurements. The most frequent measurement method is to use fingertip or toe PPG sensors for the SpO2 and heart rate measurements. Our goal is to use sensors which are easy to place and make minimum discomfort to the babies. Therefore only optical sensors are used. It will limit the number of acquired signals, which do not provide enough information for the full PSG but is sufficient for the home screening. Instead of using fingertip sensors we place it into the shoe which helps to increase the quality of acquired signal. For example is is possible to perform measurements simultaneously from more than one body location. In addition to that, using more wavelengths instead of two in one sensor, helps to decrease the influence of the artefacts [4]. Both methods increase the required amount of signal processing that affects the power consumption. For power constrained devices having energy efficient algorithms for signal processing gives extended battery lifetime and smaller dimensions.

3.3.1 Data acquisition

Reference data has been collected from the PhysioNet MIMIC II Waveform Database [27]. It contains recordings from bedside patient monitors in neonatal intensive care units. Our collected signals include fingertip PPG and respiration signals. Recordings are digitized with sampling rate of 125 Hz and resolution of 8-, 10-, or 12-bit. The recordings are from twelve different neonates, each with the length of 60 minutes. Exact age is not specified.

3.3.2 Algorithm structure

One approach to extract the breathing rate information is based on connecting the peaks of each PPG pulse wave, thus constructing a continuous envelop along the top edge of the PPG signal, marked with the red continuous line in Figure 3.1. Through the use of the Fourier transform, a prominent high-amplitude peak can be identified that corresponds to the frequency of the subject's breathing rate. Respiration cycle modulates the pulse wave that is causing amplitude changes. When we look at many continuous pulse waves in Figure 3.1, it can be seen that there is a repeating pattern caused by the respiration, which is marked with the pink dotted line. If the PPG signal is without any artefact we can easily detect the patterns based on local maxima and minima. After each oxygen intake following pulse wave ($P3$), marked with the continuous blue line, has lower amplitude compared with the previous $P1$ and the next one $P5$. Maximum pattern ($P1 - P3 - P5$) was detected correctly. Local minima $P0$ was detected but as $P2$ did not match to the criteria it will be disregarded automatically and next minima will be stored with the name $P4$. Similar analysis has been done in [45]. In addition to that we also analyse the bottom of each PPG pulse wave because artefacts and baseline movements may change the pulse wave so that modulated signal can not be detected. Analysing the lowest points of each amplitude adds extra information and comparing the results with the peaks, gives better results.

According to our tests it is possible to stay in the time domain and detect breathing based on the top and bottom edge of the PPG signal. Our proposed algorithm receives PPG signal from the SpO2 sensor. FIR notch filter removes 50/60Hz and 100/120Hz noise. The PPG signal was also filtered with median filtering over 125 samples to remove small glitches and make the signal smoother. The signal was then normalized and DC part was removed. In the following algorithm, N represents the number of current sample and will be increased after next minimum or maximum point is found. There are five main steps that describe the algorithm in Figure 3.2.

1. Buffer the signal with length of five seconds
2. Detect and count number of local minimas $minP$ and maximas $maxP$
3. IF $maxP(N-1) > maxP(N) < maxP(N+1)$
   THEN found $maxPtrn \leftarrow 1$
4. IF $minP(N-1) < minP(N) > minP(N+1)$
   THEN found $minPtrn \leftarrow 1$
5. IF
   $minPtrn(startT) > maxPtrn(startT)$
   AND $minPtrn(startT) < maxPtrn(endT)$
   AND $minPtrn(endT) > maxPtrn(endT)$
   THEN found $doublePattern \leftarrow 1$

Figure 3.2: Algorithm1. Respiration extraction using pulse wave amplitude variation [57]

To analyse the signal we collect in step 1 five seconds of the signal into the buffer. In step 2, new local minimas $minP$ and maximas $maxP$, that arrive alternately with the continuous pulse wave, will be detected. In step 3, after finding a new local maxima $maxP(N)$, it will be compared with the previous one $maxP(N-1)$. If the previous maximum point $maxP(N-1)$ has larger amplitude than the last one, it will be included as a part of the detected pattern. If next local maxima $maxP(N+1)$ has bigger amplitude than the last one $maxP(N)$ then respiration pattern, based on the maximum points, has been found and value $maxPtrn$ gets value "1" or "TRUE". Same methodology is repeatead in step 4 but with the minimum points ($minP$). In step 5 we compare start $startT$ and end time $endT$ of the minimum and maximum patterns. If the minimum pattern has started and ended after the maximum one, then respiration signal has double detected, value $doublePattern$ gets "TRUE" and we can disregard last detected pattern.

Figure 3.3 describes the simplified block diagram of the proposed algorithm. There are three main parts for pattern detection. The first one is detecting patterns based on the local maxima, on the left side. Second one is detecting patterns based on the local minima. In the middle part, double patterns are detected and removed, if necessary. The logic of how double detected patterns were removed was described in Section 3.3.

3.3.3 Algorithm implementation

PPG signals are usually analysed in the wearable device for sleep apnea diagnosis. There are three main steps that are performed during the anal-

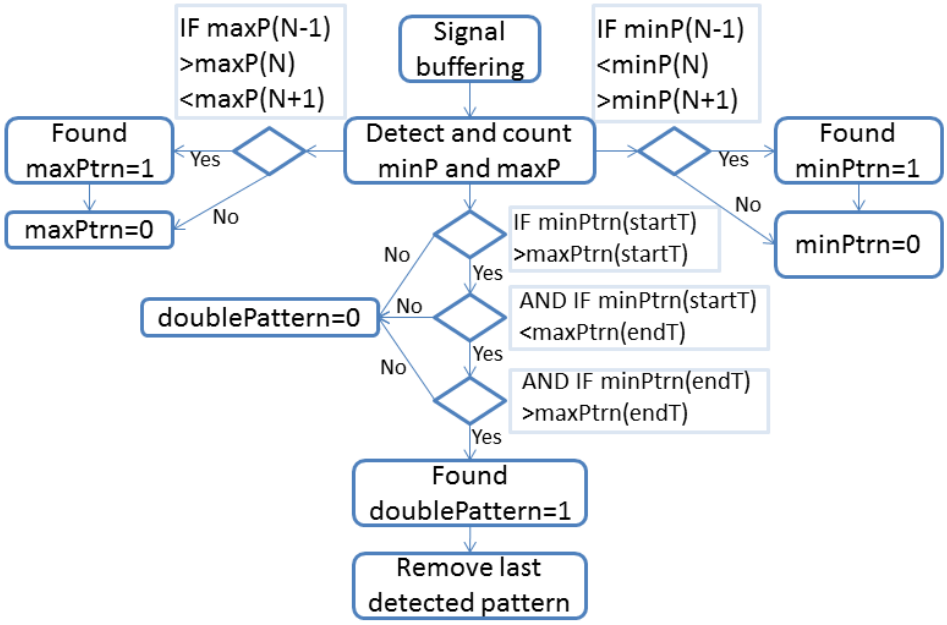

Figure 3.3: Block diagram of the proposed algorithm [57]

ysis - preprocessing, features extraction and classification, as described in Figure 3.4. Preprocessing stage removes artefacts and noise from the PPG signal. In the features extraction stage, respiration rate, heart rate, and SpO2 level are extracted. Classification stage depends on the goal of the processing. In our case, all signals, that are extracted, could be used for sleep quality diagnosis.

Most common source of interferences is the mains power and background lighting, that causes 50/60Hz sinusoidal spikes with its higher harmonics. Motion artifacts that are caused by poor contact to the photo sensor, need much more processing. There are two types of PPG measurements, transmittal and reflective. Although these two arrangements have no fundamental difference from the optics point of view, their practical properties and performance differ significantly with respect to the motion artifact, signal-to-noise ratio, and power requirements. Reflective PPG needs more secure attachment of the LED and photo-diode to the skin surface, when compared to transmittal PPG. Once an air gap is created between the skin surface and the optical components due to some disturbance, a direct optical path from the LED to the photo-diode may be created [31]. Possibility of using either method depends highly on the position from where the measurements will be taken. Attachment of the sensor on the right body location has direct impact to the signal amplitude. Low amplitude PPG signal is mostly caused by the automatic gain controller. Detecting heart beats from low amplitude the PPG signal is considered difficult. Under the placed position

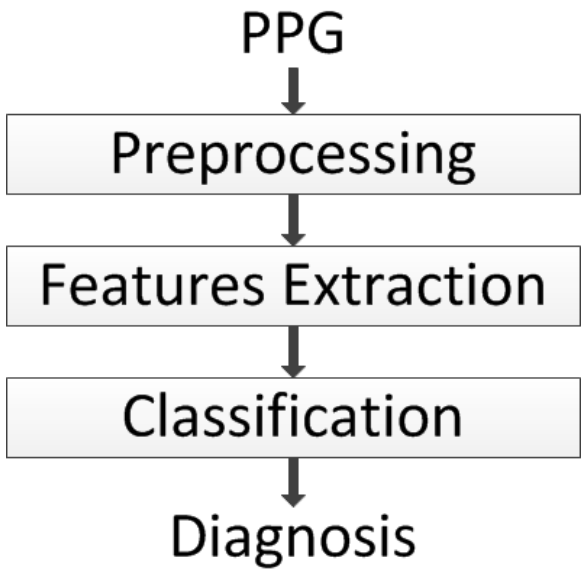

Figure 3.4: Three stages common structure of PPG diagnostic system [57]

there should be a thin epidermal tissue layer through which photons can reach the target blood vessels with less attenuation. In the arterial end of the capillaries the pressure is 30 to 40 mm Hg and in the venous ends 10 to 15 mm Hg [31]. Greater arterial pulsation than cutaneous pulsations in magnitude makes it less suspective to motion to the naturally higher internal pressure. Simultaneous measurements from different body positions increase measurement reliability. These factors generate several type of additive artifacts which may be contained within PPG signals. This may affect the extraction of features and hence the overall diagnosis, especially, when the PPG signal and its derivatives will be assessed in the algorithmic fashion.

3.3.4 Application areas

One possible application of the extracted respiration rate is OSA detection. There are certain thresholds that point to the apneic episode. Specific pattern for apneic episode was described in Chapter 3.1.4.

As the sleep apnea could be a result of arrhythmia, individual signals could be used in order to detect any critical changes. For sleep apnea detection and Apnea Hypopnea Index (AHI) calculation, respiration signal is mandatory. Implementing vital signal monitoring with the thresholds makes it possible to develop OSA screening application for home monitoring. It could be used in case sleep apnea is suspected or there is a recommendation from the doctor to monitor premature babies also at home

conditions. Figure 3.5 describes proposed algorithm that consists all main parts of the sleep apnea detection. It is capable to detect apneic cases to calculate AHI index.

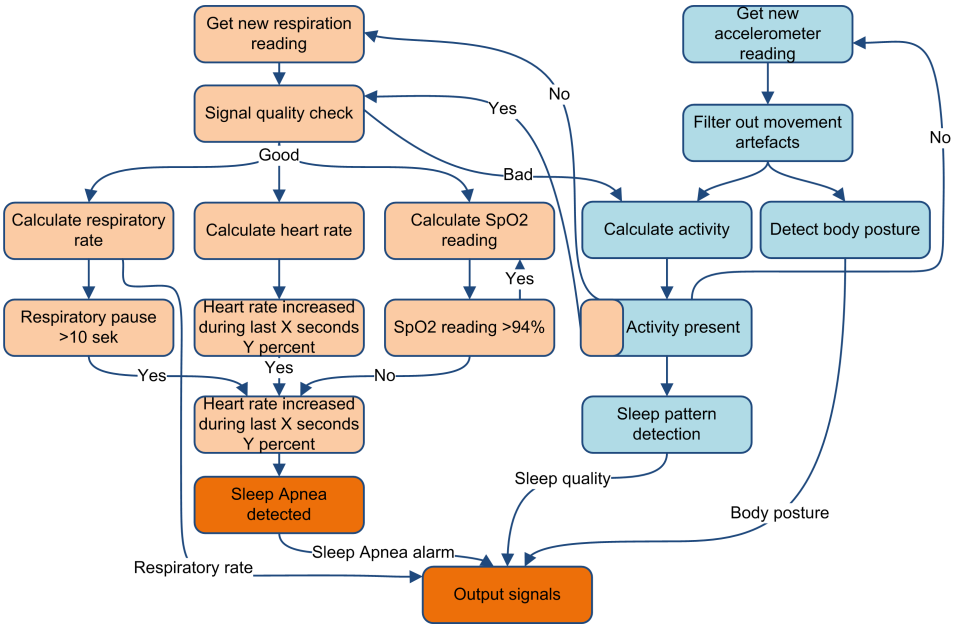

Figure 3.5: Sleep Apnea detection algorithm [55]

The purpose of this algorithm is to provide a general overview about all the steps that are needed to perform in order to process the acquired signal and provide output signals for the user feedback and further analysis. Many of these steps include sophisticated signal processing tasks. Describing individual steps in detailed level is not the scope of this chapter rather describe the architecture of proposed sleep apnea detection method.

3.4 Experimental results

An algorithm for respiration signal extraction from PPG signal has been implemented in MATLAB environment to perform experimental results. The aim of these experiments is to validate our proposed algorithm suitable for using on children.

3.4.1 Detection of respiration rate

Respiration causes variation in the peripheral circulation that affects the pulse wave. There is a great correlation between breathing effort and changes in the amplitude of pulse wave. Figure 3.6 describes the situation where the signal is clean and without any artefact. There are high and

low peaks on top and bottom of the high amplitude signal which describes the periodical amplitude variation that is caused by the respiration.

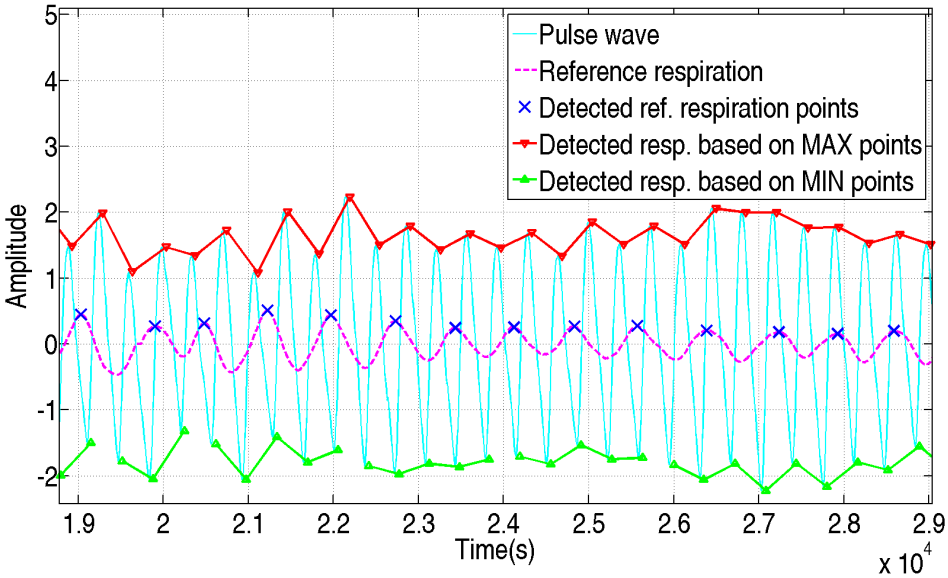

Figure 3.6: Correlation between the respiration and pulse wave [57]

Mean accuracy of the respiration detection of our method is 101.92% with the Standard Deviation (SD) of ±7.65%. Accuracy over 100% means that there were more respiration elements detected than exist in the reference signal. Table 3.1 describes tests with twelve different subjects to validate our proposed algorithm. First column is the signal name that corresponds to the name in the PhysioNet MIMIC II Waveform Database. Second column is the number of respirations in the reference signal. Next two columns describe the accuracy of minima and maxima based methods. Last column is the final accuracy we get after using both, minima and maxima based pattern detections and eliminating double patterns.

If we would use only local minima based detection, mean accuracy would be 80.28% ±5.36%. Maxima based detection rate has mean accuracy of 80.73% ±5.53%. There is a significant accuracy increase, 32.24% ±6.73%, using double pattern detection. It helps to increase the accuracy in the situation where the signal is distorted within some tens of milliseconds or DC component moves the signal baseline away from the zero point.

3.4.2 Comparison with other results

Mobile sleep apnea screening platforms have been in interest of different research groups. One similar platform was described in [50]. They connected several bio-sensors to the smart phone and use FFT to calculate

Table 3.1: Estimating the breathing rate with pulse wave amplitude variation detection [57]

Signal name	Ref. resp.	Accuracy (%)		
		Min based	Max based	Total
3000358_0010m	3972	76.86	82.30	101.33
3505210_0002m	4172	77.59	74.98	90.65
3470111_0006m	4095	78.44	79.61	104.66
3900726_0001m	4355	69.48	74.95	94.12
3601304_0001m	4139	84.13	86.25	111.11
3000858m	4376	81.67	81.26	92.62
3047119m	4065	90.09	91.76	114.32
3047445m	3465	85.83	84.27	108.54
3048124m	3748	77.51	76.25	95.84
3048455m	3553	80.86	80.83	102.26
3048754m	4232	75.21	71.15	96.93
3049672m	3578	85.63	85.16	110.65
Avarage		80.28 ±5.36	80.73 ±5.53	101.92 ±7.65

the heart and breathing rate. Oxygen saturation was calculated from the PPG signal. OSA estimation was done based on the heart rate and oxygen saturation rate because fluctuations in the blood oxygen level and heart rate are detected during the apnea periods. Spectral analysis of Arterial Oxygen Saturation (SaO2) or heart rate variability have been suggested as potential diagnostic tools for this disease [104]. Some studies show that some patients may not even have variations in SaO2 or heart rate signals, therefore pre-screening may not give adequate answer to the suspicions and full PSG is needed.

Because the SpO2 measurement accuracy is very sensitive to the body movements and amplitude of the pulse wave, several methods have been applied to suppress motion artefacts. Kalman filter has been used to improve the results to derive the pulse rate with 3% of error [103].

Table 3.2 compares different techniques to extract the respiration rate from the PPG signal. First column is a short name of the method, that is explained at the end of the table. Second column describes number of the subjects to validate the method. There is a difference in the age groups, described in the third column. Most of the algorithms are validated with mid-age adults not with neonates nor children as we have done, except one. Comparing the number of studies with adults and children, there is still need for extended research with neonates and children. As there are slight differences in signal waveforms between children and adults, there could be some deviations in the results when applying on children. Last column describes accuracy of extracting the respiratory information with the SD.

Comparing the PWV method with PRV and PAV, it has the most accurate results because PRV and PAV are more affected by the sympathetic modulation. The accuracy of our method is also comparable with the PTT method which needs ECG in addition to the PPG signal [16].

Table 3.2: Comparison of different respiration extraction methods [57]

Method	No of subj.	Age	Absolute accuracy
IMF	4	NA (adults)	99.48±0.44%
PRV	17	28.5±2.5	86.93±15.34%
PWV	17	28.5±2.5	101.27±7.81%
PAV	17	28.5±2.5	84.55±15.34%
PWV+PAV+PRV	17	28.5±2.5	99.74±7.30%
BML	10	25±3	98.63±1.24%
TMI	10	25±3	98.54±1.12%
PTT	15	4.47±2.04	100.96±9.26%
Our prop.	12	NA (neonates)	101.92±7.65%

*BML - beat morphology [102]; TMI - time interval [102]; IMF - Instrinsic Mode Functions; PRV - pulse rate variability [51];PAV - pulse amplitude variability [51]; PWV - pulse width variability [51]; PTT - pulse transit time [16]

Our proposed method, last row in the table, has excellent results compared with the other ones. The main difference is that our proposed algorithm has low computational needs and we stay in the time domain. That makes our proposed algorithm suitable for using on energy constrained embedded systems while still getting excellent results. We need to detect only amplitude minimas and maximas and compare those values with the previous ones. The most important requirement is a source signal with good quality that can be achieved with high-end electronics and different artefact suppression methods. It needs an extended testing and implementing various artifact suppression techniques to validate the accuracy in different real-time situations. Initial results show that using pulse wave amplitude variation based detection, it is possible to estimate the respiration signal with high confidence.

However there is a need for extended tests to demonstrate the reliability of our proposed algorithm in different real-life situations when there could be significant amplitude changes. To increase the accuracy of breathing rate estimation there is a need to identify and throw away distorted parts from the signal. There are many possibilities how pulse wave can be distorted which makes features extraction unusable. If we would use two optical sensors to measure the pulse wave, we could have significantly better signal quality. If readings from one sensor are out of limits or distorted, we could replace some parts of the signal with readings from the second one or estimate the signal with the help of second one. Another option is to increase

the number of wavelengths adding additional LEDs which could decrease the effect of artifacts with more sophisticated signal processing. Drawback of this solution is increased power usage due to the increased number of optical sensors. On the other hand, our goal is to increase the accuracy of the measurements from the optical sensors.

3.5 Chapter summary

To goal of this chapter was to present an algorithm for respiration signal extraction from pulse wave and provide a possible application areas such as sleep quality estimation and the diagnosis of sleep diseases. Using the prototype, described in Chapter 1.2, and optical sensors, described in Chapter 2.2, there was a need to apply signal processing to detect the pulse wave and extract interested signals. Proposed algorithm could be used for this purpose to extract the respiration rate and use it for further diagnosis.

The first part of this chapter gave a background information about the sleep and history of sleep research. There was also a discussion about sleep apnea and its classification to understand better the purpose of this work.

The second part of this chapter gave an overview which methods have been used for respiration signal extraction from pulse wave and how the respiration signal differs between different age groups.

The third part of this chapter introduced our proposed algorithm for respiration signal extraction from pulse wave using pulse wave amplitude variation. It was also discussed about possible application areas.

The fourth part of this chapter described experimental results how respiration signal was extracted. Comparison with other results gave a good overview about the efficiency of our proposed method. Our proposed algorithm had low computational needs that makes it suitable for using on energy constrained portable devices.

Chapter 4

Self-Awareness in Health Monitoring

During the continuous development remote monitoring health-care systems become smaller, more powerful and draw less energy. Those features increase the freedom to use them in more complex situations. Modular monitoring platform, proposed in Chapter 1, was designed taking into account possible future directions. Together with proposed optical sensors, described in Chapter 2, this system could be used for either long- or short-term monitoring purposes. As this system has several integrated sensors, it gives some level of awareness to estimate and analyze some of the most important parameters autonomously. To give systems some level of awareness is the future direction where smart devices will move. The objective of this chapter is to present this direction as one of the possible application areas of the proposed system.

In this chapter a self-aware health system is presented. To understand the concept of self-aware system, there is an explanation of situation awareness. The architecture for the first version of the prototype is proposed and tested in [83]. As the first version of the prototype was used for offline analysis, there is also a new version of the prototype presented that is capable to collect, abstract and categorize inputs from various sensors online. Main results of this chapter have been reported in [83].

4.1 Background

B.J. Baars observes that "like any other biological adaptation, consciousness is functional" [5]. The same can be claimed about awareness and indeed, the insight that a sense of awareness of a system's own situation can facilitate robust and dependable behavior even under radical environmental changes and drastically diminished capabilities, has resulted in a proliferation of work on self-awareness and other system properties such as

self-organization, self-configuration, self-optimization, self-protection, self-healing, etc., which are sometimes subsumed under the term "self-*". Thus, awareness enables to improve the behavior of systems, making them more robust and reducing processing, communication and energy requirements. However, designing and implementing it in an ad-hoc manner for every new system is not feasible. Introducing awareness as a separate concept in the Cyber-Physical System (CPS) infrastructure rather than as part of the application functionality, promises to simplify development and operation of such systems. As CPS are typically Systems of Systems (SoS), the awareness must be solved comprehensively, ensuring that the understanding of the situation is coherent and consistent across the SoS.

Self-awareness, situation awareness, and attention are key enablers for efficient Fog and Mist computing. Situation awareness [18] facilitates the continuous interpretation of the stream of data collected from the environment in the context of the goals and objectives of the CPS. A situation is defined by the values and interpretation of a set of situation parameters [82]. A situation parameter can be monitored or computed independently and represents a property of the situation of interest. In our example the information for generating situation awareness is exchanged by a proactive middleware, that is independent of the application functionality and can be considered as part of the CPS platform [83].

4.1.1 Fog and mist computing

Mist and fog computing are described in more detail in [83]. Due to its distributed and localized architecture, computing is a natural platform for a variety of critical Internet of Things (IoT) applications such as connected vehicles, smart grids, smart cities, and, in general, wireless sensor and actuator networks [10]. To that end several programming models and application frameworks have been developed for fog computing [92, 38]. However, in a strict definition of fog computing the devices at the very edge are not involved in computation but only in data acquisition while the interpretation occurs in the gateway. Hence, network delay and inefficient bandwidth utilization may still be problematic. Mist Computing pushes the processing even further to the edge of the network involving the sensor and actuator devices, thus decreasing latency further and increasing the autonomy of subsystems. In such scenarios awareness and self awareness of every individual device is critical as the computation and actuation is dependent on the individual device's perception of the situation. The challenge with implementing mist computing systems lies in the complexity of the resulting network and the interactions in the network, which must be managed by the devices themselves as central management of such systems is not feasible.

4.1.2 Situation awareness

To understand the essence of the self-aware system, it needs a specific terminology that is fully explained in [83]. Self-awareness monitors overall system performance in a dynamically changing environment. It includes self-monitoring, situation awareness and attention because the system must understand both its own state and the environmental conditions. A system that only tracks its own state has a very limited view of its situation.

Situation awareness enables the continuous interpretation of data collected from the environment in the context of the CPS's goals and objectives [25]. A situation is defined by the values and interpretation of a set of situation parameters [69]. A situation parameter can be monitored or computed independently and represents a property of the situation of interest. In our example, the information for generating situation awareness is exchanged via proactive middle-ware, which is independent of the application functionality and can be considered part of the CPS platform. Attention helps balance the competing tasks of collecting, processing, and responding to the data by prioritizing scarce system resources for the CPS's tasks and objectives. These priorities dynamically change depending on the situation and system state.

The concept of situation awareness originated in psychology, but its concepts are applicable to embedded systems. Just as humans process data from their senses to develop situation awareness, a CPS must be aware of its situation to perform optimally, as the "correct" behavior is dependent on the current situation. For instance, the meaning of a low fuel warning light in a vehicle is different when that vehicle is in the middle of a desert than when it is close to a gas station. Although the sensor value is identical, the interpretation of the sensor reading and consequent actions can be very different.

Complex phenomena require using data from several sensors with diverse modalities to generate an adequate level of situation awareness. The sensors may be attached to distinct, physically disjointed computing nodes, which presents the challenge of distributing the computation among individual nodes.

One example of distributed sensing and processing involves monitoring the human body during everyday activities. Evaluating the body's state requires measuring physiological parameters (such as heart rate) and interpreting their meaning (for example, the person is sleeping or running). Thus, sensors of different modalities must be attached to different areas of the body, leading to a distributed sensor system. However, wiring the human body is impractical, necessitating a network of autonomous wireless sensors.

4.2 Overview

The initial version of proposed system is presented in [83]. As it supports many different types of health care sensors and systems, the proposed modular health-monitoring system is one of the examples that could be integrated into this system. The most common way is to receive health related monitoring messages via smart-phone which requires installation of special software that is developed only for this type of sensor. Instead of our prototype, it can be any device and there are wide range of similar health-care devices on the market. All of them are designed for special purposes and send out health data that is analyzed by the software suitable only for that particular device.

There are several possible problems related to the smart-phones as a monitoring gateway for health-care devices. Up to 1-2 days long battery lifetime and in case the smart-phone has to be taken into use for other purposes, may interrupt health data receiving and analyzing. There are also applications that may automatically limit or turn off data, WIFI or Bluetooth connection if the phone is in standby mode to increase battery life. That makes smart-phone unreliable for automatic health-care data processing and alarming purposes.

To increase the reliability and make everything related to the device configuration, data reception and analysis invisible for the end-user, there can be independent self-aware health monitor installed to the home that takes care of everything in the background. All health-devices, that send out any data, are received by the self-aware health monitor, collected, abstracted, categorized and classified. The system has a knowledge about the status of connected devices, itself and could give a feedback depending on the current situation.

4.3 Self-aware health monitor

Figure 4.1 shows the conceptual architecture of a self-aware health monitor that makes use of the middleware ProWare and was developed at the Research Laboratory for Proactive Technologies at Tallinn University of Technology. The prototype monitor abstracts and classifies inputs from various sensors including altitude, location, heart rate, accelerometers, temperature, and oximeter and then compares the identified input pattern class with a pre-built or dynamically updated model. In the case of a mismatch, an anomaly signal is generated that induces attention. An attention control mechanism triggers the collection of complementary data or additional analysis steps if an anomaly appears and the analysis is not conclusive. Depending on the intensity and duration of the anomalous situation, the

monitor alerts the person or changes the health goal, thereby adapting to a new situation. In highly anomalous cases, it alerts other higher-level devices, emulating an emergency call.

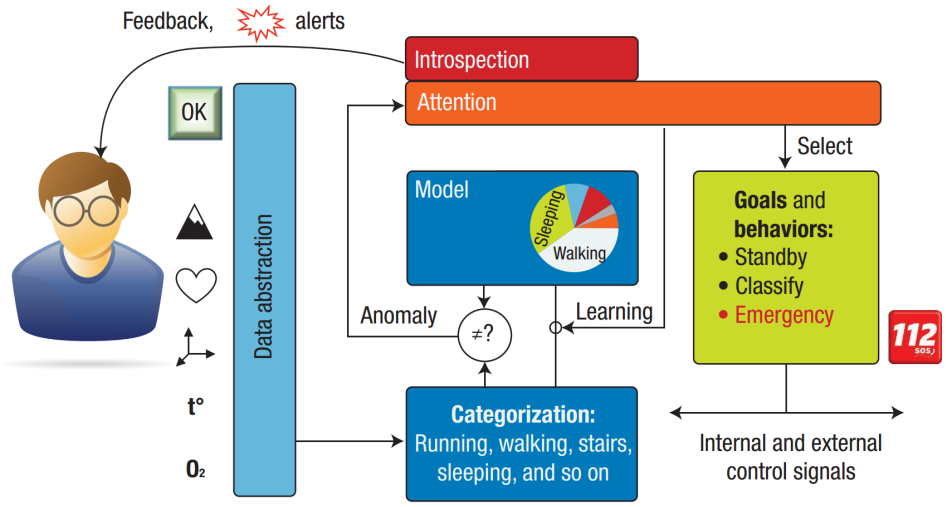

Figure 4.1: The architecture of a prototype self-aware health monitor [83]

Abstracting data in the sensor nodes reduces bandwidth and helps the system cope with changes to its structure. We apply the same mist computing principles to monitor vital human body parameters in the context of the individual's activity. In addition to the interpretation of sensor data differing in various situations, the fidelity of individual sensor data acquisition and processing is dependent on the person's activity—for example, monitoring requirements for sleeping are different from those for running. Monitoring requirements can be guided by a health practitioner, who could instruct the system in certain situations to increase the fidelity of monitoring or to log the data with finer granularity.

The situation parameter reflecting the heart rate is only meaningful in context. To evaluate whether a person's heart rate at a given moment is within a safe range, the algorithm must at minimum consider the specific current activity and the immediate history of activities, as it takes time for the human body to adapt to or recover from a specific activity. The larger context is also relevant: how well rested the person is, how much food has been consumed, and so on. In a health monitoring application, parameter types can reflect a person's activity (such as resting, walking, or running), the state of the body (stressed, rested, or tired), and the current physical load (high or medium).

Monitoring a person's daily activities has been an active research area for some time. Liang Dong and his colleagues placed several accelerometers on an individual, using a Kalman filter to track and classify the individ-

ual's daily physical routines [15]. The body segment status was categorized into static and dynamic, and further differentiated into periodical and non-periodical status using discrete Fourier transform. A hidden Markov model was used for training data and periodical movement modeling. The researchers reported overall classification accuracy at about 90 percent.

Davide Curone and his colleagues developed a similar physical activity assessment system for emergency intervention rescuers [13]. They integrated wearable electronics into textile fabrics to automatically identify potentially dangerous conditions for the monitored subject. The system achieved overall classification accuracy of 88.8 percent.

As these examples illustrate, the evaluation of a person's activity might use a range of sensors as input, and the sensor data must be interpreted differently for different activities. A heart rate of 130 might be normal for climbing stairs or jogging, but the same heart rate is worrying when the person is at rest or working at a desk.

4.4 System architecture

System design is a process that has many iterations. In this chapter we introduce the first version of the prototype that has limited functionality, and the second version that meets our requirements to perform real experiments.

4.4.1 Initial version of the prototype

To have a first proof of concept and develop the idea further a prototype with offline processing functionality was built. In this way it took the least amount of time to get first results, analyze these and continue with developing a prototype with real-time functionality that could also include the proposed modular platform.

The first version of the prototype is introduced in [83]. The heart rate data was logged using a BM-Innovations chest strap BM-CS5 [9]. The pulse rate was communicated once per second using the Bluerobin wireless protocol to the Texas Instruments eZ430-Chronos watch. The watch was equipped with an internal pressure sensor for altitude measurements. The heart rate and altitude were saved with a full time stamp temporarily in the internal memory of the watch. Data logs from the experiments were communicated to a PC for analysis using wireless SimpliciTI protocol.

For evaluating the activity of the person an accelerometer in a smartphone was used and the phone was carried in the pocket of the subject during experiments. The G-Sensor Logger Android application was used to collect accelerometer measurements.

4.4.2 A prototype with real-time functionality

To automate the manual work during experiments and simulate more real-life situations, the second version of the prototype was developed. Although, it is not yet published at the time of writing, first experimental tests were performed and there are high expectations on this version. The architecture of the new prototype is depicted on Figure 4.2. Green color modules are communicating with BLE protocol. Orange color boxes are using WSN protocol for long range communication.

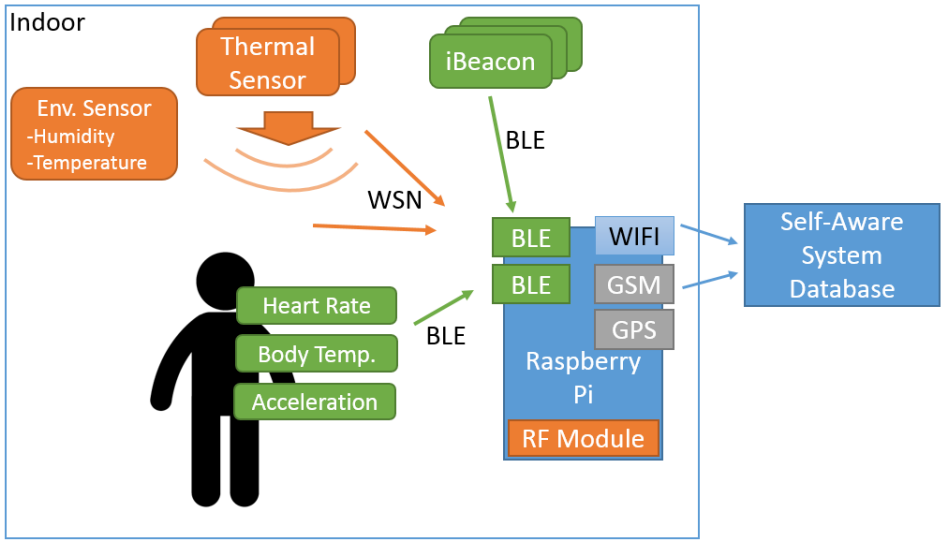

Figure 4.2: The architecture of self aware system

The system is suitable for using in indoor and outdoor. The main functionality has built into the Raspberry Pi module. There are two BLE modules connected to it. The reason for two modules is that to detect iBeacons, transceiver must be in receiving mode all the time. iBeacon is a protocol standardized by Apple to broadcast the identifier of the device to nearby portable electronic devices. The technology enables smart-phones , tablets and other devices to perform actions when in close proximity to an iBeacon [39]. The purpose of using iBeacons is to detect the location of human for indoor positioning. There is no limitation how many iBeacons can be used but we have chosen currently to use three of them concurrently in order to perform triangulation for exact positioning.

The second BLE modules is used to connect to the BLE peripheral devices. Peripheral device can advertise, to let other devices know that it's there, but it is only a Central that can actually send a connection request to estalish a connection. When a link has been established, the Central is sometimes called a Master, while the Peripheral could be called a Slave. It

is possible to have established connections with many peripheral devices. However, it is not possible to have a connection with peripheral device and also listen for advertisements from iBeacons using the same radio. In our case, we are using a SensorTag [44] and Polar H7 chest strap [78] as a peripheral devices. With the SensorTag, it is possible to to receive acceleration and body temperature information. Body temperature is measured with infrared temperature sensor together with ambient temperature. Polar H7 chest strap is used for heart rate measurements on the chest.

One of the possible use case of self-aware system is to detect lying human on the floor. This becomes more important for elderly people monitoring. Similar functionality has been studied in [70] using non-contact D6T-44L thermal sensors from Omron [76]. The sensor has chip arrays of 16 channels (4x4) to measure the surface temperature of an object. It can be used for detecting the presence of human beings by detecting the far-infrared ray of an object. For human detection the sensor is placed to the ceiling. The data about temperature readings is sent over wireless link to the Raspberry Pi.

Raspberry Pi has been chosen as a gateway because of the functionality. It has powerful processor, enough internal storage, possibilities for different communication interfaces and reasonable price. GPS module connected to the Raspberry adds possibility to perform locationing in outdoor conditions. GSM module makes possible to exchange real-time data between the Raspberry Pi and rest of the self-aware system. Instead of using GPS and GSM modules connected to the Raspberry Pi, it could also be a smartphone that collects the GPS data and use smart-phone as a WIFI hotspot for data connection. For research purposes and easier administration we have chosen the version depicted on Figure 4.2.

All data that is collected by the Raspberry Pi is sent to the Self-Aware Health sytem database for further processing. The communication between the server and client is implemented using Node.js architecture. It is an open-source, cross-platform runtime environment for server-side and networking application written in JavaScript. It is widely used in real-time web applications. On server side, data is saved into MySQL database.

4.5 Experimental results

Even though the complete system of Figure 4.2 has not yet been realized, we conducted a series of experiments in a health monitoring scenario to validate key assumptions and show the viability of identification of awareness properties in a mist computing approach. The data relevant for situation assessment was collected from individual sensors.

In the experiments a test person was involved in the following activities:

resting on a couch, working at a table, walking slowly indoors, climbing stairs indoors and walking at a rapid pace outdoors. The sensors used in the tests were accelerometer, altitude meter and a heart rate monitor.

The collected data was analyzed to determine if local situation assessment by combining data from individual embedded sensor nodes is feasible. Although the collected data was analyzed off-line the algorithms applied are sufficiently light-weight to be executable in embedded low-power computing nodes.

The data logged during the tests from all the sensing devices was analyzed with MATLAB. Our aim was to investigate if the performed activities can be detected (i.e., situation parameter values determined) from individual data streams.

As noted above, the sampling rate for pulse rate and altitude estimate was 1Hz while the average sampling rate for the accelerometer was 16Hz, therefore the raw sensor data was synchronized before analysis. We employed the modulus of the acceleration vector

$$|a| = \sqrt{a_x^2 + a_y^2 + a_z^2}, \tag{5}$$

to estimate the personal activity level, which proved to be sufficient.

Figure 4.3 (a) depicts the average values of observed pulse rates and acceleration over 10-second periods. Figure 4.3 (b) depicts the average values of observed pulse rates and acceleration over 10-second periods.

The results from the different experiments populate distinct areas in the pulse rate/activity space. The activities of sitting, driving, indoor walking, and outdoor walking can be well categorized using only two sensors: the pulse rate meter and the accelerometer. However, stair climbing forms a rather large area in the pulse rate/accelerometer space, triggering the attention mechanism to seek further data from the altitude sensor. The additional data allows the health monitor to identify the activity as stair climbing and to distinguish between moving upward (green) and downward (blue).

The results from different experiments populate rather distinct areas in the pulse rate/activity space. The activities sitting, car driving, indoor walking, outdoor walking can be well categorized using only two sensors, the pulse rate meter and the accelerometer. However, the green and cyan dots (stair climbing) form a rather large area in the pulse rate/accelerometer space triggering the attention mechanism to consult further data from the altitude sensor. These additional data allow to identify the activity as stair climbing and to distinguish between moving upwards (green) and moving downwards (cyan). More generally, this illustrates the benefit of attention directed data collection and analysis. If data from a few sensors, processed with a simple analysis algorithm, comes to an unambiguous con-

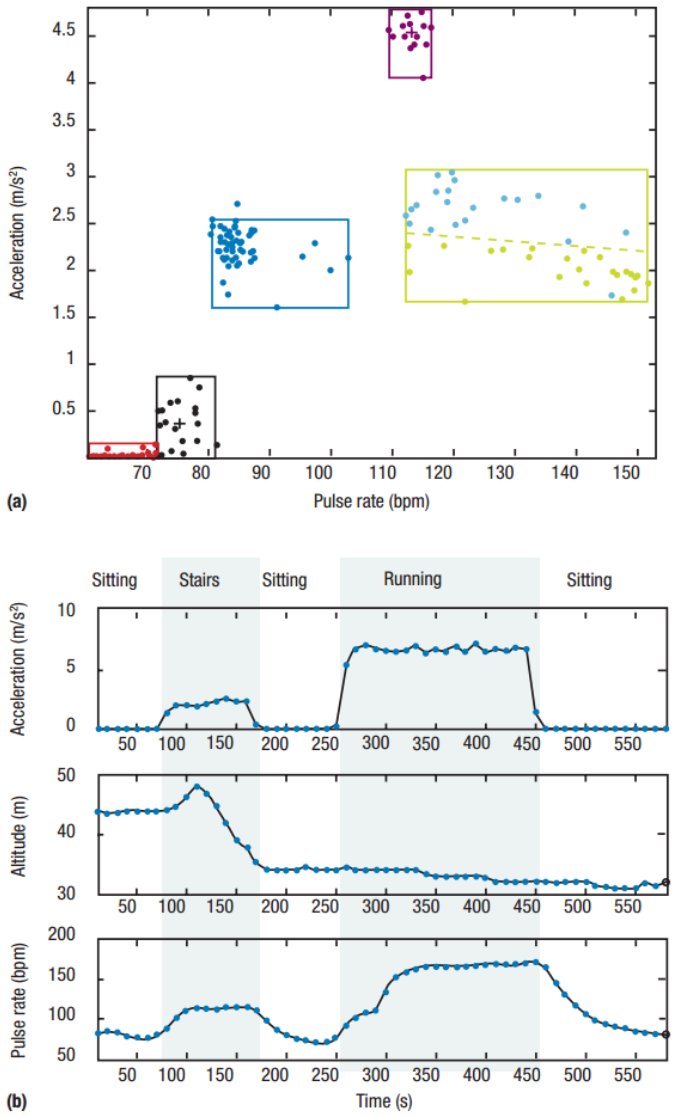

Figure 4.3: Experimental evaluation results. (a) Pulse rate versus activity, sitting or resting (red), driving a car (black), indoor slow walking (dark blue), outdoor rapid walking (magenta), walking upstairs (green), and walking downstairs (light blue). (b) The modes are correctly tracked as the subject performs different activities.

clusion, unnecessary data collection and processing is avoided. Only cases when anomalies are detected or the analysis is inconclusive warrant a more elaborate and expensive procedure of data collection, communication and computing. Thus, attention based sensing and analysis has potential to

save significant time and energy. To quantify this potential in various applications remains the objective in future work.

It has to be taken into account that these states in the figure are mostly what can be considered the steady states for given exercises, although some transitional states are also observed (the samples between the boxes). Pulse rate changes are never instantaneous. This is clearly visible in the right side of Figure 4.3 that depicts a series of exercises explains why the temporal aspect of human physiology must be considered.

From the experiments it can be concluded that relatively simple sensors can be used to determine the activity the person is involved in and correlate physiological parameters to individual activities. Moreover, most of the time only a subset of the available sensors have to be employed leading to a lean approach of monitoring.

For a more accurate estimation, however, additional phenomena need to be measured. Naturally such a monitoring system must adapt to an individual but once the adaption phase is complete, the CPS is able to monitor the person and determine if the physiological parameters are within the typical range for a given activity.

4.6 Chapter summary

Self-awareness, situation awareness and attention are powerful concepts with the potential to lead to high efficiency in various sensor and actuator networks. Inspired by biological example, studies and proposals that touch upon various aspects of self-awareness have proliferated during recent years. Still, its potential is hardly understood and by far not yet exploited. Contributing to this broad effort, we have explored situation awareness and attention, concluding that the principles of generating situation awareness using the situation parameter concept are well applicable for health monitoring. We argue that situation awareness is an inherent part of self-awareness. A system has to know its own inner state (self-awareness in a narrow sense) and where it is in the world and what the environment looks like to make a proper assessment of its own state and performance. Only with the understanding of the context it is justified to call the system self-aware in a broader sense.

Situation awareness is jointly generated by a group of sensors, thus distributing the burden over several nodes and leading to Fog computing. Fairly simple algorithms, executed by resource constrained embedded nodes, compute the situation parameters.

We have shown in our experiments with only three sensors (for pulse rate, acceleration, altitude) how the different measurements complement each other to allow for a precise assessment of typical activities and how

attention can steer data collection and processing for the benefit of lean and efficient system. Multiple sensors facilitate distributed data collecting and processing based on fog and mist computing paradigms.

In this chapter the working prototype of initial self aware health-system was introduced. Also the definition of self-aware system and situation awareness was discussed to give a better overview how the data from sensor networks could be processed in more efficient way. Initial experiments show the potential how simple sensors can be used to determine the activity and correlate it physiological parameters of the human.

Chapter 5

Conclusions and Future Work

The discussion about methods to speed up health care monitoring experiments in different application areas is summarized. As a result the proposed hardware solution to perform such experiments would give a valuable benefit designing further open-source platforms. In this chapter we summarize the thesis and discuss about possible directions for future research.

5.1 Conclusions

This thesis is focusing on the personalized health care that requires new type of technological solutions to support this direction. One part of this ecosystem is modular, small size and portable health monitoring devices that does not require highly qualified medical personnel to use it. As the health care covers all age groups and wide range of diseases there is a need for modular solutions that bring down health care costs, have some level of autonomy and are easy to handle. Proposed architecture in this thesis is one possible solution for these issues. Also some use cases for different diseases and age groups were demonstrated.

We have proposed a portable modular architecture for health care monitoring. Its small dimensions together with high flexibility and modularity make this solution usable from infants up to elderly people. There is readiness to extend system functionality with new type of modules. Two use cases were presented to demonstrate system capabilities. Foot sensor for sleep quality analysis for infants and smart sensor for pulse wave detection for adults. A working prototype was built and tested on the first test subjects. All technical functionality was implemented and tested with built-in software tests.

New type of dual optical sensor was developed to increase the noise immunity caused by the movements. On one hand, infants need always special care and developing unobtrusive sensors is complicated, on the other hand

sleep analysis on infants need unobtrusive sensors with good source signal. Proposed solution is using dual optical sensors to increase the quality of optical signal by analyzing continuously signal to noise ratio and choosing the best signal source. Compared to conventional optical sensors with one optical element we get increased noise immunity but also slightly increased energy consumption. First version of the prototype was developed and tested in-together with modular platform. Although some physical connection errors on the sensor appeared, initial tests were performed successfully. First tests showed that having multiple optical sensors with adaptive source signal selection helps to improve overall quality of the optical signal.

Smart photoplethysmographic sensor was developed for pulse wave detection from different tissue layers. Its main purpose is to detect the location and pulse wave only from arteries. As one application, this type of optical sensor decreases the time needed for the measurement of arterial stiffness. Initial results with adults showed that it is possible to detect the location of artery.

Respiration extraction algorithm from pulse wave with low computational requirements was proposed for portable health monitoring devices. The main difference is that our proposed algorithm has low computational needs and we stay in the time domain. That makes our proposed algorithm suitable for using on energy constrained embedded systems while still getting excellent results. The most important requirement is a source signal with good quality that can be achieved with high-end electronics and different artifact suppression methods. First experiments with clinically validated signals gave excellent results with low computational requirements. Experiments were performed using signals measured from toddlers and children.

As health care is moving more and more into everyone's home, it requires increased autonomy. There is a need for better understanding about the conditions person is being monitored and how to take environmental changes into account. We have proposed a self-aware health care system that could help to add some level of situation awareness and avoid unexpected results. First version of the prototype was built for proof of concept. Results with this prototype were promising to develop this idea further and continue with the experiments with the second version of the prototype. The second version of the prototype had a real-time data analysis functionality. By integrating various health-care and environmental sensors it was possible to increase the quality of the decisions.

5.2 Future Work

There is a wide range of possible directions how this work could be further extended. Some of most relevant ones are discussed below.

Proposed modular system is a good starting point to provide an open-source platform to perform different kind of measurements. Developing new type of modules helps to extend system functionalities into different health care areas. This kind of platform could become a standard that is used for research experiments and as first prototype for developing a new type of wearable device. Open-source hardware together with firmware helps to build the community that takes care of developing these ideas even further. Sharing existing design under the GPL license would give the biggest benefit for others.

Proposed smart photoplethysmographic sensor is planned with increased capabilities and reduced dimensions. As current prototype was the initial attempt with successful results to prove the idea, it is the starting point do develop it further and perform additional experiments with larger number of test group.

Proposed self-aware health system is the first version of real-time system that implements wide range of sensors for health care monitoring. Middle-ware, that takes care of decisions and provides situation awareness capabilities needs more focus. As it is complex system that needs cooperation in different areas the development continues in hardware compatibility, software functionality and learning method direction.

Bibliography

[1] N.J. Ali, D. Pitson, and J.R. Stradling. Natural History of Snoring and Related Behavious Problems Between the Ages of 4 and 7 Years. *Arch. Dis. Child*, 71:74–76, 1994.

[2] John Allen. Photoplethysmography and Its Application in Clinical Physiological Measurement. *Eur J Pain*, 8:163–71, 2007.

[3] R. R. Anderson and J. A. Parrish. The optics of human skin. *J. Invest. Dermatol.*, (77):13–9, 1981.

[4] T. Aoyagi, M. Fuse, N. Kobayashi, and et al. Multiwavelength Pulse Oximetry: Theory for the Future. *Anaesthesia and Analgesia*, 105(6):53–58, Dec 2007.

[5] B. Baars. A Cognitive Theory of Consciousness. *Cambridge University Press*, 1989.

[6] R. Bailon, L. Sornmo, and P. Laguna. A Robust Method for ECG-based Estimation of the Respiratory Frequency During Stress Testing. *TBME*, 53(7):1273–1285, 2006.

[7] Bluegiga Technologies. Maximize throughput with the BLE112/BLED112, 2014. [WWW] https://bluegiga.zendesk.com/entries/22400867–HOW-TO-Maximize-throughput-with-the-BLE112-BLED112.

[8] Bluetooth SIG. *Health Device Profile.* [WWW] https://www.bluetooth.org.

[9] BM-Innovations. BM-Innovations chest strap BM-CS5, 2015. [WWW] http://bm-innovations.com.

[10] Flavio Bonomi, Rodolfo Milito, Jiang Zhu, and Sateesh Addepalli. Fog computing and its role in the internet of things. In *Proceedings of*

the First Edition of the MCC Workshop on Mobile Cloud Computing, MCC '12, pages 13–16, New York, NY, USA, 2012. ACM.

[11] R. Boushel and C.A. Piantadosi. Near-infrared spectroscopy for monitoring muscle oxygenation. *Acta Physiol Scand*, 68:615–22, 2000.

[12] N.A. Collop and S.L. Tracy. Obstructive Sleep Apnea Devices for Out-Of-Center (OOC) Testing: Technology Evaluation. *Clin. Sleep Med*, 7(5):531–548, Oct 2011.

[13] D. Curone, A. Tognetti, and E. L. Secco et al. Heart Rate and Accelerometer data Fusion for Activity Assessment of Rescuers During Emergency Interventions. *ICSENS*, 14(3):702–710, May 2010.

[14] Cypress Semiconductor Corporation. 1-Mbit Serial FRAM Datasheet, 2015. [WWW] http://www.cypress.com/?docID=48138.

[15] Liang Dong, J. Wu, and X. Chen. Real-Time Physical Activity Monitoring by Data Fusion in Body Sensor Networks. *10th Int. Conf on Inf. Fusion*, pages 1–7, Jul 2007.

[16] E.Gil, R. Bailon, and J.M. Vergara. PTT Variability for Discrimination of Sleep Apnea Related Decreases in the Amplitude Fluctuations of PPG Signal in Children. *IEEE Transactions of Biom. Eng.*, 57(5):1079–1088, May 2010.

[17] Salvatore Emma. A Brief Look at ECG Sensor Technology, 2015. [WWW] http://www.mdtmag.com/articles/2011/08/brief-look-ecg-sensor-technology.

[18] Mica R. Endsley. Design and evaluation for situation awareness enhancement. In *Proceedings of the Human Factors and Ergonomics Society 32th Annual Meeting*, pages 97–101, 1988.

[19] eOrtopod. Foot Anatomy, 2015. [WWW] http://www.eorthopod.com/foot-anatomy/topic/30.

[20] FFT Designer. Tutorial 1. Creating and Testing MSP430 FFT Code, 2015. [WWW] http://www.fftdesigner.com/tutorial_1/.

[21] Jens Fiala, R. Gehrke, N. Weber, and et al. Implantable Optical Sensor for Continuous Monitoring of Various Hemoglobin Derivatives and Tissue Perfusion. *ICSENS*, pages 1971–1974, 2009.

[22] S.G. Fleming and L. Tarassenko. A Comparison of Signal Processing Techniques for the Extraction of Breathing Rate from the Photoplethysmogram. *World Academy of Science*, 2007.

[23] Food and Drug Administration. Is The Product A Medical Device?, 2015. [WWW] http://www.fda.gov/MedicalDevices/DeviceRegulationandGuidance/Overview/ClassifyYourDevice/ucm051512.htm.

[24] Freescale Semiconductor. Pulse Oximeter Fundamentals and Design, 2015. [WWW] http://www.freescale.com/files/32bit/doc/app_note/AN4327.pdf.

[25] Sigmund Freud. *Dora: An Analysis of a Case of Hysteria*. Touchstone, New York, 1997.

[26] T. Gislason and B. Benediktsdottir. Snoring, Apneic Episodes, and Nocturnal Hypoxemia Among Children 6 Months to 6 Years Old. *CHEST*, 107:963–66, Apr 1995.

[27] A.L. Goldberger and L.A.N. Amaral. PhysioBank, PhysioToolkit, and PhysioNet: Components of a New Research Resource for Complex Physiologic Signals. *Circulation*, 101(23):215–220, Jun 2000.

[28] A. Grabovskis and Z. Marcinkevics et al. Usability of photoplethysmography method in estimation of conduit artery stiffness. *Biomedical Optics*, Jun 2011.

[29] Reut Gruber, A. Sadesh, and A. Raviv. Instability of Sleep Patterns in Children with Attention-deficit Hyperactivity Disorder. *Am. Acad. Child. Adolesc. Psych*, 39(4):495–501, April 2000.

[30] C. Guilleminault and R. Korobkin. A Review of 50 C hildren with Obstructive Sleep Apnea Syndrome. *Lung*, 159:275–287, 1981.

[31] John Hall. *Textbook of Medical Physiology*. Saunders, Philadelphia, PA, 2000.

[32] harward Medical School. Why Do We Sleep, Anyway, 2015. [WWW] http://healthysleep.med.harvard.edu/healthy/matters/benefits-of-sleep/why-do-we-sleep.

[33] A. B. Hertzman. The blood supply of various skin areas as estimated by the photoelectric plethysmograph. *Am. J. Physiol.*, 124:328–340, 1938.

[34] A. B. Hertzman and J. B. Dillon. Distinction between arterial, venous and flow components in photoelectric plethysmography in man. *Am. J. Physiol.*, 130:177–185, 1940.

[35] Timothy F. Hoban. Assessment and Treatment of Disturbed Sleep in Attention Deficit Hyperactivity Disorder. *Expert Review of Neurotherapeutics*, 4(2):307–316, Mar 2004.

[36] Timothy F. Hoban. Sleep Disorders in Children. *Ann. N. Y. Acad. Sci.*, 1184:1–14, 2009.

[37] Timothy F. Hoban. Pediatric plysomnography, 07 2012.

[38] Kirak Hong, David Lillethun, Umakishore Ramachandran, Beate Ottenwälder, and Boris Koldehofe. Mobile fog: A programming model for large-scale applications on the internet of things. In *Proceedings of the Second ACM SIGCOMM Workshop on Mobile Cloud Computing*, MCC '13, pages 15–20, New York, NY, USA, 2013. ACM.

[39] ibeacon.com. iBeacon, 2015. [WWW] http://www.ibeacon.com/what-is-ibeacon-a-guide-to-beacons/.

[40] IDTechEx. Wearable Sensors 2015-2025: Market Forecasts, Technologies, Players, 2015. [WWW] http://www.idtechex.com/research/reports/wearable-sensors-2015-2025-market-forecasts-technologies-players-000431.asp.

[41] iHealth Lab Inc. Wireless Blood Pressure Monitor, 2015. [WWW] http://www.ihealthlabs.com/blood-pressure-monitors/wireless-blood-pressure-monitor/.

[42] iHealth Lab Inc. Wireless Pulse Oximeter, 2015. [WWW] http://www.ihealthlabs.com/fitness-devices/wireless-pulse-oximeter/.

[43] Schlumberger Excellence in Education Development. History of Medicine, 2015. [WWW] http://www.planetseed.com/relatedarticle/20th-century-and-drugs-treat-sicknesses.

[44] Texas Instruments. SensorTag, 2015. [WWW] http://www.ti.com/sensortag.

[45] W.S. Johnston and Y. Mendelson. Extracting Breathing Rate Information from a Wearable Reflectance Pulse Oximeter Sensor. *IEMBS*, 2:5388–5391, 2004.

[46] Yeun-Ho Joung. Development of Implantable Medical Devices: From an Engineering Perpective. *Int. Neurourol. J.*, 17(3):98–106, Sep 2013.

[47] J. M. Kang and T. Yoo et al. A Wrist Worn Integrated Health Monitoring Instrument with a Tele-Reporting Device for Telemedicine and Telecare. *TIM*, 55(5):1655–61, Oct 2006.

[48] E.S. Katz and J. Lutz. Pulse Transit Time as a Measure of Arousal and Respiratory Effort in Children with Sleep-Disordered Breathing. *Pediatric Research*, 53(4):580–588, Feb 2003.

[49] R. Krishnan and B. Natarajan et al. Two-Stage Approach for Detection and Reduction of Motion Artifacts in Photoplethysmographic Data. *Biomed. Eng.*, 57(8):1867–1876, Aug 2010.

[50] S.C.K. Lam and Kai Lap Wong. A Smartphone-centric Platform for Personal Health Monitoring Using Wireless Wearable Biosensors. *ICICSdiatrics*, pages 1–7, 2009.

[51] J. Lazaro and E. Gil. Deriving Respiration From the Pulse Photoplethysmographic Signal. *Computing in Cardiology*, 38:713–716, 2011.

[52] B.L.; Xu W. et al. Lee, S.; Ibey. Processing of pulse oximeter data using discrete wavelet analysis. *IEEE Trans. Biomed. Eng.*, (52):1350–1352, 2005.

[53] J.; Baek H.-J. Lee, B.; Han and et al. Improved estimation of motion artifacts from a photoplethysmographic signal using a Kalman smoother with simultaneous accelerometry. *Physiol. Meas.*, (31):1585–1603, 2010.

[54] M. Leier and K. Pilt et al. Smart Photoplethysmographic Sensor for Pulse Wave Registration at Different Vascular Depths. *EMBC*, Aug 2015.

[55] M. Leier and G. Jervan. Sleep Apnea Pre-Screening on Neonates and Children with Shoe Integrated Sensors. *Norchip*, pages 1–4, 2013.

[56] Mairo Leier and G. Jervan. Miniaturized Wireless Monitor for Long-term Monitoring of Newborns. *BEC*, 10 2014.

[57] Mairo Leier and G. Jervan. Respiration Signal Extraction from Photoplethysmogram Using Pulse Wave Amplitude Variation. *ICC*, pages 3535–3540, Jun 2014.

[58] P. A. Leonard and J. G. Douglas. A Fully Automated Algorithm for the determination of Respiratory Rate From the Photoplethysmogram. *Clinical Monitoring and Computing*, 20:33–36, 2006.

[59] Keija Li and S. Warren. Initial Study on Pulse Wave Velocity Acquired from One Hand Using Two Synchronized Wireless Reflectance Pulse Oximeters. *IEMBS*, Sep 2011.

[60] LifeSync. Wireless ECG/EKG System, 2015. [WWW] http://lifesynccorp.com/products/wireless-ecg-system.

[61] L.G. Lindberg and P.A. Oberg. Photoplethysmography. Part 2. Influence of light source wavelength. *Med. Biol. Eng. Comput.*, 29:48–54, 1991.

[62] C. Linti, H. Horter, and P. Osterreicher. Sensory Baby Vest for the Monitoring of Infants. *BSN*, pages 133–137, Nov 2006.

[63] S. Loukogeorgakis, R. Dawson, and N. Phillips et al. Validation of a device to measure arterial pulse wave velocity by a photoplethysmographic method. *Physiol Meas.*, (23):581–96, 2002.

[64] Luna. Luna bed cover, 2015. [WWW] http://lunasleep.com/.

[65] M. Maattala, A. Konttila, and E. Alasaarela. Optimum Place for Measuring Pulse Oximeter Signal in Wireless Sensor-Belt or Wrist-Band. *ICCIT*, pages 1856–1861, 2007.

[66] K. Madhav, Venu and R. Ram, M. Estimation of Respiration Rate from ECG, BP and PPG signals using Empirical Mode Decomposition. *I2MTC*, pages 1–4, May 2011.

[67] K. Venu Madhav, M. Raghuram, and E. H. Krishna. Monitoring Respiratory Activity Using PPG Signals by Order Reduced-Modified Covariance AR Technique. *iCBBE*, pages 1–4, Jun 2010.

[68] J. M. May, P. A. Kyriacou, and A. J. Petros. Development of an Optoelectronic Sensor for the Investigation of Photoplethysmographic Signals from the Anterior Fontanel of the Newborn. pages 18–21, 2011.

[69] Alain Morin. Levels of Consciousness and Self-Awareness: A Comparison and Integration of Various Neurocognitive Views. *Consciousness and Cognition*, 15(2):358–371, Feb 2006.

[70] Christel Nilsen. Localization methods for elderly people assistance. Master's thesis, Tallinn Univ. of Technology, Dep. of Comp. Eng., 2015.

[71] Lena Nilsson and A. Johansson. Respiration Can be Monitored by Photoplethysmography with High Sensitivity and Specifity Regardless of Anaesthesia and Ventilatory Mode. *Acta Anaesthesiol. Scand.*, 49(8), Sep 2005.

[72] M. Nitzan, A. Romen, and R. Koppel. Pulse oximetry: fundamentals and technology update. *Medl Devices*, page 231–239, Jul 2014.

[73] N.M. Noor and M.N. Taib. Using Pulse Oximetry Method as a Non Invasive Indicator of Blood Perfusion in Neonates. *ICICI-BME*, pages 254–8, Nov 2011.

[74] L. M. O'brien and D. Gozal. Consequences of Obtructive Sleep Apnea Syndrome. pages 211–222, 2005.

[75] Am. Acad. of Sleep Med. The AASM manual for the Scoring of Sleep and Associated Events. 2007. [WWW] http://www.nswo.nl/userfiles/files/AASM

[76] Omron. *D6T Thermal Sensors*. [WWW] http://www.omron.com/ecb/products/pdf/en-d6t.pdf.

[77] Philips. Stardust II Sleep Recorder, 2014. [WWW] http://www.healthcare.philips.com/main/homehealth/sleep/stardust.

[78] Polar. H7 heart rate sensor, 2014. [WWW] http://www.polar.com/en/products/accessories/H7_heart_rate_sensor.

[79] Richard. A. Polin and William W. Fox. *Fetal and Neonatal Physiology*. W. B. Saunders Company, 1992.

[80] D. Potuzakova and W. Chen. Innovative design for Monitoring of Neonates Using Reflectance Pulse Oximeter. In *7th ICIE*, 2011.

[81] PR Newswire. Monitoring and Diagnostic Devices to Drive the Global Wearable Medical Devices Market, 2015. [WWW] http://www.prnewswire.com/news-releases/monitoring-and-diagnostic-devices-to-drive-the-global-wearable-medical-devices-market-at-a-213-cagr-through-2020-296689841.html.

[82] J. Preden, J. Llinas, G. Rogava, R. Pathma, and L. Motus. Online data validation in distributed data fusion. In T. Pham, M. A. Kolodny, and K. L. Priddy, editors, *Ground/Air Multisensor Interoperability, Integration, and Networking for Persistent ISR IV: SPIE Defense, Security and Sensing*. SPIE - International Society for Optics and Photonics, 2013.

[83] Jurgo S. Preden, K. Tammemae, A. Jantsch, and M. Leier et al. The Benefits of Awareness and Attention in Fog and Mist Computing. *IEEE Computer*, pages 37–45, Jul 2015.

[84] S. Qurat-ul Ain Ali and V. Jeoti. DWPT Based Sleep Apnea Detection. *NPC*, pages 1–4, Sep 2011.

[85] M. Raghu Ram, K. V. Madhav, and E. H. Krishna. Computation of SpO2 Using Non-parametric Spectral Estimation Methods from Wavelet Based Motion Artiface Reduced PPG Signals. *ICSCCN*, pages 776–780, July 2011.

[86] Y. Rimet and Y. Brusquet. Surveillance of Infant at Risk of Apparent Life Threatening Events (ALTE) with the BBA Bootee: a Wearable Multiparameter Monitor. *EMBS*, pages 4997–5000, Aug 2007.

[87] E. Saadatian, S.P. Iyer, and O.N.N. Fernando. Low Cost Infant Monitoring and Communication System. *CHUSER*, pages 503–508, 2011.

[88] J.W. Salyer. Neonatal and Pediatric Pulse Oximetry. *Respitory Care*, 48, 2003.

[89] M. Sandberg and B. Larsson et al. Different patterns of blood flow response in the trapezius muscle following needle stimulation (acupuncture) between healthy subjects and patients with fibromyalgia and work-related trapezius myalgia. *Eur J Pain*, 9:497–510, 2005.

[90] M. Sandberg, L.G. Lindberg, and B. Gerdle. Peripheral effects of needle stimulation (acupuncture) on skin and muscle blood flow in fibromyalgia. *Physiol. Meas.*, 28:1–39, 2004.

[91] E. Espiritu Santo and C. Carbajal. Respiration Rate Extraction from ECG Signal via Discrete Wavelet Transform. *IEEE*, 2010.

[92] Ichiro Satoh. A framework for data processing at the edges of networks. In *Database and Expert Systems Applications*, pages 304–318. Springer, 2013.

[93] Bluetooth SIG. The Bluetooth SIG Health Device Profile, 2015. [WWW] https://www.bluetooth.org/en-us/specification/assigned-numbers/health-device-profile.

[94] J. Spigulis, L. Gailite, and A. Lihachev et al. Simultaneous recording of skin blood pulsations at different vascular depths by multiwavelength photoplethysmography. 46:1754–9, 2007.

[95] Stanford University Sleep Research Center. A Brief History of Sleep Research, 2015. [WWW] http://web.stanford.edu/đement/history.html.

[96] Statista Inc. Facts and statistics on Wearable Technology, 2015. [WWW] http://www.statista.com/topics/1556/wearable-technology/.

[97] Toshiyo Tamura and Y. Maeda et al. Wearable Photoplethysmographic Sensors - Past and Present. *Electronics*, (3):282–302, Apr 2014.

[98] MJ. Thorpy and Diagnostic Classification Steering Commitee. Periodic Limb Movement Disorder. In *International Classification of Sleep Disorders*, pages 65–68. American Sleep Disorder Association, Rochester, MN, USA, 1990.

[99] E. Tur and M. et al Tur. Basal perfusion of the cutaneous microcirculation: Measurements as a function of anatomic position. *J. Invest. Dermatol.*, (81):442–446, 1983.

[100] Withings. Wireless Scale, 2015. [WWW] http://www2.withings.com/us/en/store/details/ws_30.

[101] World Health Organization. Cardiovascular diseases (CVDs), 2015. [WWW] http://www.who.int/mediacentre/factsheets/fs317/en/.

[102] Dan Wu and G-Z. Liu. The Accuracy of Respiratory Rate Estimation Using Electrocardiography and Photoplethysmography. *ITAB*, (10):1–3, 2010.

[103] Masaru Yarita, Naoki Kobayashi, and S. Takeda. Compensation for Two Specific Types of Artifact in Pulse Wave Using a Kalman Filter. *ITAB*, pages 269–272, 2007.

[104] Carlos Zamarron and F. Gude. Utility of Oxygen Saturation and Heart Rate Spectral Analysis Obtained From Pulse Oximetric Recordings in the Diagnosis of Sleep Apnea Syndrome. *CHEST*, 123(5):1–7, May 2003.

[105] Q. Zhang, L. G. Lindberg, and R. Kadefors et al. A Non-invasive Measure of Changes in Blood Flow in the Human Anterior Tibial Muscle. *Eur J Appl Physiol*, 84:448–52, 2001.

[106] G.E. Ziganshin, A. M. Numerov, and A.S. Vygolov. UWB Baby Monitor. *UWBUSIS*, pages 159–61, Sep 2010.

[107] A. Zourabian, A. Siegel, and B. Chance et al. Trans-abdominal monitoring of fetal arterial blood oxygenation using pulse oximetry. *J. Biomed Opt.TAB*, 4(5):391–405, 2000.

Appendices

List of Publications

Appendix A

Leier M.; Jervan G. (2013). Sleep Apnea Pre-Screening on Neonates and Children with Shoe Integrated Sensors. *In: Norchip*, Vilnius, Lithuania, 2013, pp. 1-4

Sleep Apnea Pre-Screening on Neonates and Children with Shoe Integrated Sensors

Mairo Leier, Gert Jervan
Department of Computer Engineering
Tallinn University of Technology, Tallinn, Estonia
Email: mairo.leier@ttu.ee, gert.jervan@ttu.ee

***Abstract*—The aim of this paper is to provide a high level architectural description of portable sleep apnea screening system. Proposed patient mobile monitoring solution increases their mobility, flexibility and measures vital data with minimal patient disturbance with increased reliability. Data is acquired with synchronous dual multi-wavelength optical sensors, placed on the foot. Movement artefacts are reduced with the correlation of accelerometer readings. Results are sent over the wireless link to the smartphone for further diagnosis which gives also feedback to the end user. Because of the limitation of the measuring device dimensions and computational power some of the signal processing is done on the smartphone. Combining different latest technology achievements makes our proposed solution suitable for neonates and children for sleep apnea pre-screening.**

I. Introduction

The need for sleep apnea monitoring devices for babies and children at home environment shows an increasing interest. Currently available devices monitor only baby's breathing and movements. In addition to that, measuring heart rate and blood oxygen saturation (SpO2) level have huge benefits. In case of Obstructive Sleep Apnea (OSA) breathing movements continue but an obstruction in the windpipe prevents any oxygen reaching the baby's lung. This is causing sudden SpO2 drop in blood, that is related often to the Sudden Infant Death Syndrome (SIDS). Clinical polysomnograms, which are used for sleep disorder detection, are expensive and require special hospital or sleep disorder centre to monitor patients overnight. Our developed solution includes in addition to breathing detection also heart rate, which is calculated from the SpO2 signal, and accelerometer used for body posture detection and sleep pattern diagnosis. Those inexpensive at-home self-recording devices can reduce costs by screening out patients who do not need a full sleep study. For babies and children it is also the most comfortable way to perform pre-screening. Having diagnostic data from large number of patients gives a better quality to perform larger-scale research studies.

II. Sleep Apnea

The term apnea means absence of spontaneous breathing. It is a common disorder that is estimated to occur in about 7% of the population of which more than 85% remain undiagnosed. SIDS accounts for 22% of all post-neonatal deaths and affect infants with ages 1 month to 1 year. OSA is currently estimated to affect between 1% and 3% of 2- to 8-year old children and is most commonly found in children between 3 to 6 years of age.
Overnight sleep study test includes usually electrical activity of the heart, breathing patterns, SpO2 level, muscle activity and eye movements. For pre-screening purposes collecting all of those signals is not practical. Therefore current research is focusing on the most important signals that give immediate feedback about critical conditions.

III. State of the Art

The diagnostic devices and therapeutic devices segments will grow at a Compound Annual Growth Rate (CAGR) of 15% and 17%, respectively, by 2017. The diagnostic devices market is propelled by Polysomnography (PSG) devices, particularly clinical PSG devices. The usage of Ambulatory PSG devices is slated to increase in the next few years due to observed patient preference to be tested at home for convenience reasons, patients inclination to skip the unfamiliar environment of sleep labs, and cost-effectiveness of these devices. The global demand for other diagnostic devices such as respiratory polygraphs, two channel screening devices, single channel screening devices, and actigraphy systems is also on the rise due to their low costs. These devices serve as cost-effective and convenient options, as compared to PSG devices, especially for the low-economic class patient pool.
Stardust II Sleep Recorder device developed by Philips is capable of measuring respiratory airflow, pulse, SpO2, chest effort and body position without wireless transmission. There are also sleep mats available which are measuring breathing and waking movements and mats which are put 8-11 cm deep below foam or sprung mattresses. Some of them have additional body sensor which is attached to the baby's lower abdomen with micro-pore tape. Some of these are built for infants which use Ultra Wide Band (UWB) technology [1].
Our proposed solution uses high-end components to achieve high precision but with smaller size and wireless technology. It makes possible to extend sleep monitoring for home conditions and lower the cost. Current paper describes the general concept of the portable monitoring system which is under development.

IV. Proposed solution

A. Design Concept

The aim of this portable sleep apnea monitoring system is to provide a higher comfort while monitoring the heart rate, saturation of oxygen, respiration rate and body movements when the neonate is sleeping in the bed. Proposed solution has to meet the following design requirements:

- Easy sensor placing even for untrained personnel

- Newborn sleep cycle could last up to 18 hours. Monitoring should be performed without the charging during one full sleep time
- Long term monitoring should provide a high comfort without any consequences on the body
- Continuous and reliable measurement even during normal body movements during the sleep
- Electronic parts have to be easy detachable for cleaning purposes

B. System Overview

Proposed solution is focusing on infants from the newborn up to the first year and children between years 2 to 8 who need to be monitored in case sleep apnea is suspected. Based on the research most important parameters that are needed for continuous monitoring of vital signs are heart rate, SpO2 level, respiration, body posture and activity. Since the solution is mostly used during the sleep time, it should have a minimal effect on disturbing normal sleep. Therefore it is chosen to integrate sensing module of the system into the shoe that is carried by the patient during the sleep. Similar solution is proposed by [2] but without respiration signal measurement which is mandatory for detecting sleep apnea.

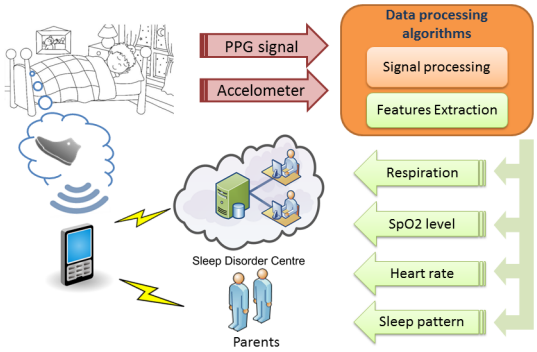

Fig. 1. The conceptual image of a portable sleep apnea pre-screening system

Figure 1 describes the conceptual image of portable sleep apnea pre-screening system. Shoe, that consists highly integrated sensors with microcontroller and wireless connectivity, is worn by the neonate or child during the sleep. Measurements are performed continuously and sent over the wireless link to the smart phone. Smart-phone provides additional sophisticated data processing with early warning system in case some measurements have abnormal readings. Such an early warning functionality helps parents to look after their children during the sleep. In case of abnormal readings an alarm is activated with suggested activities. In addition to that, analysed data can be used by the sleep clinic personnel to decide about the need for further sleep analysis.

Figure 2 describes the proposed solution's architectural design. Sensing device with sensors and signal processing unit, and smartphone with user interface divide it into two main parts. System consists one or more multi-wavelength optical

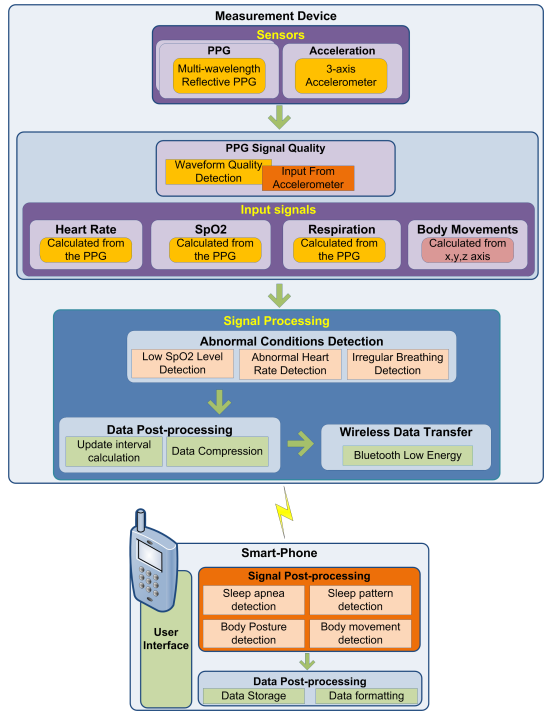

Fig. 2. System architecture of a proposed system for data processing

sensors and one accelerometer. Optical sensors are placed on the flex PCB that makes it possible to fine-tune sensor exact position on the body. Best location on the foot has to be found during the sleep tests with different patients. It was suggested by the doctors to perform measurements near Anterior tibidal which has the biggest perfusion index in the foot. Especially in cold environment perfusion index plays important role because cold reduces the amount of circulating blood in the body and signal quality gets worse.

Individual signals from the raw data are filtered and extracted in the pre-processing stage. These steps include noise reduction with low-pass and high-pass filters and DC component removal without removing useful information from the base signal.

After the signal pre-processing, abnormal condition detection algorithms are applied to perform initial analysis of patient's normal condition. Three basic signals, breathing interval, SpO2 level and heart rate are used for sleep apnea detection. To reduce the required amount of signal processing on measurement device, only individual signal components will be calculated. For breathing rate extraction from the pulse wave we have developed an algorithm that is power efficient and suitable for using on portable devices. Compared to other methods we use pulse wave amplitude modulation and get excellent results with reduced power consumption [3].

Depending on the calculated results of the signals, update interval is adjusted to reduce the amount of power usage by radio and still provide a near real-time feedback about the health conditions. Severity algorithm calculates the importance

of the readings and makes interval related decisions based on that. To reduce the radio usage even more, data compression is applied before it is sent to the smartphone.
Wireless radio is used to transmit the results to the smartphone which has to be in range to receive the alarms. Most new smartphones include dual-mode Bluetooth chips that support Classic Bluetooth (BT) and Bluetooth Low Energy (BLE). BLE has better energy saving technologies built in, that can be fully used in our proposed solution.
Second part of the solution is the smartphone. Its main purpose is to perform signal post-processing with sleep apnea detection and give first feedback to the user. It eliminates the need to develop an extra hardware for deep data analysis and storage. In case there is a need for extended monitoring in sleep clinic, smartphone is acting as a gateway to transfer analysed results to the medical personnel.

C. Electronics and Signal Acquisition

Typical pulse oximeter consists of photosensor, analogue front-end, digital processing unit with user interface. We have extended this general idea of oximeter, to provide more reliable measurements with additional sensors, with internal storage and wireless interface.

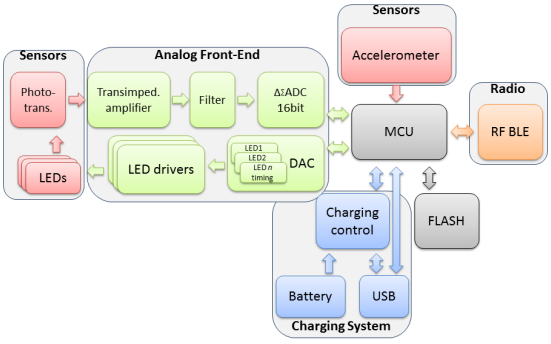

Fig. 3. Functional block diagram

Figure 3 describes our proposed hardware design. Starting with Analog Front-End and Sensors box, digital-analogue converter (DAC) controls the intensity and timing of each LED as they need to be switched on and off one with the sampling rate of 1kHz. LED driver amplifies the current that is needed for the LED. Photo-transistor receives the light that is not absorbed and current changes are converted into the voltage changes with the transimpedance amplifier. Acquired signal is filtered with several filters to eliminate high frequency noise and 50/60 Hz line interference and converted into digital form. Taking into account that prototype should consist as less overhead in hardware because of the limited size and weight, most of these filters has to be applied in the software.
Power management is done by the Charging System. Estimated battery lifetime is around 48 hours continuous monitoring which covers 2-3 full sleep times of newborn. Device is recharged over USB connection. Li-ion battery charging takes around 2 hours until fully charged. It is approximately the same time the newborn stays awake between the sleep times.
System core consists of processing unit and storage. MCU is chosen based on te required computational power in order to perform filtering and features extraction with compression. Processed data is stored on FLASH/uSD card in case wireless connection is not available to transfer it to the smartphone.
Radio module connects to the smartphone over BLE. Compared to the BT, it provides less throughput but smaller latency and better power handling that makes it perfect solution for the wireless portable devices.

D. Sensor Design

New hardware and more advanced software algorithms are being developed to reduce false alarms and provide more reliable readings under conditions of low perfusion. Compensating motion artefacts with signal processing algorithms is dealing with the consequences not with the root cause or signal acquisition. There are three main factors that affect pulse oximetry readings. A straight incident light to tissue scattered wavelength-dependently until about 2 mm depth because the inner structure of tissue is not uniform. The effect of the tissue has to be considered that affects total optical density. If using three-wavelengths, two simultaneous equations give the SpO2 without the effect of tissue coefficient dependency. At last, the effect of venous blood could be removed with five wavelengths.
Conventional oximeters use two wavelengths to perform measurements. Later technologies use wider area of wavelengths in order to increase the system reliability. Different research groups are using 3 to 12 wavelengths in oximeter. In addition to $\lambda_1 = 660$ nm and $\lambda_1 = 940$ nm, used in conventional oximeters, the most used wavelengths are $\lambda_4 = 700$ nm, $\lambda_5 = 730$ nm, and $\lambda_1 = 805$ nm [4] [5] [6].
For detection of Carboxyhemoglobin (CoHb) and methemoglobin (MetHb), four wavelengths are in principle sufficient [4]. The use of additional wavelengths allow further correction of disturbances and improves the accuracy. Using three-wavelength method improves the accuracy of SpO2 when the tissue constants are appropriately selected. With three wavelengths we can eliminate tissue effect but not venous blood effect. Therefore using five wavelengths could additionally improve the the quality of readings. Our proposed solution is using five wavelengths. Two of them , red $\lambda_1 = 660$ nm and infrared $\lambda_2 = 940$ nm are used for oxyhemoglobin (O2Hb) and deoxygenated hemoglobin (HHb) detection. Three additional wavelengths are used to detect CoHb and MetHb and improves the accuracy. It does not matter how many wavelengths are used, motion artefacts elimination is still considered difficult [6].
Signal artefacts are mostly caused by the body movements. With two optical sensors it is possible to reduce artefacts caused by the local movements. Sensors has to be placed on the body away from each other at least few centimetres. Similar method has been used to calculate pulse wave velocity (PWV) using two synchronized, wireless pulse oximeters, placed on the wrist and fingertip of the same hand [7].

V. Signal Processing

A. Sleep Apnea Detection

Normal waking and asleep SpO2 levels in healthy child or adult are 96-99% and 94-98%, respectively. Sleep apnea

has specific pattern in which order all symptoms appear. The typical cycle of sleep apnea is:

1) oxygen level begins to fall
2) breathing pauses 10 seconds or more
3) heart rate falls below normal
4) brief awakening with few large breaths
5) heart rate speeds up above normal heart rate
6) oxygen level returns to near normal

Apnea Hypopnea Index (AHI), the number of apneic episodes per hour, is used to detect the severity of sleep apnea.

- AHI of 5-15/hr - mild sleep apnea
- AHI of 16-30/hr - moderate sleep apnea
- AHI of +30/hr - severe sleep apnea

The standard definition of (AHI^s) [8] determined during attended laboratory PSG is calculated

A_{wofl} - apneas where 10 sec without flow
R_{flow} - hypopneas with reduced flow with 5% of desaturation
St_{tot} - total sleep time in hours

$$AHI^s = \frac{(A_{wofl} + R_{flow})}{St_{tot}}$$

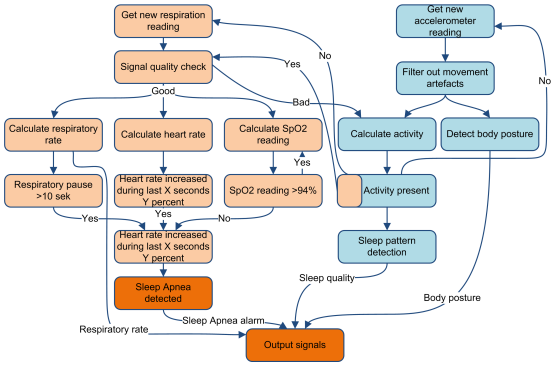

Fig. 4. Sleep Apnea detection algorithm

Figure 4 describes proposed algorithm that consists all main parts of the sleep apnea detection. It is capable to detect apneic cases to calculate AHI index. The purpose of this algorithm is to provide a general overview about all steps that are needed to perform in order to process the acquired signal and provide output signals for the user feedback and further analysis. Many of these steps include sophisticated signal processing tasks. Describing individual steps in detailed level is not the scope of this paper rather describe the architecture of proposed sleep apnea detection method.

VI. Discussion

The studies of neonates and children found that 44-63% of all critical care alarms were caused by pulse oximeters, 94% of oximeter alarms were considered clinically unimportant, and 71% were false alarms [9]. The most interest have therefore got multi-wavelength oximeters. Similar solution has been proposed in [10]. Even with the excellent LED duty cycle of 2.5%, the most power consuming component is DSP that limits the system total operating time for eight hours. Our proposed system have several advantages over other systems.

- Comfortable place to measure pulse wave on neonates and children with minimal sleep disturbance.
- Portable real-time signal processing device with RF connection with smart phone that decreases requirements for the processing power of measurement device. In addition to that it provides an early warning system with basic instructions for the parents and detailed data for the sleep physicians.
- Performing measurements simultaneously on two places and with five wavelengths helps to improve the signal quality by replacing distorted signal with the better quality one and remove several tissue and venous blood related artefacts.
- Detection of body movements help to estimate sleep pattern and give an additional information to correlate artefacts with the movements.

VII. Conclusions

Proposed solution helps to decrease cost and increase accessibility to diagnostic monitoring for sleep studies. For the neonates and children the most comfortable way to perform pre-screening is to evaluate it in the natural home situation. Our proposed solution is designed to include all the most important signals for pre-screening and give an early warning about possible life threatening situations using low energy wireless communication with smart phones.

References

[1] G. E. Ziganshin, A. M. Numerov, and A. S. Vygolov, "UWB Baby Monitor," Sep 2010.

[2] Y. Rimet and Y. Brusquet, "Surveillance of Infant at Risk of Apparent Life Threatening Events (ALTE) with the BBA Bootee: a Wearable Multiparameter Monitor," *EMBS*, pp. 4997–5000, Aug 2007.

[3] M. Leier and G. Jervan, "Respiration Signal Extraction from Photoplethysmogram Using Pulse Wave Amplitude Variation," *submitted for publication*.

[4] J. Fiala, R. Gehrke, N. Weber, and et al, "Implantable Optical Sensor for Continuous Monitoring of Various Hemoglobin Derivatives and Tissue Perfusion," *ICSENS*, pp. 1971–1974, 2009.

[5] J. M. May, P. A. Kyriacou, and A. J. Petros, "Development of an Optoelectronic Sensor for the Investigation of Photoplethysmographic Signals from the Anterior Fontanel of the Newborn," pp. 18–21, 2011.

[6] T. Aoyagi, M. Fuse, N. Kobayashi, and et al, "Multiwavelength Pulse Oximetry: Theory for the Future," *Anaesthesia and Analgesia*, vol. 105, no. 6, pp. 53–58, Dec 2007.

[7] K. Li and S. Warren, "Initial Study on Pulse Wave Velocity Acquired from One Hand Using Two Synchronized Wireless Reflectance Pulse Oximeters," *IEMBS*, Sep 2011.

[8] N. A. Collop and S. L. Tracy, "Obstructive Sleep Apnea Devices for Out-Of-Center (OOC) Testing: Technology Evaluation," *Clin. Sleep Med*, vol. 7, no. 5, pp. 531–548, Oct 2011.

[9] J. W. Salyer, "Neonatal and Pediatric Pulse Oximetry," *Respitory Care*, vol. 48, 2003.

[10] O. Guven, F. Geier, and D. Banks, "An Open-Source Platform for the Development of Microcontroller Based Multi-Wavelength Oximetry," *BioCAS*, pp. 282–285, 2010.

Appendix B

Leier M.; Jervan G. (2014). Miniaturized Wireless Monitor for Long-term Monitoring of Newborns. *In: Proceedings of the BEC 2014*, Estonia, 2014, pp. 193-196

Miniaturized Wireless Monitor for Long-term Monitoring of Newborns

Mairo Leier, Gert Jervan
Department of Computer Engineering
Tallinn University of Technology, Tallinn, Estonia
Email: mairo.leier@ttu.ee, gert.jervan@ttu.ee

***Abstract*—Wireless infant monitoring system is a small-size wearable sensor platform. There is a growing trend to simplify the measuring methods to allow a real-time monitoring of the vital signals in home environment. Most of these devices have cables, are quite large in size that may disturb infant's everyday life and need continuous supervising from parent. In this paper we propose a monitoring system that detects the most important vital signals of baby and transmits results over wireless link to the control device that could be any smart-phone. The system is capable of measuring blood oxygen level, heart rate, respiration rate, body temperature, body posture and legs activity. Combining all of these raw signals it is possible to use this system in different, possible life-threatening situations during long-term monitoring. Compared to other similar solutions it has small dimensions, low weight, increased reliability of measuring photoplethysmography signal and extended battery life because of the usage of Bluetooth Smart wireless protocol.** [1]

I. Introduction

In the last years there are an increasing number of monitoring devices for adults and elderly people available. These systems can monitor their health status and send out automatically emergency signals. However, the care methods for infants are different. The only way how infants could express themselves is crying. The most critical time when infants may need to be monitored is during the sleep, in case of birth defects and in times of illness.

The most critical age in the infant's life is first 6 months when different complications may appear and cause an unexpected death. According to the statistics, the average infant mortality rate is around 45 per 1000 live births and is even bigger in developing countries. The most frequent causes of infant death during first year of life are birth defects, low birth weight, Sudden Infant Death Syndrome (SIDS), maternal complications, accidents and respiratory distress of newborn [1].

There are several real-time infant monitoring systems being developed and already on the market. Most of them have the functionality to measure heart rate, body temperature and motions [2] [3]. Some of them also have a possibility to have respiration and humidity level information [4]. Comparison of similar devices is discussed also in [5]. There are also available different sleep mattresses and vests. Some research is done measuring respiration and heart rate with Ultra Wide Band (UWB) wireless technology [6]. In clinical environment most of the sensors are wired and placed all over the body. Even there are different places from where to measure vital signals on infant, one of the most comfortable place is on feet. It allows a quick replacement of the sensor and has a reliable signal quality [3].

Our proposed infant monitoring device consists of many new aspects regarding continuous long-term monitoring. Usage of Bluetooth Smart wireless protocol increases the monitoring device life cycle several times. We propose the system with increased reliability of the photoplethysmography (PPG) signal which has been an active research topic already some time by different groups [7]. In addition to the usage of more sophisticated signal processing methods, our proposed solution adds increased reliability also from the hardware side [5].

In the following section we present in depth system description with technical characterization and discuss about clinical and technical requirements, system architecture, embedded algorithms and wireless communications. Section 3 describes the initial results and evaluates the performance. Section 4 discusses future work. Finally section 5 gives some conclusions.

II. System Description and characterization

A. Clinical and technical requirements

To increase the reliability of the health-care device, it needs to be tested with some number of test-persons. For clinical trials the monitoring device should meet the several clinical and technical requirements. Requirements were chosen based on the normal monitoring process so that it does not need much additional effort to perform the measurement, is comfortable for the clinician and infant, gives the meaningful output for the clinician and stores enough information for further data analysis.

First, the system should be suitable for monitoring newborns from the birth up to 1 year old (Req #1). The system shall be easy to use and be convenient for the clinician during manipulation of the patient (Req #2). The position of the monitoring device on the body should be comfortable and safe, and not to cause any harm during long term contact with the newborn's skin (Req #3). The size of the device shall be lightweight and so small that it does not make any discomfort during the wearing (Req #4).

Concerning the hardware aspects the monitoring device shall be as unobtrusive and robust as possible. Neither buttons nor external wires must be apparent to avoid disturbing the patient or obstruct the measurement process (Req #5). The electrical and physical design of the monitor shall be such that, however the conditions, it presents no risk of harming the patient, e.g. by injecting current to the body (Req #6).

[1]This work was jointly supported by EU through European Regional Development Fund, and by the institutional research funding IUT 19-1 of the Estonian Ministry of Education and Research.

Monitoring device shall be able to measure pulse wave on the foot, skin temperature, body position and movements (Req #7). The pulse wave shall be analyzed in real-time and the result of the analysis shall be directly and wirelessly sent to a control unit (Req #8). At the same time a raw pulse wave signal should be logged for further off-line analysis (Req #9). Wireless exchange information between the operator and the body-worn monitoring device must be possible. The control unit shall enable the operator to send the start and stop command of a recording as well as the patient specific parameters (Req #10). The status of the monitoring device shall be displayed to the technician upon request (Req #11). The system autonomy should allow at least 24 hours of continuous monitoring (Req #12). Monitoring device shall be rechargeable over widely used charging standard to eliminate the need for special purpose charger and therefore lower the cost of additional hardware (Req #13).

B. System Architecture

The initial pre-selection of the system architecture has been done in [5]. Most of the intelligence is offloaded to the monitoring device to minimize wireless communication between the monitoring and control device that is the most power consuming process. Main tasks of the device are signal acquisition and pre-filtering, feature components extraction, storage of raw data and preparation for wireless transmission. The host application of the control device manages the monitoring device and prepares data for network upload to the historical database. Any third-party functionality is connected through the back-end interface. User interface of the control device serves a graphical interface for the operator. The figure 1 illustrates the overall data acquisition software architecture.

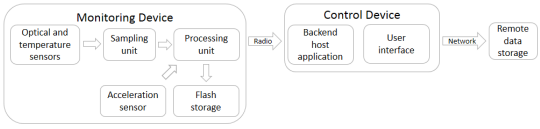

Fig. 1. Architecture overview

C. Miniaturized Monitoring Device

The monitoring device, illustrated in figure 2 is composed of:

1) Flexible board with optical and temperature sensors.
2) Analog board which provides an analog to digital conversion of optical signals.
3) Processing board which provides processing features for the monitoring system and wireless transmission.

Processing board consists of two principal electrical components selected for their low-power characteristics, a micro-controller unit and a radio transceiver. The micro-controller unit (MCU) from Texas Instrument MSP430F5528 featuring 8KB of RAM and 128KB of ROM [8]. Bluetooth Low Energy radio transceiver from Bluegiga Technologies BLE112 adds the possibility for wireless data transfer to meet the requirement #5. Wireless module offers an external communication to the control the device. On-board ferro-electric RAM (FRAM) memory module offers a compact,

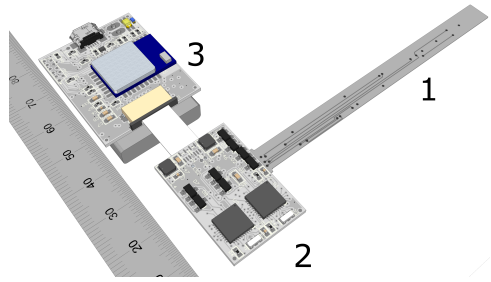

Fig. 2. Monitoring device

ultra-fast and low power storage capability. Micro-USB interface serves charging capability and wired communication to external devices. Micro-USB has been widely accepted standard on the latest cell-phones and meets therefore the requirement #13. On-board indicator LEDs indicate about the most important status conditions like battery information and wireless communication. The monitoring board is powered through a 400 mAh battery.

There are several sensors integrated into the monitoring device. Three-axes accelerometer BMA280 adds the functionality to measure body posture and activity. Optical sensors on the flex cable measure the PPG signal with two different wavelengths. Temperature sensor on the flex cable adds support for body temperature monitoring. All-together they meet the requirement #7.

The monitoring device with battery pack and silicone enclosure weights around 30g and is packaged into a 75x27x12 mm^3 silicone enclosure that meets the clinical requirements #1 and #4.

Fig. 3. Monitoring device on the foot

Monitoring device is packed into medical grade silicone, Dow Corning S40 Silicone Rubber, that is a two-part platinum-catalyzed silicone elastomer specifically designed for liquid injection moulding or supported extrusion [9]. It meets all the US and European standards for healthcare device that is necessary for clinical trials. This criteria also meets our requirement #3 in safety perspective. As the whole device is enclosed with the silicone and during the measurement the device is not charged, it also meets the clinical requirement #6 in electrical safety.

D. Embedded Algorithms

Embedded algorithms, implemented into the monitoring device, meet the real-time criteria in limited processing power environment. All discussed algorithms need the maximum length of signal buffer up to 2 seconds and don't require processor intensive calculations. In regards to that they also fulfil the requirement #8.

1) Pulse-wave detection: A robust and accurate pulse-wave detection algorithm is crucial to ensure a reliability of the system. A real-time algorithm for pulse-wave detection is implemented. It is based on detection of the pulse wave envelope, described in [10]. Compared to the wavelet transform and neural network based algorithms it is relatively quick and works in real-time. According to the results of limited testing, accuracy of the algorithm at rest claims to be 100%.

2) SpO2 calculation: A pulse oximeter analyzes the light absorption of two wavelengths from the pulse-added volume of oxygenated arterial blood that is well described in [11]. SpO_2 reading is taken out from the table stored on the memory calculated with the empirical formulas. A ratio of 1 represents a SpO_2 of 85%, a ratio of 0.4 represents SpO_2 of 100%, and a ratio of 3.4 represents SpO_2 of 0%. For increased reliability, the table must be based on experimental measurements of healthy patients.

3) Respiration detection: To extract the respiration information, the most interested frequency band stays between 0.2 Hz and 1 Hz. In our implementation we are using PPG signal to extract the respiration information. One efficient way to calculate the breathing rate is based on connecting the peaks and bottoms of each PPG pulse wave accordingly, thus constructing a continuous envelop along the top and bottom edge of the PPG signal [12].

4) Body posture detection: As the system is used mostly on babies up to 1 year old who have not learned yet to walk we are focusing only in which position baby is sleeping or lying. Most of the time an infant is sleeping on the back and sideways and in rare cases also lying face down. With roll and pitch calculations we get any position of the foot that is sufficient to estimate the position of the body. All inclination angles are calculated with he help of three-axis accelerometer. Sensor inclination angles with respect to the ground are calculated to get the pitch and roll of the body. Implemented formulas are fully described in [13].

5) Activity detection: There are three most frequent activity types that should be detected: sleep, crying and awake. Each of them has a slightly different threshold. In some cases an activity detection could increase the detection rate of another function. Table I describes different type of activities that could be detected with the measurement of accelerometer on the foot. The most important vital signals, that describe the status of baby's health, are respiration frequency and heart rate. Combining those signals as described in the table I we could significantly increase the reliability of each particular algorithm, listed in the activity type column.

When a baby's body is in static position, the accelerometer responds only to the gravitiy acceleration of 1 G. In motion and change of the motion, an accelerometer produces corresponding acceleration. Activity signal magnitude area method provides a good way to detect kinematic changes of the body [13]. Using different time frames it gives a good opportunity to analyze the specificity of movements and propose particular type of activity.

TABLE I. ACTIVITY COMPARISON

Activity type	Activity level	Activity frequency	Respiration frequency	Heart rate
Sleep	low	low	low	low
Awakening	medium	medium	low	low
Awake	medium	low	medium	medium
Crying	high	high	med.-high	high

E. Wireless Communication Services

The monitoring device features two wireless communication modes: (1) a two-way event-based mode for data visualization, algorithm output transmission and online algorithm parameter setting; (2) a wireless data transmission mode to transfer raw PPG and acceleration data, if requested, to the control device.

The up-link, from the control device to the monitoring device, provides the communication with the possibility to send information as well as query the monitoring device status. Information such as the algorithm parameters, PPG signal ADC module, accelerometer configuration, radio module configuration can be transferred.

As the system uses Bluetooth Smart wireless communication protocol, throughput is limited to around 60 kbps in case of unacknowledged packets. In a typical environment the fastest reliable throughput with acknowledged packets, according to Bluegiga Technologies tests, is 8-10 kbps [14]. Transmitting raw PPG signal with the sampling rate of 250 Hz and 22-bit of data, we need throughput of 5,9 kbps. 14-bit digital accelerator with the sampling rate of 100 Hz needs 1,6 kbps. In total there is a need for throughput up to 7,5 kbps.

Bluetooth Smart communication is based on Generic Attribute (GATT) profiles. Services that are advertised under each according profile by our monitoring device are listed in the table II.

TABLE II. BLUETOOTH SMART PROFILES

Service name	Service type	Update interval	Value descriptor
Device Information	global	N/A	uint16
Health Thermometer	global	2 Hz	uint16
Heart Rate	global	1 Hz	uint8/uint16
Respiration Rate	local	1 Hz	uint8
Blood Oxygen Level	local	1 Hz	uint8
Body Position	local	1 Hz	uint8
Activity	local	1 Hz	uint8
Alert Status	local	1 Hz	uint8
Raw PPG	local	250 Hz	uint8
Raw acceleration	local	100 Hz	uint16

First column describes name of the service. Second column defines whether the service is globally defined by the Bluetooth Smart specification or own defined. The biggest difference between global and local service is that global services are defined by specifications and with known Universally Unique Identifiers (UUID) but local services can be defined according to specific need and with own-generated 128-bit UUID. Supporting globally defined services adds

better integration with Bluetooth Health Device Profile [15]. Third column defines the frequency of each service update interval. If particular service does not support notification based automatic update it is marked with N/A. Last column defines number format of the service descriptor value. Type "uint" means unsigned integer and number after uint is the number of bits that represents the length of data. Heart Rate service supports two type of lengths depending the value that is currently transmitted. For raw data transfer there are two services, "Raw PPG" and "Raw acceleration" that support indication types that allows to send unacknowledged packets to speeds up data transfer. Raw data storage and wireless transfer also meets the requirement #9.

III. Results

A. Memory footprint

Including all functionality the measurement system requires 1,5 kB of RAM and 22,8 kB of program memory. The biggest size of the program memory is occupied by USB, accelerometer and functionality that analyses the digitized optical signal. Algorithms that are handling accelerometer and optical signals consume also most of the used size of RAM.

B. Power consumption profile

In the "operating" mode, the total system power budget is 71 mW. The measured average MCU active duty-cycle is 40% yielding to an average power consumption of 28,4 mW that meets well the requirement #12, representing about 50 hours of autonomy for a 400-mAh battery. For data storage we use an external FRAM memory modules that support over 100 times faster data throughput and consume 3 times less power compared to FLASH based modules. Figure 4 illustrates power consumption breakdown of measuring device.

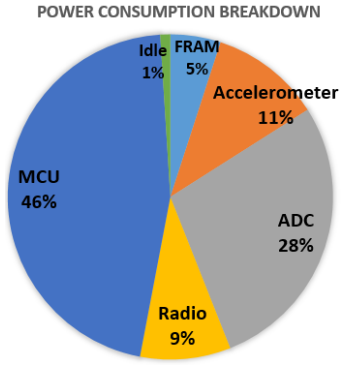

Fig. 4. Power consumption of the measuring device

The biggest amount of power is consumed by the MCU that has several tasks. Embedded algorithms that are activated by external interrupts consume most of the MCU execution mode. PPG signal sampling with the rate of 250 Hz adds a new sample in every 4 ms. If there are at least 5 continuous unprocessed samples a pulse-wave detection algorithm is executed. Acceleration information is sent only if there is a movement over preset threshold. The remaining, 60 % of the time, MCU is idling that leaves room for additional processing algorithms.

IV. Future work

The current infant monitoring device has up to 50 hours of autonomy. Extending the battery life even further could benefit arrangement of the monitoring. Several actions can be taken to decrease the overall system power usage: apply compression algorithm for wireless raw data transfer, optimize the duty cycle and power level of optical sensors, optimize embedded algorithms and increase the time in deep sleep mode of processing unit. Optimizing the usage of accelerometer could also benefit overall power consumption.

V. Conclusions

In this paper, a wireless infant monitor system is presented. Efforts towards miniaturizing the form factor and improving the comfort of the system have been made. The resulting prototype weights with battery pack and silicone enclosure around 30 g and is packaged into 75x27x12 mm^3 silicone enclosure. It has an autonomy of up to two days with continuous measurement mode. The system was fixed on the newborn's foot, as in figure 3. During one week the several hours long measurements were performed and within this time no remarkable discomfort was observed.
Our proposed solution is designed to include all the most important signals for pre-screening and give an early warning about possible life threatening situations using low energy wireless communication with smart phones.

References

[1] M. Heron and D. L. Hoyert, "National vital statistics report," 2009.

[2] E. Saadatian, S. Iyer, and O. Fernando, "Low Cost Infant Monitoring and Communication System," *CHUSER*, pp. 503–508, 2011.

[3] Y. Rimet and Y. Brusquet, "Surveillance of Infant at Risk of Apparent Life Threatening Events (ALTE) with the BBA Bootee: a Wearable Multiparameter Monitor," *EMBS*, pp. 4997–5000, Aug 2007.

[4] C. Linti, H. Horter, and P. Osterreicher, "Sensory Baby Vest for the Monitoring of Infants," *BSN*, pp. 133–137, Nov 2006.

[5] M. Leier and G. Jervan, "Sleep Apnea Pre-Screening on Neonates and Children with Shoe Integrated Sensors," *Norchip*, pp. 1–4, 2013.

[6] G. E. Ziganshin, A. M. Numerov, and A. S. Vygolov, "UWB Baby Monitor," *UWBUSIS*, pp. 159–161, Sep 2010.

[7] C. Robles-Rubio, K. Brown, and R. Kearney, "A New Movement Artifact Detector for Photoplethysmographic Signals," *EMBC*, pp. 2295–2299, 2013.

[8] MSP430F551x, MSP430F552x Mixed Signal Microcontroller. Texas Instruments. [Online]. Available: http://www.ti.com/product/msp430f5528

[9] *S40 Liquid Silicone Rubber Parts A and B Product Information*, Dow Corning. [Online]. Available: http://www3.dowcorning.com/DataFiles/090007c880114a68.pdf

[10] M. Hong, "A Real-Time Pulse Wave Detection Device Basing on Signal Envelope," *BMEI*, no. 5, pp. 812–816, 2012.

[11] S. Bagha and L. Shaw, "A Real Time Analysis of PPG Signal for Measurement of SpO2 and Pulse Rate," *IJCA*, vol. 36, no. 11, pp. 45–50, Dec 2011.

[12] M. Leier and G. Jervan, "Respiration Signal Extraction from Photoplethysmogram Using Pulse Wave Amplitude Variation," *ICC*, 2014.

[13] C.-F. Lai and Y.-M. Huang, "Adaptive Body Posture Analysis for Elderly-Falling Detection with Multisensors," *MIS*, vol. 25, no. 2, pp. 20–30, 2010.

[14] Maximize throughput with the BLE112/BLED112. Bluegiga Technologies. [Online]. Available: https://bluegiga.zendesk.com/entries/22400867--HOW-TO-Maximize-throughput-with-the-BLE112-BLED112

[15] *Health Device Profile*, Bluetooth SIG. [Online]. Available: https://www.bluetooth.org

Appendix C

Leier M.; Jervan G. (2041). Respiration Signal Extraction from Photoplethysmogram Using Pulse Wave Amplitude Variation *In: IEEE International Conference on Communications ICC2014*, Sydney, Australia, 2014, pp. 3535-3540

Respiration Signal Extraction from Photoplethysmogram Using Pulse Wave Amplitude Variation

Mairo Leier, Gert Jervan
Department of Computer Engineering
Tallinn University of Technology, Tallinn, Estonia
Email: mairo.leier@ttu.ee

***Abstract*—Respiratory information is usually measured directly with chest and abdominal belt or from the nasal airflow. There are several methods to extract respiration also from the electrocardiogram (ECG) and photoplethysmogram (PPG). In this paper we propose a methodology that detects the amplitude changes in the PPG signal to estimate the respiration rate. During exhalation, our parasympathetic nervous system makes the blood vessels more flexible than during inhalation. Blood vessels flexibility affects the propagation velocity of the pulse wave. In that way respiration also modulates the amplitude of the pulse wave signal. Comparing with other respiration signal extraction techniques our method has excellent results with limited processing power. The long-term objective of this work is to use the respiration signal together with heart rate and blood oxygen saturation level (SpO2), that are extracted from the pulse wave, for sleep apnea detection and screening purposes.**

I. Introduction

Pulse oximetry is frequently used in clinical situations for non-invasive measurement of heart rate and arterial oxygen saturation. Photoplethysmogram (PPG) is obtained optically illuminating the skin and measuring changes in light absorption with the pulse oximetry. In many clinical situations breathing rate is extracted from the PPG, which is known to cause a minimum of inconvenience to the patient. A number of methods for deriving the breathing rate from the PPG have been suggested in the literature. One possible application area to extract respiration rate is to diagnose an Obstructive Sleep Apnea (OSA). It is a respiratory disorder characterized by recurrent airflow obstruction caused by total or partial collapse of the upper airway. It is believed to cause often for the babies Sudden Infant Death Syndrome (SIDS) to occur.

As the need for remote health monitoring systems increases, the complexity of such systems also grows significantly. For pre-screening purposes there is no need to use systems that provide full clinical analysis. Signals measured by few attached sensors consist usually complex signals that are used to extract different features.

In this paper we propose an algorithm to extract respiration rate from the PPG signal. We analyse the amplitude variations in the PPG signal that are caused by the respiration and demonstrate experimentally efficiency of our proposal.

In the following section we present background on blood oxygen saturation measurement and discuss related work with some possible application areas. In section 3 we describe the methodology that is used to analyse the PPG signal. Section 4 describes the initial results and evaluating the performance. Finally section 5 discusses future work and gives some conclusions.

II. State of the art

A. Blood oxygen saturation measurement

Blood oxygen saturation level (SpO2) is one of the most direct measurement of a baby's health condition. Although the primary cause of SIDS has not been determined, there is a growing evidence that the victims have had previous hypoxic episodes that may be an early warning sign of SIDS [1]. It can be detected by measuring a person's SpO2 level, that is also a general indicator of the baby's condition which is perpetually monitored on premature babies [2]. Healthy baby at normal conditions should have a reading of 97% to 99%. Some authors claim that nocturnal arterial blood oxygen saturation level (SaO2) alone allows for confident recognition of moderate and severe OSA cases, but it is likely to be inadequate for excluding milder cases in clinical practice [3].

Low SpO2 level is the direct result of apnea or insufficient oxygen intake. If there is a sudden drop in the SpO2 level $\geq$ 4% and if it stays below 90%, this is an early warning sign of trouble. Several indices derived from overnight pulse oximetry may predict the presence of OSA, such as the number of oxyhemoglobin desaturations below a threshold, usually a 3 or 4 % decline from the baseline or the cumulative time spent below an oxyhemoglobin saturation of 90%, among others [4].

Lethal arrhythmia had been proposed by several groups as the primary cause of SIDS. The authors of [2] argued that the arrhythmia may be the result of hypoxic apnea, rather than a cause of SIDS. Bradycardia (low heart rate) is also indicator of trouble. Therefore measuring heart rate has a definite advantage over detecting hypoxic episodes alone.

SpO2 is usually measured by using a finger probe or ear lobe saturation. This is considered as a reliable and practical when patient is steadily in the bed. There are also experiments where SpO2 readings were taken on wrist and chest belt [5] with good quality readings. Studies [6] also show that pulse oximetry measurements on foot are reliable and have also good correlation with perfusion index.

Different studies have been done measuring the SpO2 level on neonates. For that purpose reflectance pulse oximeter based on Near Infra-red Spectroscopy (NIRS) technique was used which are more comfortable in long term monitoring [7]. Prototypes with reflectance sensors embedded in soft foam and fabric materials give an opportunity to integrate them into snuggle

and mattresses where baby lays on most of the time. Drawback of this solution is that it is very sensitive to the movements and requires certain body positions that may give many false alarms.
Pulse oximetry and accelerometer has also been integrated into the infant shoe [8]. Accelerometer is used as an actimetry and position measurement of infant. It is also stated that oximeter performance is mostly affected by low peripheral perfusion states and patient motion. Therefore greater likelihood of false alarms is caused by a false low reading or no reading at all. The studies of neonates and children found that 44-63% of all critical care alarms were caused by pulse oximeters, 94% of oximeter alarms were considered clinically unimportant, and 71% were false alarms [9].

B. Sleep apnea classification

Corkum and colleagues studied the sleep of 25 medication-free pre-adolescent children and reported sleep problems such as bedtime resistance, restless sleep and longer sleep duration were significantly more frequent in the Attention Deficit with Hyperability (ADHD) group. An early case series of 50 children with polysomnography proven OSA demonstrated hyperactivity in 42% of subjects and decreased school performance in 16% [10]. A subsequent examination of the natural history of snoring between 4 to 7 years of age found that hyperactivity, restless sleep and excessive sleepiness were significantly more common among habitually snoring children compared with youngsters who had never snored, lending further support to the notion that a causative relationship may exist [11].
There is also an emerging evidence that periodic limb movement disorder (PLMD) may be associated with prominent attentional/behavioural symptoms in children. Diagnostic criteria for PLMD is typically met when PSG exhibits greater than five PLMs per hour of sleep and symptomatic sleep disruption is reported, altough universally accepted paediatric criteria have not yet been established [12].
Existing research suggests that daytime inattention, hyperactivity and behavioural problems are likely to be caused or worsened by OSA or PLMD for a substantial minority of patients. This will remain an active area of investigation, with substantial efforts toward development of reliable and cost-effective screening tools which will permit screening for these primary sleep disorders without the time and expense of a full polysomnography (PSG). Development of outcome-based treatment guidelines for these conditions will improve assessment of the impact of treatment on day and night time symptoms [13].

C. Difference between full polysomnography and screening

Full PSG is an overnight monitoring in the sleep laboratory. Each subject is monitored with EEG, right and left electrooculogram, submental EEG, EMG, ECG, chest and abdominal wall motion by respiratory inductance plethysmography, oronasal airflow, SaO2, P_{ETCO2} by infrared capnometry at the nose. Subjects are also monitored with infrared video camera [14].
For screening purposes simplified tests may be used at home. These tests usually involve measuring heart rate, SpO2 level, airflow and breathing patterns. If you have sleep apnea, the test results will show drops in the SpO2 level during apneas and subsequent rises with awakening. Portable monitoring devices don't detect all cases of sleep apnea. In some cases you still may go through the full PSG even if your initial results are normal. It is considered also as a reliable and comfortable way to diagnose the OSA in babies and children.

III. Materials and Methods

Proposed solution is focusing on infants from the newborn up to first year and children between the year 2 to 8 who need to be monitored in case sleep apnea is suspected. Our goal is to use sensors which are easy to place and make minimum discomfort to the babies. Therefore only optical sensors were used. It will limit the number of acquired signals, which do not provide enough information for full PSG but is sufficient for the home screening.

A. Difference in signal characteristics between neonates and adults

The biggest difference between adults and neonates is the heart rate and breathing rate. Strong sympathetic stimulation can increase the heart rate in young adults from the normal rate of 70 beats per minute up to 180 to 200 and, rarely, even 250 beats per minute. Resting heart rate for the newborns is similar, 70 to 190 beats per minute. Well-trained athletes has the lowest heart rate, as low as 40 to 60 beats per minute. In case of 250 beats per minute time between every beat is 240 ms and biologically it can not be less than 200 ms.

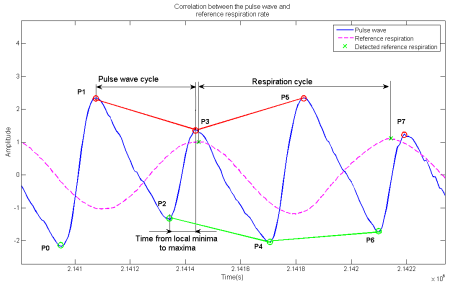

Fig. 1. Analysis of pulse and respiration wave

Figure 1 describes morphological changes of the pulse wave. Time from local minima ($P2$) to maxima ($P3$) is about 80 ms. With 125 Hz sampling rate it is enough to analyse up to 10 samples at the time, that corresponds to the 80 ms, not to miss any important changes in the pulse wave.
To compare the shape of the currently analysed signal with the next one, we buffer it. It causes a slight delay for the analysis but helps to detect whether the next local minima or maxima belongs to the current respiration pattern or is the beginning of the next one. As we also need to catch also a low heart rate and some possible missing beats, we buffer 5 seconds at the time, that is enough to include the next pulse wave and not to cause big delays in case some critical changes have happened.

B. Data Acquisition

Reference data has been collected from the PhysioNet MIMIC II Waveform Database. It contains recordings from

bedside patient monitors in adults and neonatal intensive care units. Our collected signals include fingertip PPG and respiration signals. Recordings are digitized with sampling rate of 125 Hz and resolution of 8-, 10-, or 12-bit. The recordings are from six different neonates, each with the length of 60 minutes.

C. Pulse wave signal processing

The main challenges in processing the PPG signals can be divided into three main groups, preprocessing, feature extraction, and diagnosis as described in Figure 2.

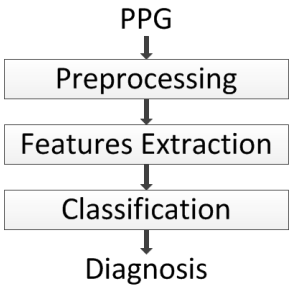

Fig. 2. Three stages common structure of PPG diagnostic system

Preprocessing stage removes the artefacts from the PPG signal. Most common source of interferences is the mains power, that causes 50/60Hz sinusoidal spikes with its higher harmonics. Motion artefacts that are caused by poor contact to the photo sensor, need much more processing. There are two types of PPG measurements, transmittal and reflective. Although these two arrangements have no fundamental difference from the optics point of view, their practical properties and performance differ significantly with respect to the motion artefact, signal-to-noise ratio, and power requirements. Reflective PPG needs more secure attachment of the LED and photo-diode to the skin surface, when compared to transmittal PPG. Once an air gap is created between the skin surface and the optical components due to some disturbance, a direct optical path from the LED to the photo-diode may be created [15]. Possibility of using either method depends highly on the position where the measurements will be taken.
These factors generate several type of additive artefacts which may be contained within PPG signals. This may affect the extraction of features and hence the overall diagnosis, especially, when the PPG signal and its derivatives will be assessed in the algorithmic fashion.
Under the placed position there should be a thin epidermal tissue layer through which photons can reach the target blood vessels with less attenuation. In the arterial end of the capillaries the pressure is 30 to 40 mm Hg and in the venous ends 10 to 15 mm Hg [15]. Greater arterial pulsation than cutaneous pulsations in magnitude makes it less suspective to motion to the naturally higher internal pressure.

D. Respiration signal extraction

Physiological monitoring of breathing interval is important in many clinical settings, including critical and neonatal care, sleep study assessment and anaesthetics. Respiration causes variation in the peripheral circulation, making it possible to monitor breathing using a PPG sensor attached to the skin. The low frequency respiratory-induced intensity variations (RIIV) in the PPG signal are considered that RIIV includes contribution from the venous return to heart caused by alterations in intra-thoracic pressure and also changes in the sympathetic tone control of cutaneous blood vessels. The physiological mechanisms relating to the RIIV are, however, not fully understood. Baharav and colleagues found that increased respiratory effort occurs throughout the night in OSA patients, with the subsequent hypoxia and arousal, may become one of the useful parameters for the OSA screening of snoring children [16] [14].
There are several methods extracting respiratory information from the PPG signal. Pulse rate variability (PRV), pulse amplitude variability (PAV) and pulse width variability (PWV), which all are related to respiration [17], are used to estimate the respiration using a spectrum-based algorithm [18]. Respiratory estimation errors are quite comparable and stay around $-0.26 \pm 7.30\%$.
Empirical Mode Decomposition (EMD) method, that is robust, simple and makes use of derived Intrinsic Mode Functions (IMF), have shown good results in [19] with the accuracy of estimating respiratory rate between 98.73% and 99.87%. Some research has been done to efficiently extract respiration from the PPG using order reduced modified covariance AR technique [20]. It gives an improvement in frequency resolution compared to the traditional Fast Fourier Transform (FFT) method.
Discrete Wavelet Transform (DWT) is widely used when extracting respiration signal from Electrocardiogram (ECG) [21]. An absolute average error of 6.8% was obtained, considered highly acceptable for ambulatory patient monitoring. One variant of the DWT is Discrete Wavelet Packet Transform (DWPT) which tiles the frequency space in a discrete number of intervals. According to the literature [22] the accuracy of the DWPT technique is 85%. Wavelets have advantages over traditional Fourier methods in analysing physical situations where the signal contains discontinuities and sharp spikes. Daubechies wavelet based method was used and proved to be efficient in reducing motion artefacts restoring all the morphological features of the PPG signal [23].
Attachment of the sensor on the right body location has direct impact to the signal amplitude. Low amplitude PPG signal is mostly caused by the automatic gain controller. Detecting the heart beats in low amplitude PPG signals is considered difficult.
By filtering the data, it is possible to extract the respiratory rate harmonic from the filtered signal. Nilsson et al. [24] suggested the use of a 3rd order Butterworth band-bass filter with a pass-band from 0.1 to 0.3Hz to filter the PPG signal. Autoregressive based method [25] is aiming to provide more accurate results than existing techniques but it needs to be tuned to an individual, or at best, to specific age groups and/or for specific time periods. Some more complex techniques are using time-frequency spectra (TFS) for analyzing non-stationary signals. In this category, several studies have utilized short-time Fourier transform (STFT) and continuous wavelet transform (CWT) [26] to extract the respiration rate from the PPG signal. While the studies show relatively good results, the CWT is impractical because the extraction of the RR is done in

some cases with the use or frequency modulation (FM) while in other cases with the amplitude modulation (AM) of the heart rate. This requires additional adaptive decision-making schemes, to determine when to use either FM or AM of the heart rate signal, making this kind of approach not suitable for a low power resource constrained application.

E. Our proposed method for respiration signal extraction

One approach to extract the breathing rate information is based on connecting the peaks of each PPG pulse, thus constructing a continuous envelop along the top edge of the PPG signal. Then, through the use of the Fourier transform, a prominent high-amplitude peak can be identified that corresponds to the frequency of the subjects
Respiration cycle modulates the pulse wave that is causing amplitude changes. When we look at many continuous pulse waves in Figure 1 it can be seen that there is a repeating pattern that respiration is causing. If the PPG signal is without any artefact we can easily detect patterns based on local maxima and minima. After each oxygen intake following pulse wave ($P1$) has lower amplitude breathing signal [27].
According to our tests it is possible to stay in the time domain and detect breathing based on the top and bottom edge of the PPG signal. Our proposed algorithm receives PPG signal from the SpO2 sensor. FIR notch filter removes 50/60Hz and 100/120Hz noise. The PPG signal was also filtered with median filtering over 125 samples to remove small glitches and make the signal smoother. The signal was then normalized and DC part was removed. In the following algorithm N represents the number of current sample and will be increased after next minimum or maximum point is found. There are five main steps that describe the algorithm:

1) Buffer the signal with length of five seconds
2) Detect and count number of local minimas $minP$ and maximas $maxP$
3) IF $maxP(N-1) > maxP(N) < maxP(N+1)$ THEN found $maxPtrn \leftarrow 1$
4) IF $minP(N-1) < minP(N) > minP(N+1)$ THEN found $minPtrn \leftarrow 1$
5) IF $minPtrn(startT) > maxPtrn(startT)$ AND $minPtrn(startT) < maxPtrn(endT)$ AND $minPtrn(endT) > maxPtrn(endT)$ THEN found $doublePattern \leftarrow 1$

To analyse the signal we collect five seconds of the signal into the buffer. Each pulse wave has its local minima $minP$ and maxima $maxP$ that will be detected in the second step. After finding a new local maxima $maxP(N)$, it will be compared with the previous one $maxP(N-1)$. If the previous maximum point has larger amplitude than the last one, it will be included as a part of the pattern. If next local maxima $maxP(N+1)$ has bigger amplitude than the $maxP(N)$ then respiration pattern, based on the maximum points, has been found and $maxPtrn$ gets value "1" or "TRUE". Same methodology is repeatead in step 4 but with the minimum points ($minP$). In step 5 we compare start and end time of the minimum and maximum patterns. If the minimum pattern has started and ended after the maximum one, then respiration signal has double detected ($doublePattern$) and we can disregard last detected pattern. Figure 1 describes how double detected patterns were removed. Maximum pattern ($P1 - P3 - P5$) was detected correctly. Local minima $P0$ was detected but as $P2$ did not match to the criteria it will be disregarded automatically and next minima will be stored with the name $P4$.

F. Sleep apnea detection

One possible implementation of the extracted respiration rate is OSA detection. There are certain thresholds that point to the apneic episode. In case an air volume is measured, decrease the amount of air through the lungs at least 50% with the duration over 10 seconds, are signs of apnea. Saturation level decreases 3-4% from the baseline, which may end up with awakening. Cumulative time when saturation level is below 90% is also often an early sign of trouble [2]. Normal waking and asleep SpO2 levels in healthy child or adult are 96-99% and 94-98%, respectively. Sleep apnea has specific pattern in which order all symptoms appear. The typical cycle of sleep apnea is:

1) oxygen level begins to fall
2) breathing pauses 10 seconds or more
3) heart rate falls below normal
4) brief awakening with few large breaths
5) heart rate speeds up above normal heart rate
6) oxygen level returns to near normal

Apnea Hypopnea Index (AHI), the number of apneic episodes per hour, is used to detect the severity of sleep apnea.

- AHI of 5-15/hr - mild sleep apnea
- AHI of 16-30/hr - moderate sleep apnea
- AHI of +30/hr - severe sleep apnea

The standard definition of (AHI^s) [28] determined during attended laboratory PSG is calculated
A_{wofl} - apneas where 10 sec without flow
R_{flow} - hypopneas with reduced flow with 5% of desaturation
St_{tot} - total sleep time in hours

$$AHI^s = \frac{(A_{wofl} + R_{flow})}{St_{tot}}$$

As the sleep apnea could be the result of arrhythmia, individual signals could be used in order to detect any critical changes. We have tested our respiration extraction results with OSA detection algorithm. Three signals, heart rate, respiration rate and SpO2 values were used. In order to test our OSA detection algorithm we had to simulate SpO2 values because the reference database did not contain these signals. We have created random array of SpO2 values between 90% and 100% with one value per second. In every apneic episode, SpO2 level stays below the 94% at least 10 seconds, that is essential to simulate the real apneic episode.

Implementing vital signal monitoring with the thresholds makes it possible to develop OSA screening application for home monitoring. It could be used in case sleep apnea is suspected or there is a recommendation from the doctor to monitor premature babies also at home conditions.

TABLE I. ESTIMATING THE BREATHING RATE WITH PULSE WAVE AMPLITUDE VARIATION DETECTION

Signal name	Reference respirations	Accuracy (%)		
		MIN	MAX	Total
3000358_0010m	3972	76.86	82.30	101.33
3505210_0002m	4172	77.59	74.98	90.65
3470111_0006m	4095	78.44	79.61	104.66
3900726_0001m	4355	69.48	74.95	94.12
3601304_0001m	4139	84.13	86.25	111.11
3000858m	4376	81.67	81.26	92.62

IV. RESULTS

A. Detection of respiration rate

Respiration causes variation in the peripheral circulation that affects the pulse wave. There is a great correlation between breathing effort and changes in the amplitude of pulse wave. Figure 3 describes situation where the signal is clean and without any artefact. There are high and low peaks on top and bottom of the high amplitude signal which describes the periodical amplitude variation that is caused by the respiration.

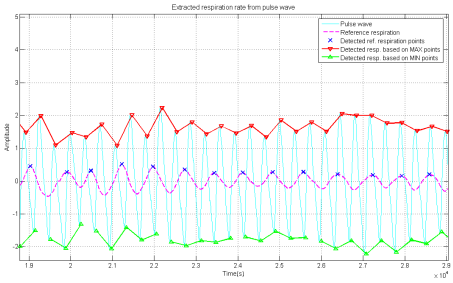

Fig. 3. Correlation between respiration and pulse wave

Mean accuracy of the respiration detection is 99.08% with the Standard Deviation (SD) of ±7.28%. Table I describes tests with six different subjects to validate our proposed algorithm. First column is the signal name that corresponds to the name in the PhysioNet MIMIC II Waveform Database. Second column is the number of respirations in the reference signal. Next two columns describe the number of extracted respirations from the pulse wave converted into the percentage. Last column is the final accuracy we get after using both, minima and maxima based pattern detection and eliminating double patterns. There is a significant accuracy increase, 30.65% ±8.74%, using double pattern detection.

B. Comparison with other results

Mobile sleep apnea screening platforms has been interest by different research groups. One similar platform was built by [29]. They connected several bio-sensors to the smart phone and using FFT pulse rate, breathing rate. Oxygen saturation was calculated from the PPG signal. OSA estimation was done based on the pulse rate and oxygen saturation rate because fluctuations in the blood oxygen level and heart rate are detected during the apnea periods. Spectral analysis of SaO2 or heart rate variability have been suggested as potential diagnostic tools in this disease [30]. Some studies show that some patients may not even present variations in SaO2 or heart rate signals, therefore pre-screening may not give adequate answer to the suspicions and full PSG is needed.

TABLE II. COMPARISON OF DIFFERENT RESPIRATION EXTRACTION METHODS

Method	Number of subjets	Age	Absolute accuracy
IMF	4	NA (adults)	99.48±0.44%
PRV	17	28.5±2.5	86.93±15.34%
PWV	17	28.5±2.5	98.83±9.44%
PAV	17	28.5±2.5	84.55±15.34%
PWV+PAV+PRV	17	28.5±2.5	99.74±7.30%
BML	10	25±3	98.63±1.24%
TMI	10	25±3	98.54±1.12%
Our proposed	6	NA (neonates)	99.08±7.28%

*BML - beat morphology [32]; TMI - time interval [32]; IMF - Instrinsic Mode Functions; PRV - pulse rate variability [17];PAV - pulse amplitude variability [17]; PWV - pulse width variability [17]; PAVD - our proposed pulse amplitude variability based pattern detection

Because the SpO2 measurement accuracy is very sensitive to the body movements and amplitude of the pulse wave, several methods have been applied to suppress motion artefacts. Kalman filter has been used to improve the results to derive the pulse rate with 3% of error [31].
Table II compares different techniques to extract respiration rate from the PPG signal. First column is a short name of the method, that is explained at the end of the table. Second column describes number of the subjects to validate the method. There is a difference in the age groups, described in the third column. Most of the algorithms are validated with the mid-age adults not with the neonates nor children as we have done. As there are slight differences in signal waveforms between the children and adults, there could be some deviations in the results when applying on children. Last column describes the accuracy of extracting the respiratory information with the SD.

Our proposed method, last row in the table, has excellent results compared with the other ones. It needs an extended testing and implementing various artefact suppression techniques to validate the accuracy in different real-time situations. Initial results show that using pulse wave amplitude variation based detection, it is possible to estimate the respiration signal with high confidence.

V. CONCLUSIONS AND FUTURE WORK

Our evaluation of the proposed algorithm demonstrates that pulse amplitude variation could effectively be derived from the PPG signal analysis. It does not need as much processing power as FFT or DWT based algorithms.
However there is a need for extended tests to demonstrate the reliability of our proposed algorithm in different real-life situations when there could be significant amplitude changes. To increase the accuracy of breathing rate estimation there is a need to identify and throw away distorted parts from the signal. There are may possibilities how pulse wave can be distorted which makes features extraction unusable. If we would use two optical sensors to measure the pulse wave, we could have significantly better signal quality. If readings from one sensor are out of limits or distorted, we could replace some parts of the signal with readings from the second one or estimate the signal with the help of second one. Drawback of this solution is increased power usage due to the increased number of optical

sensors. On the other hand, our goal is to increase the accuracy of the measurements from the optical sensors.

REFERENCES

[1] S. Q. ul Ain Ali and V. Jeoti, "Sudden infant death syndrome (crib death)," *American Heart Journal*, vol. 93, no. 6, pp. 784–793, Jun 1977.

[2] R. A. Polin and W. W. Fox, *Fetal and Neonatal Physiology*. W. B. Saunders Company, 1992.

[3] F. Series and I. Marc, "Utility of nocturnal home oximetry for case finding in patients with suspected sleep apnea hypopnea syndrome," *Ann. Intern. Med.*, vol. 119, pp. 449–453, 1993.

[4] R. Golpe and A. Jimenez, "Utility of Home Oximetry as a Screening Test for Patients with Moderate to Severe Symptoms of Obstructive Sleep Apnea," *Sleep*, vol. 22, no. 7, pp. 932–7, Nov 1999.

[5] M. Maattala, A. Konttila, and E. Alasaarela, "Optimum Place for Measuring Pulse Oximeter Signal in Wireless Sensor-Belt or Wrist-Band," *ICCIT*, pp. 1856–1861, 2007.

[6] N. M. Noor and M. N. Taib, "Using Pulse Oximetry Method as a Non Invasive Indicator of Blood Perfusion in Neonates," *ICICI-BME*, pp. 254–258, Nov 2011.

[7] D. Potuzakova and W. Chen, "Innovative design for Monitoring of Neonates Using Reflectance Pulse Oximeter," in *7th ICIE*, 2011.

[8] Y. Rimet and Y. Brusquet, "Surveillance of Infant at Risk of Apparent Life Threatening Events (ALTE) with the BBA Bootee: a Wearable Multiparameter Monitor," *EMBS*, pp. 4997–5000, Aug 2007.

[9] J. W. Salyer, "Neonatal and Pediatric Pulse Oximetry," *Respitory Care*, vol. 48, 2003.

[10] C. Guilleminault and R. Korobkin, "A review of 50 Children with Obstructive Sleep Apnea Syndrome," *Lung*, vol. 159, pp. 275–287, 1981.

[11] N. J. Ali, D. Pitson, and J. R. Stradling, "Natural History of Snoring and Related Behavious Problems Between the Ages of 4 and 7 Years," *Arch. Dis. Child*, vol. 71, pp. 74–76, 1994.

[12] M. Thorpy and D. C. S. Commitee, "Periodic Limb Movement Disorder," in *International Classification of Sleep Disorders*. American Sleep Disorder Association, Rochester, MN, USA, 1990, pp. 65–68.

[13] T. F. Hoban, "Assessment and Treatment of Disturbed Sleep in Attention Deficit Hyperactivity Disorder," *Expert Review of Neurotherapeutics*, vol. 4, no. 2, pp. 307–316, Mar 2004.

[14] E. S. Katz and J. Lutz, "Pulse Transit Time as a Measure of Arousal and Respiratory Effort in Children with Sleep-Disordered Breathing," *Pediatric Research*, vol. 53, no. 4, pp. 580–588, Feb 2003.

[15] J. Hall, *Textbook of Medical Physiology*. Philadelphia, PA: Saunders, 2000.

[16] L. M. O'brien and D. Gozal, "Consequences of Obtructive Sleep Apnea Syndrome," pp. 211–222, 2005.

[17] J. Lazaro and E. Gil, "Deriving Respiration From the Pulse Photoplethysmographic Signal," *Computing in Cardiology*, vol. 38, pp. 713–716, 2011.

[18] R. Bailon, L. Sornmo, and P. Laguna, "A Robust Method for ECG-based Estimation of the Respiratory Frequency During Stress Testing," *TBME*, vol. 53, no. 7, pp. 1273–1285, 2006.

[19] K. V. Madhav and M. R. Ram, "Estimation of Respiration Rate from ECG, BP and PPG signals using Empirical Mode Decomposition," *IEEE*, 2011.

[20] K. V. Madhav, M. Raghuram, and E. H. Krishna, "Monitoring Respiratory Activity Using PPG Signals by Order Reduced-Modified Covariance AR Technique," *iCBBE*, pp. 1–4, 2010.

[21] E. E. Santo and C. Carbajal, "Respiration Rate Extraction from ECG Signal via Discrete Wavelet Transform," *IEEE*, 2010.

[22] S. Q. ul Ain Ali and V. Jeoti, "DWPT Based Sleep Apnea Detection," *IEEE*, 2011.

[23] M. R. Ram, K. V. Madhav, and E. H. Krishna, "Computation of SpO2 Using Non-parametric Spectral Estimation Methods from Wavelet Based Motion Artiface Reduced PPG Signals," *ICSCCN*, pp. 776–780, July 2011.

[24] L. Nilsson and A. Johansson, "Respiration Can be Monitored by Photoplethysmography with High Sensitivity and Specifity Regardless of Anaesthesia and Ventilatory Mode," *Acta Anaesthesiol. Scand.*, vol. 49, no. 8, Sep 2005.

[25] S. Fleming and L. Tarassenko, "A Comparison of Signal Processing Techniques for the Extraction of Breathing Rate from the Photoplethysmogram," *World Academy of Science*, 2007.

[26] P. A. Leonard and J. G. Douglas, "A Fully Automated Algorithm for the determination of Respiratory Rate From the Photoplethysmogram," *Clinical Monitoring and Computing*, vol. 20, pp. 33–36, 2006.

[27] W. Johnston and Y. Mendelson, "Extracting Breathing Rate Information from a Wearable Reflectance Pulse Oximeter Sensor," *IEMBS*, vol. 2, pp. 5388–5391, 2004.

[28] N. A. Collop and S. L. Tracy, "Obstructive Sleep Apnea Devices for Out-Of-Center (OOC) Testing: Technology Evaluation," *Clin. Sleep Med*, vol. 7, no. 5, pp. 531–548, Oct 2011.

[29] S. Lam and K. L. Wong, "A Smartphone-centric Platform for Personal Health Monitoring Using Wireless Wearable Biosensors," *ICICSdiatrics*, pp. 1–7, 2009.

[30] C. Zamarron and F. Gude, "Utility of Oxygen Saturation and Heart Rate Spectral Analysis Obtained From Pulse Oximetric Recordings in the Diagnosis of Sleep Apnea Syndrome," *CHEST*, vol. 123, no. 5, pp. 1–7, May 2003.

[31] M. Yarita, N. Kobayashi, and S. Takeda, "Compensation for Two Specific Types of Artifact in Pulse Wave Using a Kalman Filter," *ITAB*, pp. 269–272, 2007.

[32] D. Wu and G.-Z. Liu, "The Accuracy of Respiratory Rate Estimation Using Electrocardiography and Photoplethysmography," *ITAB*, no. 10, pp. 1–3, 2010.

Appendix D

Leier M.; Pilt K.; Karai D.; Jervan G. (2015). Smart Photoplethysmographic Sensor for Pulse Wave Registration at Different Vascular Depths *In: EMBC*, Milano, Italy, 2015, pp. 1849-1852

Smart Photoplethysmographic Sensor for Pulse Wave Registration at Different Vascular Depths

Mairo Leier[1], Kristjan Pilt[2], Deniss Karai[3] and Gert Jervan[4]

Abstract— **The aim of this paper is to propose a smart optical sensor for cardiovascular activity monitoring at different tissue layers. Photoplethysmography (PPG) is a noninvasive optical technique for monitoring mainly blood volume changes in the examined tissue. However, different important physiological parameters, such as oxygen saturation, heart and breathing rate, dynamics of skin micro-circulation, vasomotion activity etc., can be extracted from the registered PPG signal. The developed sensor consists of 32 light emitting sources with four different wavelengths, which are located to the four different distances from four photo detectors. Compared to the existing sensors, the system enables to select the optimal LED (light emitting diode) and photo detector couple in order to obtain the pulse wave signal from the interested blood vessels with the highest possible signal to noise ratio. In this study, the designed PPG sensor was tested for the pulse wave registration from radial artery. The highest efficiency and signal to noise ratio was achieved using infrared LED (940 nm) and photo-diode pair.**

I. Introduction

Photoplethysmography (PPG) is a noninvasive optical technique for monitoring mainly blood volume changes in the examined tissue. Light from a light source, e.g. LED (light emitting diode), laser, halogen lamp, is emitted to the examined tissue, where it is scattered and absorbed. The transmitted or back-scattered light intensity changes from the tissue can be detected by using photo-diode. This technique has been clinically widely used for example in pulse oximetry systems, where the blood oxygenation rate is calculated based on the simultaneous amplitude measurement of PPG signal on two or more wavelength bands [1]. However, the research and application areas of the PPG technique have been expanding during the recent years. The PPG signal registration and analysis has been used for heart and breathing rate measurement, heart rate variability analysis, pulse transit time, arterial stiffness and vasomotion estimation [2]. PPG sensors are designed mainly for the pulse wave registration from peripheral vascular beds, such as finger, ear lobe, forehead etc. Nevertheless, the pulse wave registration from the artery is needed in order to exclude the influence of the peripheral blood vessels (arterioles, capillaries) and to estimate the stiffness changes of the central arteries or certain segment of artery [3].

Our proposed system consists of 32 LEDs in four different wavelengths and four photo-diodes. Distances between the photo-diodes and LEDs vary to analyze different tissue layers. LEDs can be grouped in order to analyze automatically larger tissue areas without moving the sensor on the skin. The sensor is controlled by the previously proposed miniaturized monitoring device [4]. The designed PPG sensor is tested for the pulse wave registration from radial artery.

In the following section we present background on the PPG measurement and discuss related work together with some possible application areas. In section 3 we describe the methodology that is used to analyze the PPG signal. Section 4 describes the experiments and initial results. Finally section 5 discusses the future work and gives some conclusions.

II. State of the art

The alternating current (AC) component in the PPG signal is synchronous with heart cycle and it is related to the heart generated pulse wave [2]. The pulse waveform carries important clinical information about the arterial system, including the micro-circulation of the skin. The detection of the PPG signal from different tissue layers may give a better understanding of the changes in the arterial system [5]. Techniques and applications to obtain the information from deeper tissue layers, such as blood flow monitoring in the tibial anterior muscle [6] [7], foetal oxygen saturation monitoring [8], estimation of pulse wave velocity in larger arteries [9] have been developed.

The light penetration volume-depth in skin depends on the selection of the wavelength [10]. Absorption of the light in the visible and near infrared wavelengths depends mainly on chromophores such as water, hemoglobin, and melanin. There is an "optical window", where the light is less absorbed by tissue. Therefore, red and near infrared light can penetrate deeper layers of tissue than shorter (green, blue) or longer (infrared) wavelengths and the absorption of blood is more prevalent. In addition to the absorption, tissue is a highly scattering medium, where the light behaves diffusely. Photons are scattered from cell membranes and organelles. Generally, in shorter wavelengths the light is more scattered than in longer wavelengths. Due to the scattering and absorption properties of the tissue there is possibility to obtain the PPG signal from different tissue layers, which is based on the combination of wavelength and distance between the LED and photo-diode (PD) [11]. In addition, earlier

*This work was jointly supported by EU through European Regional Development Fund, and by the institutional research funding IUT 19-1 and IUT 19-2 of the Estonian Ministry of Education and Research.

[1]Mairo Leier is with the Department of Computer Engineering, Tallinn University of Technology, Tallinn, Estonia mairo.leier@ttu.ee

[2]Kristjan Pilt is with the Department of Biomedical Engineering, Tallinn University of Technology, Tallinn, Estonia kristjan.pilt@cb.ttu.ee

[3]Deniss Karai is with the Department of Biomedical Engineering, Tallinn University of Technology, Tallinn, Estonia deniss@cb.ttu.ee

[4]Gert Jervan is with the Department of Computer Engineering, Tallinn University of Technology, Tallinn, Estonia gert.jervan@ttu.ee

studies, using extremely short light pulses and time-of-flight analysis, have reported that the distance photons travel in tissue is approximately 4-6 times the distance between the light source and photo detector [12]. Generally, in case of short distance between the LED and photo-diode, and short wavelength (green, blue), the penetration volume-depth is small. On the other hand in case of long distance between the LED and photo-diode, and longer wavelength (near infrared), the penetration volume-depth is larger.

PPG sensor development for the signal registration from the different penetration volume-depths, has been described earlier [6] [7] [13]. The advantage of our proposed sensor is to combine PDs and LEDs with different wavelengths into groups so that they can be driven independently. The distance between the LEDs and PDs and selection of the wavelength in proposed smart PPG sensor has been made based on the previously mentioned studies.

III. Sensor Architecture

The proposed sensor architecture is part of the previously developed system. The architecture and the functionality of the system has been discussed in [4] and [14]. Smart PPG sensor consists of LED and photo-diode array with control logic and optical measurement functionality.

A. Sensor

Figure 1 depicts the architecture of the optical sensor module. There are four independent LED and PD groups, and two independent channels. A channel means that all signals that are measured in this particular group are connected with one particular analog front-end (AFE) module. In total there are two identical AFEs integrated into one AFE module that are working in parallel. Each group has one PD, green (G), red (R) and two infra-red (IR) LED emitters.

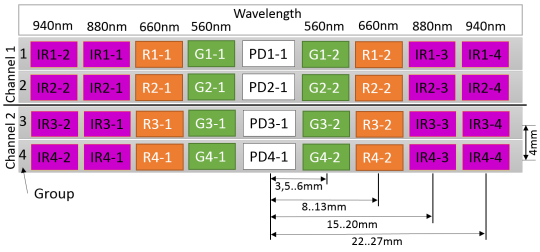

Fig. 1. Structure of optical sensor array

Four different wavelengths are used. Green LED 560 nm, red LED 660 nm, inner infrared LED (IR*n*-1 and IR*n*-3) 880 nm, and outer infrared LED (IR*n*-2 and IR*n*-4) 940 nm. All vertical and horizontal distances between LEDs and PD-s are based on the studies, mentioned in state of the art.

1) Light Source Driver: Figure 2 depicts the hardware block diagram of the smart PPG sensor. All digital control signals are marked with dotted line. Multiplexing of control signal is done by using serial in to parallel out shift registers that drive analogue switches. Each shift register controls two switches and each switch in turn two LED pairs. A LED pair means that there are two LEDs, one LED anode is connected to another's cathode so that they can be turned on alternately. With current configuration we can drive independently up to 16 LEDs per one channel. In Figure 2 an emitter-pair is drawn as emitter box. For simplicity there are four two emitter boxes drawn and inside each one there are two emitters. Depending on the used analogue switch, there can be any number of LED pairs inside each box. The switching of optical sensor is initiated by the data processing module (a). Real switching of optical sensor is performed by the integrated Control Logic (b). The current for each LED is digitally controlled with 8-bit accuracy. Current configuration allows to set up to 100 mA LED current for each LED independently by the AFE.

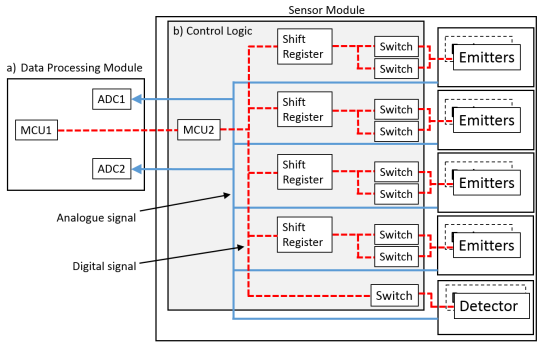

Fig. 2. Hardware block diagram

All four PD-s are driven by one analogue switch. For each channel there are two PD-s. Solid blue lines on the Figure 2 mark analogue signals. From the PD, an analogue signal goes directly to the AFE module.

2) Communication: Device is controlled by the user interface via USB connection. For better sensor management we have developed a Python based graphical user interface (GUI) that allows to set individually the current of each LED, feedback resistors and capacitors, to view the received signals and save the raw data into the file. From Analogue front-end we receive 6 signals: LED1, LED2, LED1 ambient, LED2 ambient, LED1-LED1 ambient and LED2-LED2 ambient. All signals are 22-bit long. Ambient measurement and cancellation is built into the AFE as is done automatically by the AFE.

B. Logic

1) Driving phases: The LED array driving process has two main phases. At first, the array has to be calibrated which is mandatory to start the measurement process. Calibration process analyses the acquired signal and determines LED groups that have the best signal quality.

For the calibration we group two LEDs into one group. In Figure 1 LEDs IR*n*-1 and IR*n*-2 forms one group, R*n*-1 and G*n*-1 second, R*n*-2 and G*n*-2 third, and IR*n*-3 and IR*n*-4 fourth group. Same grouping methodology is defined

in each group and on both channels. Altogether we get 16 LED groups. Each group is switched on and off for a short period of time with different pre-defined configurations.

Calibration with each group is started by setting the LED current to 100mA and amplification with the feedback resistor to the maximum level. If the signal strength goes into saturation, amplification is decreased until the AC component has the maximum value and DC component is not in the saturation. Based on the AC and DC component, we calculate the efficiency. At first, a received photo-current is calculated:

$$I_p = \frac{V_{out}}{2 * R_f}, \tag{1}$$

where I_p is photo-current, V_{out} is photo-voltage analog-digital conversion (ADC) value divided by 22-bits, R_f is feedback resistor of the amplifier. With that equation we can calculate photo-current for AC and DC component. Efficiency is calculated with the following formula:

$$\gamma_{eff} = \frac{I_{AC}}{I_{DC}}, \tag{2}$$

where γ_{eff} is the efficiency, I_{AC} is photo-current of AC component and I_{DC} is photo-current of DC component.

After all groups are toggled once with their own best settings, signal quality analysis follows to detect the presence of pulse wave. The group with the highest amplitude of AC component will be chosen automatically to start the continuous measurement process. If there are signals with identical quality from more than one group we can redefine groups and repeat the same process to find only those LEDs that give the best signal for our needs and group these into one group that will be used during the analysis.

2) Configuration of light source driver: The AFE module is capable of generating up to 5 kHz pulse repetition frequency (PRF). Each period includes two times ambient and LED sampling. The sample rate is four times PRF, up to 20 kHz. For pulse wave detection the common sampling rate is 250 Hz and up but using higher sampling rate it is possible to use built in hardware averaging functionality that gives even better signal quality. In our current configuration, we are using sampling rate of 500Hz and no averaging.

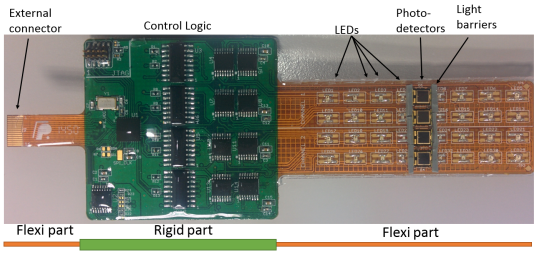

Fig. 3. Sensor module overview

Figure 3 depicts the build-up of the sensor module. Module has a connector for external system connection, that is built on the flex part. All control logic is placed on the rigid part as it helps to increase the mechanical reliability because the rigid does not bend. All optics are on the flex part as it touches directly the skin and needs to be bent accordingly. All electronics, including LEDs and photo-diodes, is poured into the medical silicone to minimize the effect of the skin.

Rigid and flex parts have 4-layer design to suppress the noise and increase the stiffness to the appropriate level. Extra care has been taken with the signal line routing of the detectors. As the length of the whole sensor part is 138 mm, there is a risk for increased noise. For that reason all detector lines are routed on the middle layer and also surrounded with shielding traces.

IV. Experiments and Results

During the real experiments we have got results that verify out expectations about obtaining the best pulse wave signal from the radial artery only from the LED and photo-diode pair with the highest efficiency, that is calculated using formula (2). Measurements were performed by placing the sensor on the wrist, as depicted on figure 4, and fastening it using bending strap.

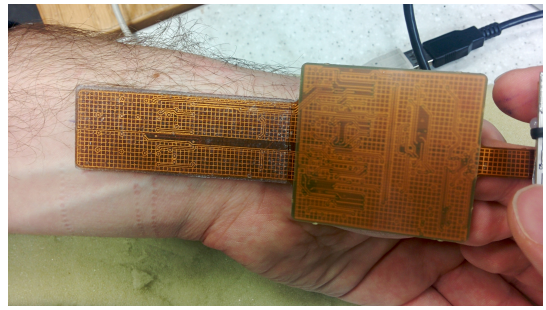

Fig. 4. Sensor placement on the wrist

Experiments were performed on different days, but on the same test person. The signals were recorded from the left hand radial artery. Efficiency was calculated as described in the previous section. Table I depicts the relative signal efficiency for each LED and photo-diode pair. The optopair with highest efficiency on each vertical group is colored. Red color marks infrared, orange red and light green marks green LED. Efficiency more than 1% is considered usually as a good signal. The bigger the efficiency number the better signal to noise ratio we get.

The signal with the highest efficiency is received with the LEDs that have the longest wavelength, marked with red. Comparing the left and right side, the signal with highest efficiency is on the right side because radial artery is more close to the surface of the skin on the wrist side. As it can be seen from Table I, there are also some differences between measurements on different days. However, it is visible, that the results are repeatable and the radial artery can be detected under certain optopair.

For the reference we have also measured noise level of photo-diode by shutting down LED driving part of the AFE

TABLE I
TEST RESULTS

Day 1

IRn-3	IRn-4	Rn-2	Gn-2		Gn-1	Rn-1	IRn-2	IRn-1
0,58%	0,68%	0,33%	0,59%	PD	1,09%	0,36%	0,67%	0,52%
1,10%	1,11%	0,68%	0,00%	PD	0,83%	0,68%	1,37%	1,61%
0,84%	0,89%	0,51%	0,47%	PD	0,63%	0,62%	1,02%	1,07%
0,58%	0,63%	0,43%	0,37%	PD	0,48%	0,55%	0,79%	0,60%

Day 2

0,26%	0,31%	0,41%	0,32%	PD	0,36%	0,29%	0,65%	0,42%
0,48%	0,69%	0,51%	0,00%	PD	0,37%	0,49%	1,46%	0,79%
0,37%	0,50%	0,46%	0,23%	PD	0,26%	0,35%	1,05%	0,61%
0,26%	0,29%	0,32%	0,16%	PD	0,21%	0,38%	0,71%	0,53%

module and putting the sensor to the dark. The average noise is 0.256 mV and it is not dependent on the feedback resistor in Eq. (1).

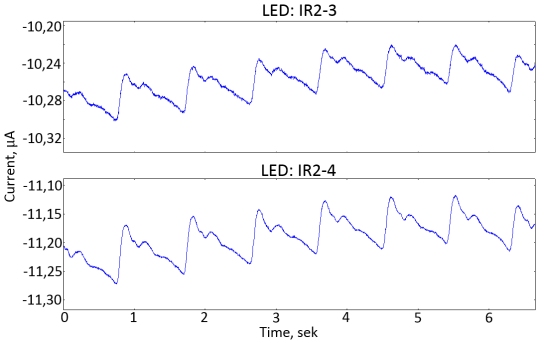

Fig. 5. Measured PPG signals; Top: IR2-3, bottom: IR2-4

Figure 5 depicts the results of one LED pair. Upper part describes the signal measured with IR2-3 and below IR2-4. Both signals have already ambient subtracted and LED current is calculated based on the Eq. (1) and (2). As this figure belongs to the measurements made on the second day, it correlates well with the Table I bottom part. Efficiency values in that table show also that IR2-4 has slightly better efficiency compared to IR2-3, 0.69% and 0.48% accordingly.

V. FUTURE WORK AND CONCLUSIONS

Currently all measurements were performed manually by switching between LED pairs, setting feedback resistor, capacitor and LED current values manually. This task will be automated in the future because this is the calibration task that needs to be performed before each measurement. During that time there should be no sensor placement changes nor any other disturbances that may change the environment conditions, which impacts heavily signal quality.

LED and photo-diode control logic is currently separated from AFE with micro-connector. To increase the physical reliability and noise immunity, AFE and LED/PD driving can be bundled into one board to reduce the physical dimensions of the module twice. This makes the placement of the sensor to the human wrist more comfortable and faster.

It is possible to decrease the ambient noise by increasing ambient cancellation current and decreasing LED duty cycle. It is also possible to enable the second stage ambient cancellation amplification to increase the noise immunity and get more noise free bits.

In this paper, the architecture and driving possibilities of smart PPG sensor is presented. We have designed the first prototype of smart PPG sensor. It has 32 independent emitters and 4 independent detectors that can be grouped and driven individually. With the current configuration the system is flexible enough to perform measurements by grouping emitters into different groups or driving all of them individually. First experiments show that it is possible to use developed sensor for registration of pulse wave from radial artery in more comfortable way and faster. According to our results the efficiency variation ca 1.46% between different optopairs and different emitter wavelengths shows clearly the usability of proposed sensor.

REFERENCES

[1] M. Nitzan, A. Romen, and R. Koppel, "Pulse oximetry: fundamentals and technology update," *Medl Devices*, p. 231239, Jul 2014.

[2] J. Allen, "Photoplethysmography and Its Application in Clinical Physiological Measurement," *Eur J Pain*, vol. 8, pp. 163–71, 2007.

[3] G. A, M. Z, and L. Z. et al, "Usability of photoplethysmography method in estimation of conduit artery stiffness," *Biomedical Optics*, Jun 2011.

[4] M. Leier and G. Jervan, "Miniaturized Wireless Monitor for Long-term Monitoring of Newborns," *BEC*, 10 2014.

[5] J. Spigulis, L. Gailite, and A. L. et al., "Simultaneous recording of skin blood pulsations at different vascular depths by multiwavelength photoplethysmography," vol. 46, pp. 1754–9, 2007.

[6] Q. Zhang, L. G. Lindberg, and R. K. et al, "A Non-invasive Measure of Changes in Blood Flow in the Human Anterior Tibial Muscle," *Eur J Appl Physiol*, vol. 84, pp. 448–52, 2001.

[7] M. Sandberg, L. Lindberg, and B. Gerdle, "Peripheral effects of needle stimulation (acupuncture) on skin and muscle blood flow in fibromyalgia," *Physiol. Meas.*, vol. 28, pp. 1–39, 2004.

[8] A. Zourabian, A. Siegel, and B. C. et al, "Trans-abdominal monitoring of fetal arterial blood oxygenation using pulse oximetry," *J Biomed Opt.TAB*, no. 5, pp. 391–405, 200010.

[9] S. Loukogeorgakis, R. Dawson, and N. P. et al, "Validation of a device to measure arterial pulse wave velocity by a photoplethysmographic method," *Physiol Meas.*, no. 23, pp. 581–96, 2002.

[10] R. R. Anderson and J. A. Parrish, "The optics of human skin," *J. Invest. Dermatol.*, no. 77, pp. 13–9, 1981.

[11] L. Lindberg and P. berg, "Photoplethysmography. Part 2. Influence of light source wavelength," *Med. Biol. Eng. Comput.*, vol. 29, pp. 48–54, 1991.

[12] R. Boushel and C. Piantadosi, "Near-infrared spectroscopy for monitoring muscle oxygenation," *Acta Physiol Scand.*, vol. 68, pp. 615–22, 2000.

[13] M. Sandberg, B. Larsson, and L. G. L. et al, "Different patterns of blood flow response in the trapezius muscle following needle stimulation (acupuncture) between healthy subjects and patients with fibromyalgia and work-related trapezius myalgia," *Eur J Pain*, vol. 9, pp. 497–510, 2005.

[14] M. Leier and G. Jervan, "Sleep Apnea Pre-Screening on Neonates and Children with Shoe Integrated Sensors," *Norchip*, pp. 1–4, 2013.

Appendix E

Preden S. J.; Tammemäe K.; Jantsch A.; Leier M.; Riid A.; Calis E. (2015). The Benefits of Awareness and Attention in Fog and Mist Computing *In: IEEE Computer*, 2015, pp. 23-31

The Benefits of Awareness and Attention in Fog and Mist Computing

Jürgo S. Preden, Kalle Tammemäe, Axel Jantsch,
Mairo Leier, Andri Riid, Emine Calis

March 8, 2016

Abstract

While situation and self-awareness facilitate a proper assessment of cost-constrained cyber-physical system, attentions serves to allocate the limited resources where they are most needed. Together they are key enablers for efficient distributed sensing and computing networks.

1 Introduction

B.J. Baars (see sidebar [S1, p.347]) observes that "like any other biological adaptation, consciousness is *functional*". The same can be claimed about awareness and indeed, the insight that a sense of awareness of a system's own situation can facilitate robust and dependable behavior even under radical environmental changes and drastically diminished capabilities, has resulted in a proliferation of work on self-awareness and other system properties such as self-organization, self-configuration, self-optimization, self-protection, self-healing, etc., which are sometimes subsumed under the term self-* (see sidebar). Thus, awareness enables to improve the behavior of systems, making them more robust and reducing processing, communication and energy requirements. However, designing and implementing it in an ad-hoc manner for every new system is not feasible. Introducing awareness as a separate concept in the Cyber-Physical System (CPS) infrastructure rather than as part of the application functionality, promises to simplify development and operation of such systems. As CPS are typically Systems of Systems (SoS), the awareness must be solved comprehensively, ensuring that the understanding of the situation is coherent and consistent across the SoS.

We argue that self-awareness, situation awareness, and attention are key enablers for efficient *Fog* and *Mist computing* (See the sidebox on *Fog* and *Mist Computing*). *Situation awareness* [1] facilitates the continuous interpretation of the stream of data collected from the environment in the context of the goals and objectives of the CPS. A situation is defined by the values and interpretation of a set of *situation parameters* [2]. A situation parameter can be monitored or computed independently and represents a property of the situation of interest. In our example the information for generating situation awareness is exchanged by a *proactive middleware*, that is independent of the application functionality and can be considered as part of the CPS platform.

Fog and Mist Computing

Awareness in computing nodes can be achieved using several computing architectures. In the *Cloud Computing* scenarios the data from sensors is communicated to the cloud and the interpretation of sensor data is performed in the cloud environment, which results in inefficiencies in terms of bandwidth consumption and delays, while being powerful as global knowledge from all relevant nodes is available for situation evaluation. In *Fog Computing* [F1], the computation is performed at the edge of the network at the gateway devices, thereby reducing the need for communicating data to the servers, reducing bandwidth requirements and latency. Due to its distributed and localized architecture, computing is a natural platform for a variety of critical Internet of Things (IoT) applications such as connected vehicles, smart grids, smart cities, and, in general, wireless sensor and actuator networks [F2]. To that end several programming models and application frameworks have been developed for fog computing [F3, F4]. However, in a strict definition of fog computing the devices at the very edge are not involved in computation but only in data acquisition while the interpretation occurs in the gateway. Hence, network delay and inefficient bandwidth utilization may still be problematic. *Mist Computing* pushes the processing even further to the edge of the network involving the sensor and actuator devices, thus decreasing latency further and increasing the autonomy of subsystems. In such scenarios awareness and self awareness of every individual device is critical as the computation and actuation is dependent on the individual device's perception of the situation. The challenge with implementing mist computing systems lies in the complexity of the resulting network and the interactions in the network, which must be managed by the devices themselves as central management of such systems is not feasible.

References

[F1] Cisco Technology Radar, "Fog computing." https://techradar.cisco.com/trends/Fog-Computing, March 2015.

[F2] F. Bonomi, R. Milito, J. Zhu, and S. Addepalli, "Fog computing and its role in the internet of things," in *Proceedings of the First Edition of the MCC Workshop on Mobile Cloud Computing*, MCC '12, (New York, NY, USA), pp. 13–16, ACM, 2012.

[F3] I. Satoh, "A framework for data processing at the edges of networks," in *Database and Expert Systems Applications*, pp. 304–318, Springer, 2013.

[F4] K. Hong, D. Lillethun, U. Ramachandran, B. Ottenwälder, and B. Koldehofe, "Mobile fog: A programming model for large-scale applications on the internet of things," in *Proceedings of the Second ACM SIGCOMM Workshop on Mobile Cloud Computing*, MCC '13, (New York, NY, USA), pp. 15–20, ACM, 2013.

Attention is instrumental in balancing the competing tasks of data collection, processing and responses under tight resource constraints because it assigns priorities to tasks and goals. These priorities dynamically change depending on the situation and the state of the system. Thus, situation awareness assesses the observations and gives significance to data, attention directs scarce system resources to the most important tasks at hand, and by means of self-awareness

the overall system performance is monitored in a dynamically changing environment. In a nutshell, self-awareness (in a broad sense) includes self-monitoring (self-awareness in a narrow sense) and situation awareness because the system has to "understand" both its own state and the environmental conditions. A system that tracks only its own inner state has a very limited view of its situation in the world.

Below we explore these concepts in a human health monitoring scenario and we show how situation awareness facilitates the assessment of human physiological data using context information.

Self-Aware and Autonomic Systems

Already in the early days of theoretical psychology over a century ago the concepts of self-awareness and consciousness have been studied with great sophistication by William James [S2] and Sigmund Freud [S3], among others. Since the 1960s attempts to structure and categorize self-awareness into levels, degrees, and scope have proliferated, but this development has also lead to a fair amount of confusion due to lack of coherence with earlier work. To clear the fog A. Morin [S4] has put forward a comparison of nine neurocognitive models of self-awareness with an analysis of their respective differences and similarities. Morin's framework distinguishes, from lower to higher levels, *unconsciousness*, *conscious of external stimuli and events*, *self-awareness of public and private self-aspects*, and *meta self-awareness*, while interesting aspects and nuances are due to "perception of self in time and complexity of self-representations" [S4].

Beyond categorization of awareness phenomena, a number of theories of self-awareness, consciousness and attention in human brains have been developed. Baars describes the *Global Workspace Model* (GWM) [S1] of conscious processing, supposed to be located in the *Extended Reticular-Thalamic Activation System* (ERTAS) [S1, figure 3.1, page 97]. Its salient feature is that only one of the many parallel, subconscious processing modules gets access at any given time and can spread information globally and thus controlling the activation in large parts of the brain. Essentially, consciousness serves as a global resource allocator. Many of the phenomena predicted by the GWS could be confirmed in simulations and experiments, although more recent research downplays the importance of consciousness while *attention* and *goals* assume a more prominent role [S5]. The goals exert their effects on behavior by modulating attention - when people try to attain goals, attention serves to maintain a balance between focus and flexibility on actions.

Biological examples have long inspired computer engineering and the field received a boost in the 1990s due to ever growing complexity in software systems. The 1998 DARPA Broad Agency Announcement on Self-Adaptive Software (DAA-98-12) [S6] triggered a plethora of research on topics like self-adaptive, autonomic, self-aware computing. IBM picked up the thread and developed a powerful vision on autonomic computing leading to an abundance of research papers and eventually also products [S7]. Since then work on self-* topics has flourished both in the context of large software systems and of constrained embedded sys-

tems. Witness to these efforts are recent surveys and collections on self-healing [S8, S9], on-chip self-monitoring [S10], bio-inspired hardware design [S11], situation identification techniques [S12], pattern based engineering approaches [S13], and self-awareness [S14]. Also, Frameworks and platforms for self-aware computing are proliferating [S15–S17].

References

[S1] B. Baars, *A Cognitive Theory of Consciousness*. Cambridge University Press, 1989.

[S2] W. James, *The Principles of Psychology*, vol. I. New York: Dover, 1950. Originally published in 1890.

[S3] S. Freud, ed., *Fragments of an analysis of a case of hysteria*, vol. 7. London: Hogarth, 1953. Originally published in 1905.

[S4] A. Morin, "Levels of consciousness and self-awareness: A comparison and integration of various neurocognitive views," *Consciousness and Cognition*, vol. 15, no. 2, pp. 358 – 371, 2006.

[S5] A. Dijksterhuis and H. Aarts, "Goals, attention, and (un)consciousness," *Annual Review of Psychology*, vol. 61, pp. 467–490, January 2010.

[S6] R. Laddaga, "Active software," in *Self-Adaptive Software*, vol. 1936 of *Lecture Notes in Computer Science*, pp. 11–26, Springer, July 2001.

[S7] J. O. Kephart and D. M. Chess, "The vision of autonomic computing," *Computer*, vol. 36, no. 1, pp. 41–50, 2003.

[S8] D. Ghosh, R. Sharman, H. Raghav Rao, and S. Upadhyaya, "Self-healing systems - survey and synthesis," *Decis. Support Syst.*, vol. 42, pp. 2164–2185, January 2007.

[S9] H. Psaier and S. Dustdar, "A survey on self-healing systems: approaches and systems," *Computing*, vol. 91, no. 1, pp. 43–73, 2011.

[S10] G. Kornaros and D. Pnevmatikatos, "A survey and taxonomy of on-chip monitoring of multicore systems-on-chip," *ACM Trans. Des. Autom. Electron. Syst.*, vol. 18, pp. 17:1–17:38, Apr. 2013.

[S11] P. Cong-Vinh, ed., *Autonomic Networking-on-Chip: Bio-Inspired Specification, Development, and Verification*. CRC Press, December 2011.

[S12] J. Ye, S. Dobson, and S. McKeever, "Situation identification techniques in pervasive computing: A review," *Pervasive and Mobile Computing*, vol. 8, pp. 36–66, Feb. 2012.

[S13] T. Chen, F. Faniyi, R. Bahsoon, P. R. Lewis, X. Yao, L. L. Minku, and L. Esterle, "The handbook of engineering self-aware and self-expressive systems," *Computing Research Repository (CoRR)*, vol. abs/1409.1793, 2014.

[S14] P. Lewis, A. Chandra, S. Parsons, E. Robinson, K. Glette, R. Bahsoon, J. Torresen, and X. Yao, "A survey of self-awareness and its application in computing systems," in *Self-Adaptive and Self-Organizing Systems Workshops (SASOW), 2011 Fifth IEEE Conference on*, pp. 102–107, October 2011.

[S15] A. Jantsch and K. Tammemäe, "A framework of awareness for artificial subjects," in *Proceedings of the 2014 International Conference on Hardware/Software Codesign and System Synthesis*, CODES '14, (New York, NY, USA), pp. 20:1–20:3, ACM, 2014.

[S16] H. Hoffmann, M. Maggio, M. D. Santambrogio, A. Leva, and A. Agarwal, "Seec: A framework for self-aware computing," Tech. Rep. MIT-CSAIL-TR-2010-049, MIT, Cambrige, Massachusetts, October 2010.

[S17] S. Sarma, N. Dutt, N. Venkatasubramaniana, A. Nicolau, and P. Gupta, "Cyberphysical-system-on-chip (CPSoC): Sensor-actuator rich self-aware computational platform," tech. rep., Center for Embedded Computer Systems University of California, Irvine, Irvine, CA 92697-2620, USA, May 2013. CECS Technical Report No: CECS TR–13–06.

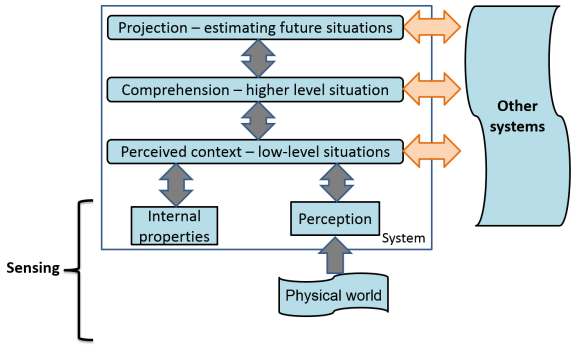

Figure 1: Hierarchical buildup of situation parameters.

2 Situation Dependent Interpretation

Both, situation awareness and attention, are an important part of self-awareness. Although the discipline of situation awareness originates from the human domain, the concepts are applicable in the domain of embedded systems. Both humans as well as computers process collected data from sensors for developing situation awareness. A cyber-physical system must be aware of the situation to perform optimally as the "correct" behavior is dependent on the current situation. For instance, the interpretation of a low fuel warning light in a vehicle is different in the middle of a desert, 300 miles from the closest gas station, and when the vehicle is pulling into a gas station. So although the sensor value is identical, the interpretation, and the consequent actions, of the sensor reading is very different.

Complex phenomena require that data from several sensors with diverse modalities are used to generate an adequate level of situation awareness. The sensors may be attached to different, physically disjoint computing nodes. This introduces the challenge (and the opportunity) of distributing the computation between individual computing nodes. One example which requires distributed sensing and processing is monitoring of the human body during everyday activities. Evaluating the state of the human body requires measuring physiological parameters and estimating the activities, because the interpretation of the measured data (e.g. heart rate) depends on the current activity (e.g. sleeping or running). Thus, sensors of different modalities must be attached in different areas of the human body, leading to a distributed sensor system. Wiring up the human body is unpleasant and hence, a network of autonomous wireless sensors should be used.

When both sensing and processing is distributed, a hierarchical buildup of situational information becomes necessary, leading to ever higher abstractions of the data. Figure 1, inspired by Mica Endsley [1], shows the main steps: sensing (perception of internal properties and the physical world), perceived context, comprehension and projection. In most computing nodes the highest level of abstraction of situational information is at the level of low-level situations (perceived context), while a few more capable computing nodes perform also the

comprehension step. Projection is a complex processing step, which may not be present at all as this requires a good understanding of the application domain as well as complex prediction methods. The concept for hierarchical buildup of situational information has first been introduced by Endsley [1] in the context of human situation awareness. J. Preden has extended it for the cyber-physical computing domain, by allowing for the exchange of situational information at the lower levels, which maps well to the computational architecture in *Fog* and *Mist computing* leading to efficient implementations.

The concept of situation parameters [2] allows to represent abstracted sensory data characterizing relevant aspects of a situation. The situation parameter types are highly domain and application dependent. It is critical that common ontology and semantics are used on the types and meaning of the situation parameters and that the parameter values are valid in the required temporal and the spatial intervals. A specific data item may be useful and valid at a certain time and location, but invalid and misleading a few seconds later at a different location. Thus, metadata must be associated with the parameter values computed by distinct computing nodes. In case of human health monitoring the minimum spatial validity criteria is that the situation parameters should characterize the same person. The temporal validity criteria specifies the temporal interval in which the parameter values are valid, e.g., the human activity assessment must reflect the activity within at least the past 10 seconds to correctly evaluate the current heart rate of the human.

Situation parameter values reflect phenomena of interest and by composing them, values of higher level parameter can be computed. The types and accuracy of situation parameters, how they are computed and their validity criteria are highly application dependent. The systems must be able to cope with inaccuracies as the values may be based on imprecise data because of inherent challenges in precisely monitoring physical processes, limited fidelity of the sensing hardware, or the approximations made in software. Examples are image processing and acoustic signal processing - the results obtained are almost always approximations, estimating the probability of the observed phenomena being of certain type or in a certain state.

One methodology that allows for combining data with varying levels of certainty is fuzzy logic [3]. Associating situation parameter types with fuzzy sets and situation parameter values with degree of membership to a given set, the set memberships can be computed at any computing node. Fuzzy rules can be used to derive higher-level situation parameter values from lower level fuzzy set membership levels. The membership functions for some fuzzy sets can be quite complex, for example a set representing the amount and quality of sleep of a person. Comprehensive solutions exist for automatic evaluation of this, for example the solution offered by Beddit Ltd. (http://www.beddit.com/), taking into account sleeping time, breathing patterns, the heartbeat rate, the amount of movement and several other factors. Thus, the function for estimating the quality of sleep itself is complex. Membership functions for other fuzzy sets may be simpler, e.g. to provide a value of the situation parameter reflecting the heart rate of the person.

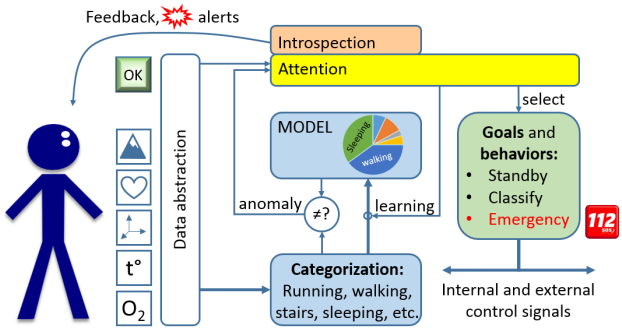

Figure 2: Architecture of self-aware Health Monitor.

3 Awareness Concepts in Health Monitoring

Our conceptual architecture of self-aware Health Monitor is provided in (Figure 2). Inputs from various sensors (altitude, location, heart rate, accelerometers, temperature, oxymeter etc.) are abstracted, attributed and categorized. The identified input pattern class is compared with a pre-built or dynamically updated model. In case of a mismatch an *anomaly* signal is generated which induces attention. An attention control mechanism triggers the collection of complementary data or additional analysis steps if an anomaly appears and the analysis is not conclusive. Depending on intensity and duration of the anomalous situation either the person is alerted or the goal is changed, adapting to a new situation. In highly anomalous cases other higher level devices are alerted (emulating emergency call).

We have previously shown how principles of using situation parameters for assessing the state of the physical world can be applied in the context of an Intelligence, Surveillance and Reconnaissance (ISR) application [2]. The benefits from abstracting data in the sensor nodes (mist computing) are the reduction of bandwidth and an adaptable system that is able to cope with changes to the system structure.

We apply the same principles to monitor the condition of a human body, where vital parameters are monitored in the context of the activity the human is involved in. In addition to the interpretation of sensor data being different in various situations, the fidelity of individual sensor data acquisition and processing is dependent on the activity of the person. For example the monitoring requirements for sleeping are different from those for running. The monitoring requirements may be also guided by a doctor, i.e. a doctor could instruct the system in certain situations to increase the fidelity of monitoring or to log the data with finer granularity.

Utilizing the value of the situation parameter reflecting the heart rate is only meaningful in the context. To evaluate if the heart rate of a person at a given moment is within a safe range the algorithm must, as a minimum, consider the specific current activity and the immediate history of activities (it takes a certain time for the human body to adapt to or to recover from a specific activity). Also, the larger context is relevant - how well rested the person is,

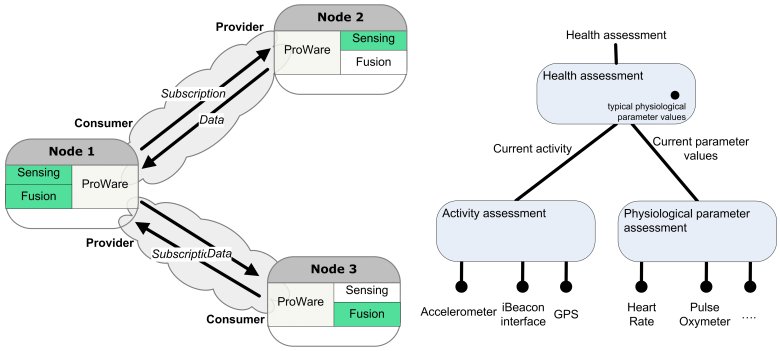

Figure 3: Left: ProWare components in individual computing nodes. Right: Hierarchies of situation parameters computed by individual computing nodes.

what food has been consumed, etc. In a health monitoring application the parameter types may reflect the activity of the person (e.g. resting, walking, running), the state of the human body (e.g. stressed, rested, tired) or the current physical load (e.g. high load, medium load). The parameter values can be computed centrally or by separate computing nodes as depicted on the right part of Figure 3.

Monitoring a person's daily activity has been an active research area for some time. Dong et al. [4] have placed several accelerometers on the body. With a Kalman filter the system tracked and classified the daily physical activities with good accuracy. The status of the body segment was categorized into static and dynamic, further differentiated into periodical and non-periodical status using Discrete Fourier Transform (DFT). A Hidden Markov Model (HMM) was used for training data and modeling of periodical movement. The overall classification accuracy is reported as about 90%.

Similar physical activity assessment for rescuers during emergency interventions has been developed by Curone et al. [5]. Wearable electronics was integrated into the textile fabrics with the goal to automatically identify potentially dangerous conditions for the monitored subject. With the triaxial accelerometer and one lead ECG (electrocardiogram), an overall classification accuracy of 88.8% was achieved.

As these examples illustrate, the evaluation of the activity of a person may use a range of sensors as input. It is clear that for different activities the interpretation of the sensor data must be interpreted differently. A heart rate of 130 may be normal for a person climbing stairs or jogging but the same heart rate is worrying when the person is resting or working at a desk. Similarly, the interpretation of other physiological signals depends on the current activity of the person.

In order to facilitate effective exchange of situation parameters, a Proactive Middleware (ProWare) has been implemented in the Research Laboratory for Proactive Technologies. The left part of (Figure 3) depicts the elements of ProWare involved in data exchange. ProWare enables dynamic establishment of communication partnerships (as service subscriptions) for exchange of situation

parameters, enabling the consumer of the situation parameters to specify the temporal and spatial constraints for the parameters [2].

The ProWare components, located in every computing node, check the validity criteria and ensure that only data that satisfies the validity criteria are delivered to the analysis algorithms. In order to facilitate the validation of the mist computing concepts we have packaged the ProWare components together with a clustered mesh protocol in a compact wireless module. This module enables fast integration with sensor devices and it is pin compatible with Raspberry PI, Arduino and Bluehex.

4 Experiments and Results

Even though the complete system of Figure 2 has not yet been realized, we conducted a series of experiments in a health monitoring scenario to validate key assumptions and show the viability of identification of awareness properties in a mist computing approach. The data relevant for situation assessment was collected from individual sensors.

In the experiments a test person was involved in the following activities: resting on a couch, working at a table, walking slowly indoors, climbing stairs indoors and walking at a rapid pace outdoors. The sensors used in the tests were accelerometer, altitude meter and a heart rate monitor.

The collected data was analyzed to determine if local situation assessment by combining data from individual embedded sensor nodes is feasible. Although the collected data was analyzed off-line the algorithms applied are sufficiently light-weight to be executable in embedded low-power computing nodes.

The heart rate data was logged using a BM-Innovations chest strap BM-CS5 (http://bm-innovations.com/). The pulse rate was communicated once per second using the Bluerobin wireless protocol to the Texas Instruments eZ430-Chronos watch (http://www.ti.com/tool/ez430-chronos). The watch was equipped with an internal pressure sensor for altitude measurements. The heart rate and altitude were saved with a full time stamp temporarily in the internal memory of the watch. Data logs from the experiments were communicated to a PC for analysis using wireless SimpliciTI protocol (http://processors.wiki.ti.com). For evaluating the activity of the person the accelerometer in a smartphone was used and the phone was carried in the pocket of the subject during experiments. The G-Sensor Logger Android application was used to collect accelerometer measurements. The data logged during the tests from all the sensing devices was analyzed with MATLAB. Our aim was to investigate if the performed activities can be detected (i.e., situation parameter values determined) from individual data streams. As noted above, the sampling rate for pulse rate and altitude estimate was 1Hz while the average sampling rate for the accelerometer was 16Hz, therefore the raw sensor data was synchronized before analysis. In a *Mist computing* implementation the synchronization will be performed by ProWare. We employed the modulus of the acceleration vector $|a| = \sqrt{a_x^2 + a_y^2}$ when data of two sensors was used, and $|a| = \sqrt{a_x^2 + a_y^2 + a_z^2}$ for data from three sensors to estimate the personal activity level, which proved to be sufficient.

The left side of Figure 4 depicts the averaged values of observed pulse rates and acceleration over ten-second periods.

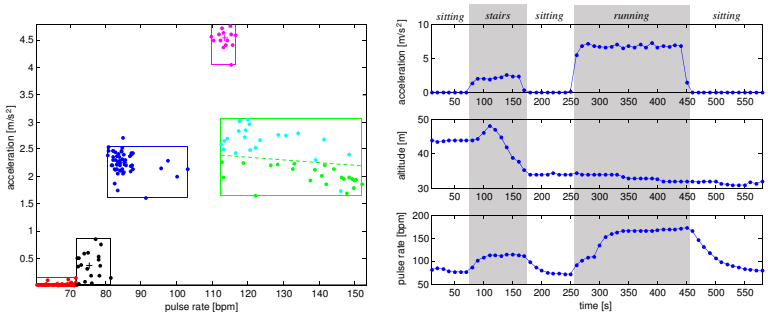

Figure 4: Left: Pulse rate versus activity: red: sitting or resting; black: car driving; blue: indoor slow walking; magenta: outdoor rapid walking; walking upstairs (green) and downstairs (cyan). Right: The modes are correctly tracked as the person performs different activities.

The results from different experiments populate rather distinct areas in the pulse rate/activity space. The activities sitting, car driving, indoor walking, outdoor walking can be well categorized using only two sensors, the pulse rate meter and the accelerometer. However, the green and cyan dots (stair climbing) form a rather large area in the pulse rate/accelerometer space triggering the attention mechanism to consult further data from the altitude sensor. These additional data allow to identify the activity as stair climbing and to distinguish between moving upwards (green) and moving downwards (cyan). More generally, this illustrates the benefit of attention directed data collection and analysis. If data from a few sensors, processed with a simple analysis algorithm, comes to an unambiguous conclusion, unnecessary data collection and processing is avoided. Only cases when anomalies are detected or the analysis is inconclusive warrant a more elaborate and expensive procedure of data collection, communication and computing. Thus, attention based sensing and analysis has potential to save significant time and energy. To quantify this potential in various applications remains the objective in future work.

Also note that these states in the figure are mostly what can be considered the steady states for given exercises, although some transitional states are also observed (the samples between the boxes). Pulse rate changes are never instantaneous. This is clearly visible in the right side of Figure 4 that depicts a series of exercises explains why the temporal aspect of human physiology must be considered.

From the experiments it can be concluded that relatively simple sensors can be used to determine the activity the person is involved in and correlate physiological parameters to individual activities. Moreover, most of the time only a subset of the available sensors have to be employed leading to a lean approach of monitoring. For a more accurate estimation, however, additional phenomena need to be measured. Naturally such a monitoring system must adapt to an individual but once the adaption phase is complete, the CPS is able to monitor the person and determine if the physiological parameters are within the typical range for a given activity.

5 Conclusions and future work

Self-awareness, situation awareness and attention are powerful concepts with the potential to lead to high efficiency in various sensor and actuator networks. Inspired by biological example, studies and proposals that touch upon various aspects of self-awareness have proliferated during recent years. Still, its potential is hardly understood and by far not yet exploited. Contributing to this broad effort, we have explored situation awareness and attention, concluding that the principles of generating situation awareness using the situation parameter concept are well applicable for health monitoring. We argue that situation awareness is an inherent part of self-awareness. A system has to know its own inner state (self-awareness in a narrow sense) and where it is in the world and what the environment looks like to make a proper assessment of its own state and performance. Only with the understanding of the context it is justified to call the system self-aware in a broader sense.

Situation awareness is jointly generated by a group of sensors, thus distributing the burden over several nodes and leading to *Fog* or *Mist computing*. Fairly simple algorithms, executed by resource constrained embedded nodes, compute the situation parameters. ProWare can be used as a platform to facilitate the information exchange of situational parameters within a resource constrained network. With the availability of a standalone RF hardware module that contains ProWare it is simple to connect any device to an existing CPS.

We have shown in our experiments with only three sensors (for pulse rate, acceleration, altitude) how the different measurements complement each other to allow for a precise assessment of typical activities and how attention can steer data collection and processing for the benefit of lean and efficient system. Multiple sensors facilitate distributed data collecting and processing based on fog and mist computing paradigms.

We are building a complete prototype CPS which is able to monitor the parameters of the human body and dynamically learn normal sensor patterns facilitating the detection of deviations and anomalies.

References

[1] M. R. Endsley, "Design and evaluation for situation awareness enhancement," in *Proceedings of the Human Factors and Ergonomics Society 32th Annual Meeting*, pp. 97–101, 1988.

[2] J. Preden, J. Llinas, G. Rogava, R. Pathma, and L. Motus, "On-line data validation in distributed data fusion," in *Ground/Air Multisensor Interoperability, Integration, and Networking for Persistent ISR IV: SPIE Defense, Security and Sensing* (T. Pham, M. A. Kolodny, and K. L. Priddy, eds.), SPIE - International Society for Optics and Photonics, 2013.

[3] A. Riid and E. Rüstern, "An integrated approach for the identification of compact, interpretable and accurate fuzzy rule-based classifiers from data," in *Intelligent Engineering Systems (INES), 2011 15th IEEE International Conference on*, pp. 101–107, June 2011.

[4] L. Dong, J. Wu, and X. Chen, "Real-Time Physical Activity Monitoring by Data Fusion in Body Sensor Networks," *10th Int. Conf on Inf. Fusion*, pp. 1–7, July 2008.

[5] D. Curone, A. Tognetti, and E. L. S. et al, "Heart Rate and Accelerometer data Fusion for Activity Assessment of Rescuers During Emergency Interventions," *ICSENS*, pp. 702–710, May 2010.

Curriculum Vitae

Personal Data

Name: Mairo Leier
Date of Birth: December 01, 1982
Place of Birth: Haapsalu, Estonia
Citizenship: Estonian

Contact Data

Address: 15A Akadeemia St., 12618 Tallinn, Estonia
Phone: +372 56 876 456
E-mail: mairo22@gmail.com

Education

2010 – ...	PhD studies in Information and Communication Technology, Tallinn University of Technology (TUT)
2008 – 2010	M.Sc. in Computer Science, Tallinn University of Technology
2004 – 2005	B.Sc. (double degree) in Fachhochschule Jena in Germany
2001 – 2005	B.Sc. in Mechanical Engineering, University of Applied Sciences

Career

2012 – ...	Early-stage researcher, Tallinn University of Technology
2012 – 2014	Co-founder and Technology leader, EWG-Tech OÜ
2006 – 2012	Engineer Multimedia Solutions, Ericsson Estonia AS
2002 – 2005	Mobile phones repair engineer, Elisa Estonia AS

Awards

2014	1^{th} Place, Summer of Startups Competition, Tallinn, Estonia
2012	2^{nd} Place, Summer of Startups Competition, Tallinn, Estonia
2011	1^{th} Place, TeamUp Competition, Tallinn, Estonia

Elulookirjeldus

Isikuandmed

Nimi: Mairo Leier
Sünniaeg: 01. Detsember, 1982
Sünnikoht: Haapsalu, Eesti
Kodakondsus: Eesti

Kontaktandmed

Aadress: Akadeemia tee 15A, 12618 Tallinn, Eesti
Tel.: +372 56 876 456
E-post: mairo22@gmail.com

Hariduskäik

2010 – ...	Doktoriõpe, info- ja kommunikatsioonitehnoloogia õppekava, Tallinna Tehnikaülikool
2008 – 2010	Magistrikraad Informaatika erialal, Tallinna Tehnikaülikool
2004 – 2005	Bakalaureusekraad (topeltkraadiõpe) Masinaehitue erialal, Jena Ametikõrgkool, Saksamaa
2001 – 2005	Bakalaureusekraad Masinaehituse ja automatiseerimise erialal, Tallinna Tehnikakõrgkool

Teenistuskäik

2012 – ...	Nooremteadur, Tallinna Tehnikaülikool
2012 – 2014	Kaasasutaja ja tehnikajuht, EWG-Tech OÜ
2006 – 2012	Multimeedialahenduste insener, Ericsson Eesti AS
2002 – 2005	Mobiiltelefonide hooldusspetsialist, Elisa Eesti AS

Saavutused ja preemiad

2014	1. koht, Summer of Startups võistlus, Tallinn, Eesti
2012	2. koht, Summer of Startups võistlus, Tallinn, Eesti
2011	1. koht, TeamUp tootearenduspäeva võistlus, Tallinn, Eesti

DISSERTATIONS DEFENDED AT TALLINN UNIVERSITY OF TECHNOLOGY ON *INFORMATICS AND SYSTEM ENGINEERING*

1. **Lea Elmik**. Informational Modelling of a Communication Office. 1992.

2. **Kalle Tammemäe**. Control Intensive Digital System Synthesis. 1997.

3. **Eerik Lossmann**. Complex Signal Classification Algorithms, Based on the Third-Order Statistical Models. 1999.

4. **Kaido Kikkas**. Using the Internet in Rehabilitation of People with Mobility Impairments – Case Studies and Views from Estonia. 1999.

5. **Nazmun Nahar**. Global Electronic Commerce Process: Business-to-Business. 1999.

6. **Jevgeni Riipulk**. Microwave Radiometry for Medical Applications. 2000.

7. **Alar Kuusik**. Compact Smart Home Systems: Design and Verification of Cost Effective Hardware Solutions. 2001.

8. **Jaan Raik**. Hierarchical Test Generation for Digital Circuits Represented by Decision Diagrams. 2001.

9. **Andri Riid**. Transparent Fuzzy Systems: Model and Control. 2002.

10. **Marina Brik**. Investigation and Development of Test Generation Methods for Control Part of Digital Systems. 2002.

11. **Raul Land**. Synchronous Approximation and Processing of Sampled Data Signals. 2002.

12. **Ants Ronk**. An Extended Block-Adaptive Fourier Analyser for Analysis and Reproduction of Periodic Components of Band-Limited Discrete-Time Signals. 2002.

13. **Toivo Paavle**. System Level Modeling of the Phase Locked Loops: Behavioral Analysis and Parameterization. 2003.

14. **Irina Astrova**. On Integration of Object-Oriented Applications with Relational Databases. 2003.

15. **Kuldar Taveter**. A Multi-Perspective Methodology for Agent-Oriented Business Modelling and Simulation. 2004.

16. **Taivo Kangilaski**. Eesti Energia käiduhaldussüsteem. 2004.

17. **Artur Jutman**. Selected Issues of Modeling, Verification and Testing of Digital Systems. 2004.

18. **Ander Tenno**. Simulation and Estimation of Electro-Chemical Processes in Maintenance-Free Batteries with Fixed Electrolyte. 2004.

19. **Oleg Korolkov**. Formation of Diffusion Welded Al Contacts to Semiconductor Silicon. 2004.

20. **Risto Vaarandi**. Tools and Techniques for Event Log Analysis. 2005.

21. **Marko Koort**. Transmitter Power Control in Wireless Communication Systems. 2005.

22. **Raul Savimaa**. Modelling Emergent Behaviour of Organizations. Time-Aware, UML and Agent Based Approach. 2005.

23. **Raido Kurel**. Investigation of Electrical Characteristics of SiC Based Complementary JBS Structures. 2005.

24. **Rainer Taniloo**. Ökonoomsete negatiivse diferentsiaaltakistusega astmete ja elementide disainimine ja optimeerimine. 2005.

25. **Pauli Lallo**. Adaptive Secure Data Transmission Method for OSI Level I. 2005.

26. **Deniss Kumlander**. Some Practical Algorithms to Solve the Maximum Clique Problem. 2005.

27. **Tarmo Veskioja**. Stable Marriage Problem and College Admission. 2005.

28. **Elena Fomina**. Low Power Finite State Machine Synthesis. 2005.

29. **Eero Ivask**. Digital Test in WEB-Based Environment 2006.

30. **Виктор Войтович**. Разработка технологий выращивания из жидкой фазы эпитаксиальных структур арсенида галлия с высоковольтным p-n переходом и изготовления диодов на их основе. 2006.

31. **Tanel Alumäe**. Methods for Estonian Large Vocabulary Speech Recognition. 2006.

32. **Erki Eessaar**. Relational and Object-Relational Database Management Systems as Platforms for Managing Softwareengineering Artefacts. 2006.

33. **Rauno Gordon**. Modelling of Cardiac Dynamics and Intracardiac Bio-impedance. 2007.

34. **Madis Listak**. A Task-Oriented Design of a Biologically Inspired Underwater Robot. 2007.

35. **Elmet Orasson**. Hybrid Built-in Self-Test. Methods and Tools for Analysis and Optimization of BIST. 2007.

36. **Eduard Petlenkov**. Neural Networks Based Identification and Control of Nonlinear Systems: ANARX Model Based Approach. 2007.

37. **Toomas Kirt**. Concept Formation in Exploratory Data Analysis: Case Studies of Linguistic and Banking Data. 2007.

38. **Juhan-Peep Ernits**. Two State Space Reduction Techniques for Explicit State Model Checking. 2007.

39. **Innar Liiv**. Pattern Discovery Using Seriation and Matrix Reordering: A Unified View, Extensions and an Application to Inventory Management. 2008.

40. **Andrei Pokatilov**. Development of National Standard for Voltage Unit Based on Solid-State References. 2008.

41. **Karin Lindroos**. Mapping Social Structures by Formal Non-Linear Information Processing Methods: Case Studies of Estonian Islands Environments. 2008.

42. **Maksim Jenihhin**. Simulation-Based Hardware Verification with High-Level Decision Diagrams. 2008.

43. **Ando Saabas**. Logics for Low-Level Code and Proof-Preserving Program Transformations. 2008.

44. **Ilja Tšahhirov**. Security Protocols Analysis in the Computational Model – Dependency Flow Graphs-Based Approach. 2008.

45. **Toomas Ruuben**. Wideband Digital Beamforming in Sonar Systems. 2009.

46. **Sergei Devadze**. Fault Simulation of Digital Systems. 2009.

47. **Andrei Krivošei**. Model Based Method for Adaptive Decomposition of the Thoracic Bio-Impedance Variations into Cardiac and Respiratory Components. 2009.

48. **Vineeth Govind**. DfT-Based External Test and Diagnosis of Mesh-like Networks on Chips. 2009.

49. **Andres Kull**. Model-Based Testing of Reactive Systems. 2009.

50. **Ants Torim**. Formal Concepts in the Theory of Monotone Systems. 2009.

51. **Erika Matsak**. Discovering Logical Constructs from Estonian Children Language. 2009.

52. **Paul Annus**. Multichannel Bioimpedance Spectroscopy: Instrumentation Methods and Design Principles. 2009.

53. **Maris Tõnso**. Computer Algebra Tools for Modelling, Analysis and Synthesis for Nonlinear Control Systems. 2010.

54. **Aivo Jürgenson**. Efficient Semantics of Parallel and Serial Models of Attack Trees. 2010.

55. **Erkki Joasoon**. The Tactile Feedback Device for Multi-Touch User Interfaces. 2010.

56. **Jürgo-Sören Preden**. Enhancing Situation – Awareness Cognition and Reasoning of Ad-Hoc Network Agents. 2010.

57. **Pavel Grigorenko**. Higher-Order Attribute Semantics of Flat Languages. 2010.

58. **Anna Rannaste**. Hierarcical Test Pattern Generation and Untestability Identification Techniques for Synchronous Sequential Circuits. 2010.

59. **Sergei Strik**. Battery Charging and Full-Featured Battery Charger Integrated Circuit for Portable Applications. 2011.

60. **Rain Ottis**. A Systematic Approach to Offensive Volunteer Cyber Militia. 2011.

61. **Natalja Sleptšuk**. Investigation of the Intermediate Layer in the Metal-Silicon Carbide Contact Obtained by Diffusion Welding. 2011.

62. **Martin Jaanus**. The Interactive Learning Environment for Mobile Laboratories. 2011.

63. **Argo Kasemaa**. Analog Front End Components for Bio-Impedance Measurement: Current Source Design and Implementation. 2011.

64. **Kenneth Geers**. Strategic Cyber Security: Evaluating Nation-State Cyber Attack Mitigation Strategies. 2011.

65. **Riina Maigre**. Composition of Web Services on Large Service Models. 2011.

66. **Helena Kruus**. Optimization of Built-in Self-Test in Digital Systems. 2011.

67. **Gunnar Piho**. Archetypes Based Techniques for Development of Domains, Requirements and Sofware. 2011.

68. **Juri Gavšin**. Intrinsic Robot Safety Through Reversibility of Actions. 2011.

69. **Dmitri Mihhailov**. Hardware Implementation of Recursive Sorting Algorithms Using Tree-like Structures and HFSM Models. 2012.

70. **Anton Tšertov**. System Modeling for Processor-Centric Test Automation. 2012.

71. **Sergei Kostin**. Self-Diagnosis in Digital Systems. 2012.

72. **Mihkel Tagel**. System-Level Design of Timing-Sensitive Network-on-Chip Based Dependable Systems. 2012.

73. **Juri Belikov**. Polynomial Methods for Nonlinear Control Systems. 2012.

74. **Kristina Vassiljeva**. Restricted Connectivity Neural Networks based Identification for Control. 2012.

75. **Tarmo Robal**. Towards Adaptive Web – Analysing and Recommending Web Users` Behaviour. 2012.

76. **Anton Karputkin**. Formal Verification and Error Correction on High-Level Decision Diagrams. 2012.

77. **Vadim Kimlaychuk**. Simulations in Multi-Agent Communication System. 2012.

78. **Taavi Viilukas**. Constraints Solving Based Hierarchical Test Generation for Synchronous Sequential Circuits. 2012.

79. **Marko Kääramees**. A Symbolic Approach to Model-based Online Testing. 2012.

80. **Enar Reilent**. Whiteboard Architecture for the Multi-agent Sensor Systems. 2012.

81. **Jaan Ojarand**. Wideband Excitation Signals for Fast Impedance Spectroscopy of Biological Objects. 2012.

82. **Igor Aleksejev**. FPGA-based Embedded Virtual Instrumentation. 2013.

83. **Juri Mihhailov**. Accurate Flexible Current Measurement Method and its Realization in Power and Battery Management Integrated Circuits for Portable Applications. 2013.

84. **Tõnis Saar**. The Piezo-Electric Impedance Spectroscopy: Solutions and Applications. 2013.

85. **Ermo Täks**. An Automated Legal Content Capture and Visualisation Method. 2013.

86. **Uljana Reinsalu**. Fault Simulation and Code Coverage Analysis of RTL Designs Using High-Level Decision Diagrams. 2013.

87. **Anton Tšepurov**. Hardware Modeling for Design Verification and Debug. 2013.

88. **Ivo Müürsepp**. Robust Detectors for Cognitive Radio. 2013.

89. **Jaas Ježov**. Pressure sensitive lateral line for underwater robot. 2013.

90. **Vadim Kaparin**. Transformation of Nonlinear State Equations into Observer Form. 2013.

92. **Reeno Reeder**. Development and Optimisation of Modelling Methods and Algorithms for Terahertz Range Radiation Sources Based on Quantum Well Heterostructures. 2014.

93. **Ants Koel**. GaAs and SiC Semiconductor Materials Based Power Structures: Static and Dynamic Behavior Analysis. 2014.

94. **Jaan Übi**. Methods for Coopetition and Retention Analysis: An Application to University Management. 2014.

95. **Innokenti Sobolev**. Hyperspectral Data Processing and Interpretation in Remote Sensing Based on Laser-Induced Fluorescence Method. 2014.

96. **Jana Toompuu**. Investigation of the Specific Deep Levels in *p*-, *i*- and *n*-Regions of GaAs p^+-*pin*-n^+ Structures. 2014.

97. **Taavi Salumäe**. Flow-Sensitive Robotic Fish: From Concept to Experiments. 2015.

98. **Yar Muhammad**. A Parametric Framework for Modelling of Bioelectrical Signals. 2015.

99. **Ago Mõlder**. Image Processing Solutions for Precise Road Profile Measurement Systems. 2015.

100. **Kairit Sirts**. Non-Parametric Bayesian Models for Computational Morphology. 2015.

101. **Alina Gavrijaševa**. Coin Validation by Electromagnetic, Acoustic and Visual Features. 2015.

102. **Emiliano Pastorelli**. Analysis and 3D Visualisation of Microstructured Materials on Custom-Built Virtual Reality Environment. 2015.

103. **Asko Ristolainen**. Phantom Organs and their Applications in Robotic Surgery and Radiology Training. 2015.

104. **Aleksei Tepljakov**. Fractional-order Modeling and Control of Dynamic Systems. 2015.

105. **Ahti Lohk**. A System of Test Patterns to Check and Validate the Semantic Hierarchies of Wordnet-type Dictionaries. 2015.

106. **Hanno Hantson**. Mutation-Based Verification and Error Correction in High-Level Designs. 2015.

107. **Lin Li**. Statistical Methods for Ultrasound Image Segmentation. 2015.

108. **Aleksandr Lenin**. Reliable and Efficient Determination of the Likelihood of Rational Attacks. 2015.

109. **Maksim Gorev**. At-Speed Testing and Test Quality Evaluation for High-Performance Pipelined Systems. 2016.

110. **Mari-Anne Meister**. Electromagnetic Environment and Propagation Factors of Short-Wave Range in Estonia. 2016.

111. **Syed Saif Abrar**. Comprehensive Abstraction of VHDL RTL Cores to ESL SystemC. 2016.

112. **Arvo Kaldmäe**. Advanced Design of Nonlinear Discrete-time and Delayed Systems. 2016.